CHAPTER 3

RESULTS AND DISCUSSION

3.1 Synthesis of Poly(L-lactide-*co*-ε-caprolactone), PLC 50:50 mole% Copolymers: Small Scale (25 g)

3.1.1 Effect of the Reaction Time on the Polymer Properties

To study the effect of the reaction time on the PLC 50:50 copolymer properties, polymerizations were carried out with the reaction time varying between 2 and 96 hours at constant the monomer to initiator molar ratio ([M]:[I] = 100:0.01 mole%) and 0.1 mole% $SnOct_2$ catalyst. The ROP was carried out in bulk at 120°C. The conditions used for synthesis of PLC copolymers, %yield and physical appearance are shown in Table 3.1.

From Table 3.1, it can be seen that the physical appearance of PLC copolymers in the initial period of reaction time were translucent brittle solid look like poly(L-lactide). Because of the reactivity of L-lactide is higher than that of ε-caprolactone, due to L-lactide has 2 ester groups that is the reactive group in the ROP reaction while ε-caprolactone has only 1 ester group. When increasing the reaction time, polymerization of ε-caprolactone is increased; as a result, PLC copolymers have the property between ε-caprolactone and L-lactide properties. At the end of the reaction period, the physical appearance of PLC copolymers was pale yellow transparent and rubbery-like solids.

Table 3.1 The effect of the reaction time on the %yield and physical appearance of PLC copolymers in small scale (25 g) using [M]:[I] molar ratio 100:0.01 mole%, 0.1 mole% $SnOct_2$ as a catalyst at 120°C.

Copolymer	Reaction time (hours)	%yield	Physical Appearance
PLC_S1	2	61.26	translucent brittle solid
PLC_S2	4	67.49	translucent brittle solid
PLC_S3	6	74.11	translucent brittle solid
PLC_S4	8	79.73	transparent solid
PLC_S5	12	83.55	transparent solid
PLC_S6	24	88.34	transparent rubbery-like solid
PLC_S7	48	91.68	transparent pale yellow rubbery-like solid
PLC_S8	72	90.31	transparent pale yellow rubbery-like solid
PLC_S9	96	92.51	transparent pale yellow rubbery-like solid

Figure 3.1 shows the effect of the reaction time on the %yield of PLC copolymers. As a mentioned above, ε-caprolactone has lower reactivity than L-lactide. Thus, in the initial reaction time, ε-caprolactone monomer remained in the polymerization system and gave low %yield of PLC copolymers. The increase in the reaction time leads to an increase in the %yield of PLC copolymers, until it reaches a maximum after 48 hours, but beyond that time, the %yield of PLC copolymers were obtained levels off at a constant value.

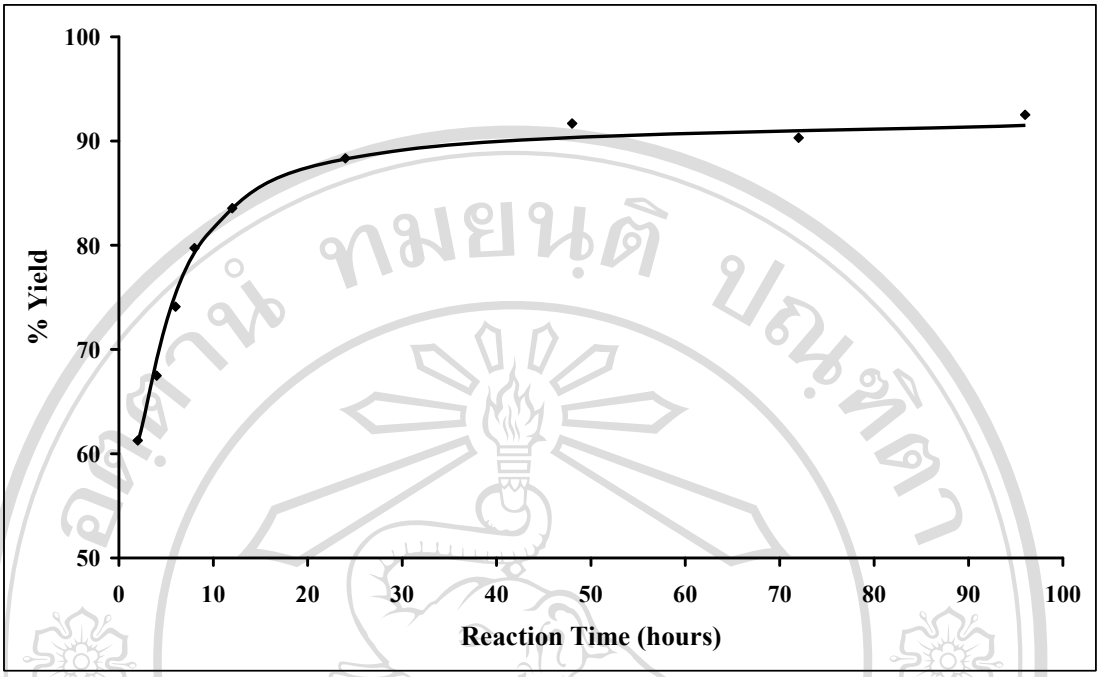

Figure 3.1 % Yield-time profile of PLC copolymers in small scale (25 g).

3.1.1.1 Structural Analysis by ^{1}H-NMR Spectroscopy

The structure of the PLC copolymers with different the reaction time were characterized by ^{1}H-NMR. The ^{1}H-NMR spectra of PLCs in deuterated chloroform solutions were recorded using a Bruker Avace 400 MHz NMR spectrometer at room temperature and the data obtained from MestRe-C data processing software. The spectra of crude and purified PLC_S1 and PLC_S8 are shown in Figures 3.2-3.5. The summarized interpretations from the proton assignments of corresponding chemical shift and peak area integration of crude and purified PLCs are given in Tables 3.2-3.5.

Figures 3.2 and 3.4 show the ^{1}H-NMR spectra of crude PLC_S1 and PLC_S8 copolymers respectively. It can be seen that the peak at δ = 5.0 – 5.3 ppm (peak b) corresponding to the methine proton (C-H) in the lactyl unit of L-lactide units, at δ = 4.0 – 4.2 ppm (peak c) and δ = 2.2 – 2.5 ppm (peak g) corresponding to methylene

proton (ε-CH_2 and α-CH_2) in the caprolactone units and at δ = 1.1 – 2.0 ppm (peak a, d, f and e) corresponding to the overlap of the methylene proton of caprolactone unit and methyl proton of L-lactide unit.

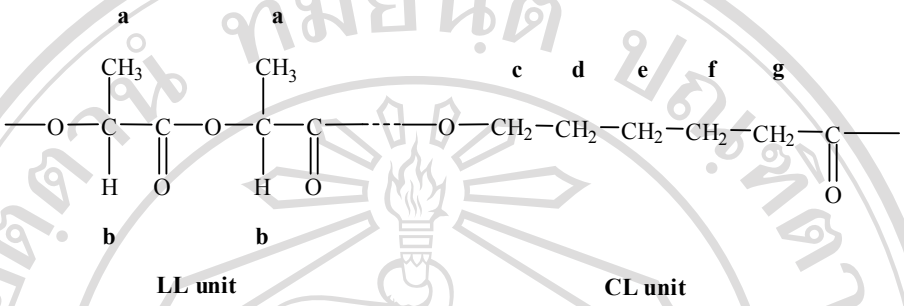

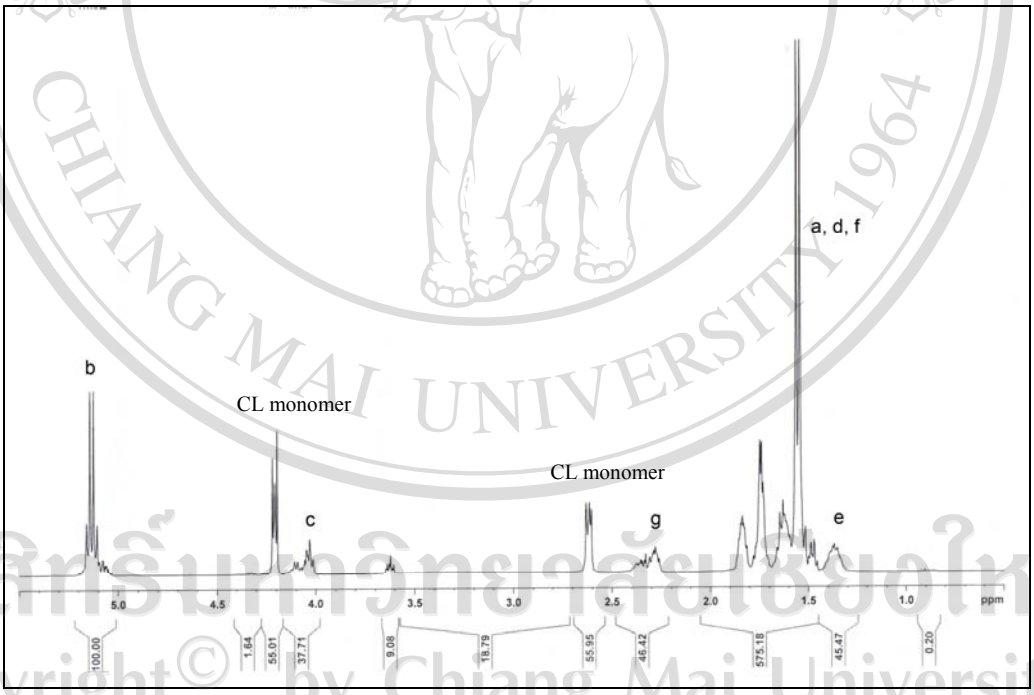

Figure 3.2 ^{1}H-NMR (400 MHz) spectrum of crude PLC_S1 in small scale (25 g).

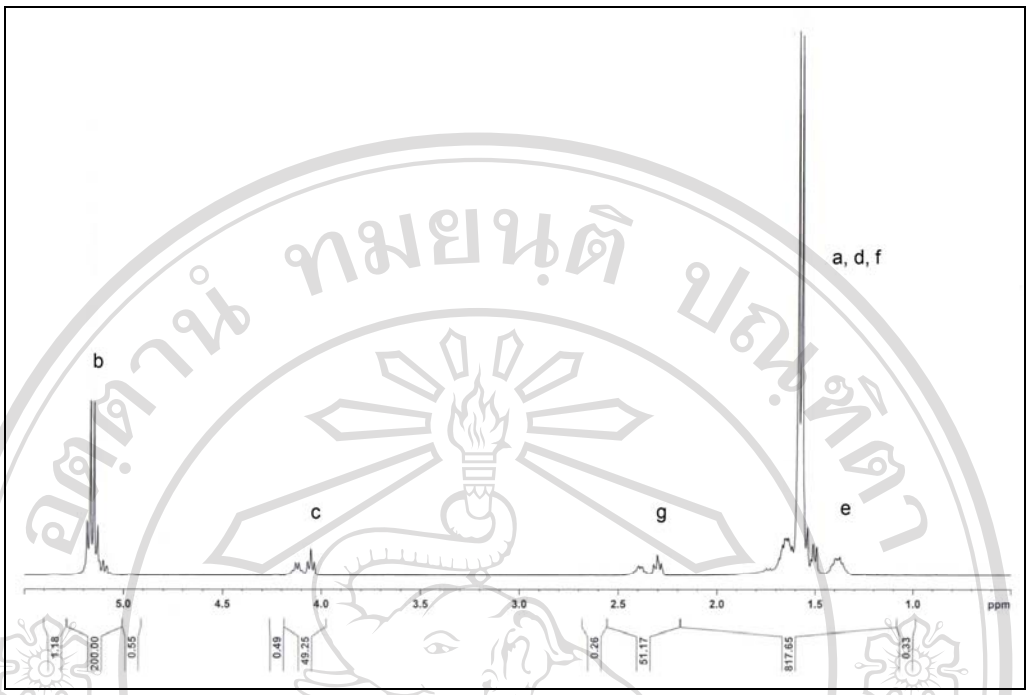

Figure 3.3 ^{1}H-NMR (400 MHz) spectrum of purified PLC_S1 in small scale (25 g).

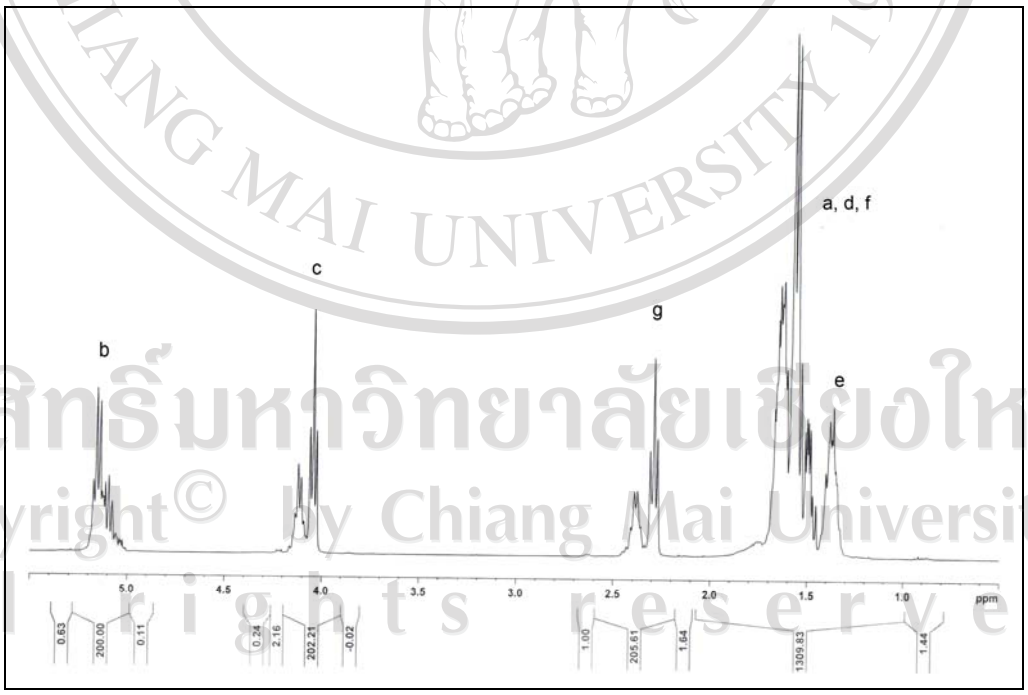

Figure 3.4 ^{1}H-NMR (400 MHz) spectrum of crude PLC_S8 in small scale (25 g).

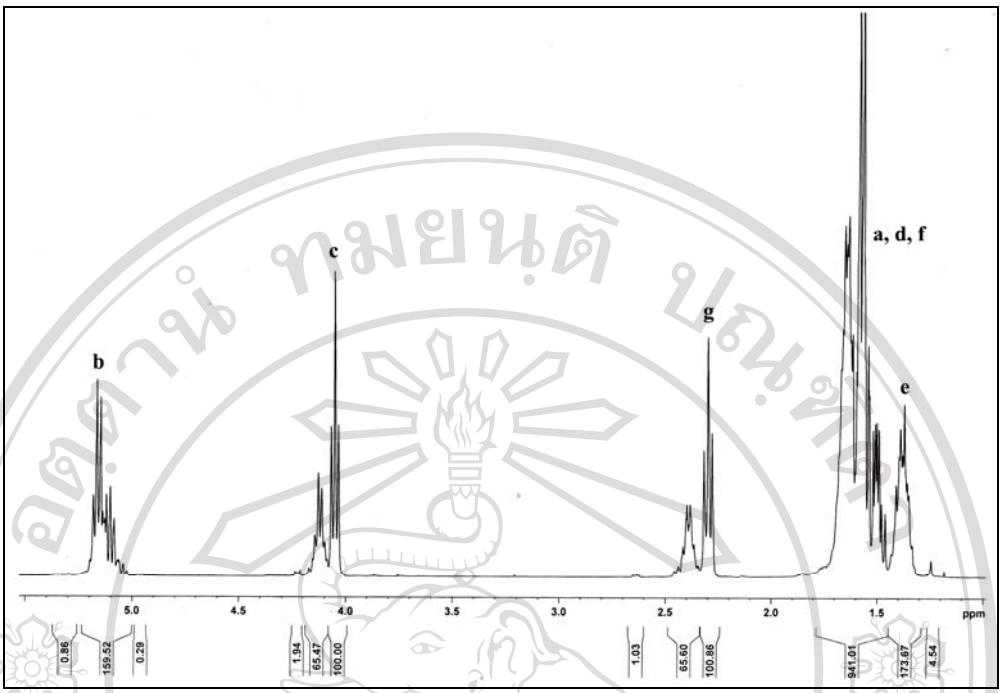

Figure 3.5 ^{1}H-NMR (400 MHz) spectrum of purified PLC_S8 in small scale (25 g).

Table 3.2 Proton assignments and corresponding chemical shift ranges for the various resonance peaks in the ^{1}H-NMR spectra of the crude PLC_S1-S9 copolymers in small scale (25 g).

Copolymer	**chemical shift range, δ (ppm)**				
	CL monomer	**b**	**c**	**g**	**a, d, f, e**
PLC_S1	2.6 , 4.2	5.3-5.0	4.2-4.0	2.5-2.2	2.0-1.2
PLC_S2	2.6 , 4.2	5.3-5.0	4.2-4.0	2.5-2.2	1.9-1.3
PLC_S3	2.6 , 4.2	5.3-5.0	4.2-4.0	2.5-2.2	1.9-1.2
PLC_S4	2.6 , 4.2	5.3-5.0	4.2-4.0	2.5-2.2	2.2-1.1
PLC_S5	2.6 , 4.2	5.3-5.0	4.2-3.9	2.5-2.2	2.1-1.2
PLC_S6	2.6 , 4.2	5.3-5.0	4.2-4.0	2.5-2.2	2.1-1.2
PLC_S7	nd	5.3-5.0	4.2-4.0	2.6-2.2	2.0-1.1
PLC_S8	nd	5.3-5.0	4.2-3.9	2.6-2.2	2.1-1.0
PLC_S9	nd	5.3-5.0	4.2-3.9	2.6-2.2	2.1-1.0

Table 3.3 Proton assignments and corresponding peak area integrations for the various resonance peaks in the ^{1}H-NMR spectra of the crude PLC_S1-S9 copolymers in small scale (25 g).

Copolymer	peak area integration					
	CL monomer		b	c	g	a, d, f, e
	2.6 ppm	4.2 ppm				
PLC_S1	55.95	55.01	100.00	37.71	46.42	620.65
PLC_S2	68.47	61.79	99.99	40.77	58.04	651.98
PLC_S3	41.47	40.91	100.00	64.88	72.06	658.09
PLC_S4	30.70	30.60	100.00	72.81	76.86	660.59
PLC_S5	52.43	52.60	200.00	146.06	150.88	1296.32
PLC_S6	14.07	15.16	200.00	190.81	194.54	1305.37
PLC_S7	nd	nd	200.00	218.21	220.72	1365.76
PLC_S8	nd	nd	200.00	202.21	205.61	1309.83
PLC_S9	nd	nd	200.00	203.65	206.01	1341.87

Table 3.4 Proton assignments and corresponding chemical shift ranges for the various resonance peaks in the ^{1}H-NMR spectra of the purified PLC_S1-S9 copolymers in small scale (25 g).

Copolymer	chemical shift range, δ (ppm)				
	CL monomer	b	c	g	a, d, f, e
PLC_S1	nd	5.3-5.0	4.3-4.0	2.6-2.2	2.2-1.1
PLC_S2	nd	5.3-5.0	4.2-4.0	2.5-2.2	2.2-1.2
PLC_S3	nd	5.3-5.0	4.2-4.0	2.5-2.2	1.8-1.3
PLC_S4	nd	5.3-5.0	4.2-4.0	2.6-2.2	1.9-1.2
PLC_S5	nd	5.3-5.0	4.2-3.9	2.6-1.9	1.9-1.1
PLC_S6	nd	5.3-5.0	4.2-4.0	2.5-2.2	1.8-1.3
PLC_S7	nd	5.3-5.0	4.2-4.0	2.5-2.2	1.9-1.3
PLC_S8	nd	5.3-5.0	4.2-4.0	2.5-2.2	1.8-1.3
PLC_S9	nd	5.3-5.0	4.2-4.0	2.5-2.2	1.8-1.3

Table 3.5 Proton assignments and corresponding peak area integrations for the various resonance peaks in the ^{1}H-NMR spectra of the purified PLC_S1-S9 copolymers in small scale (25 g).

Copolymer	peak area integration					
	CL monomer		b	c	g	a, d, f, e
	2.6 ppm	4.2 ppm				
PLC_S1	nd	nd	200.00	49.25	51.17	817.65
PLC_S2	nd	nd	100.00	35.72	36.66	447.66
PLC_S3	nd	nd	236.41	139.81	139.15	1346.47
PLC_S4	nd	nd	200.00	145.91	157.82	1085.20
PLC_S5	nd	nd	200.00	145.81	169.49	1087.09
PLC_S6	nd	nd	168.09	155.99	158.26	1120.51
PLC_S7	nd	nd	163.21	165.98	168.23	1156.35
PLC_S8	nd	nd	159.52	165.47	166.46	1114.68
PLC_S9	nd	nd	151.40	157.76	158.22	1072.57

These results confirmed that in the copolymer chain microstructure consist of L-lactide unit and ε-caprolactone unit. However, the ^{1}H-NMR spectrum of crude PLC_S1 copolymer at the reaction time of 2 hours as shown in Figure 3.2 has the peak at δ = 4.2 and 2.6 ppm corresponding to -O-C$\underline{H_2}$-CH_2- and -CO-C$\underline{H_2}$-CH_2- in caprolactone monomer unit respectively. At the longer reaction times, for example reaction times reaching 72 hours, the peak at δ = 4.2 and 2.6 ppm were disappeared as shown in Figure 3.4 because of polymerization of ε-caprolactone monomer increase and the copolymerization reaction goes to completion.

Figures 3.3 and 3.5 show the ^{1}H-NMR spectra of purified PLC_S1 and PLC_S8 copolymers respectively that similar to the ^{1}H-NMR spectra of crude PLC copolymers. The peak at δ = 4.2 and 2.6 ppm were disappeared because residual ε-caprolactone monomer was eliminated in the purification step *via* re-precipitation in cold methanol.

3.1.1.2 Copolymer Composition Analysis by ^{1}H-NMR Spectroscopy

Since the area under a ^{1}H-NMR peaks is directly proportional to the number of protons which it arises from, it follows that, in the case of a copolymer, and the relative peak areas of the respective protons can be used to calculate the copolymer composition. For the PLC 50:50 copolymers synthesized in this work, the results of these calculations are given in Table 3.6 with the final copolymer compositions being compared alongside the initial comonomer feeds.

Sample Calculation :

From Figure 3.3 and Table 3.5 the composition of the pure PLC_S1, comonomer mole ratio 50:50, sample was calculated from the relative peak area integrations of the methine proton (δ = 5.0 – 5.3 ppm) and ε-methylene protons (δ = 4.0 – 4.2 ppm) in the L-Lactide and ε-caprolactone units respectively.

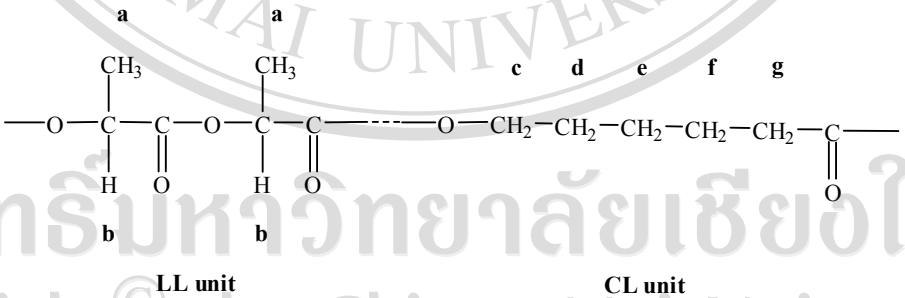

peak integration of methine protons	:	peak integration of ε-methylene protons
(2 protons / LL unit)		(2 protons / CL unit)
200.00	:	49.25

therefore

copolymer composition = LL : CL

= 200.00 / 2 : 49.25 / 2

= 100.00 : 24.625

= 80.2 : 19.8 (mole%)

This comonomer mole ratio of 80.2:19.8 mole% in the final copolymer composition can be compared with the 50:50 mole% ratio in the initial comonomer feed.

Table 3.6 Comparison of the initial comonomer feeds with the final copolymer compositions of the PLC copolymers in small scale (25 g).

Copolymer	**Initial comonomer feeds LL:CL (mole%)**	**Final copolymer compositions LL:CL (mole%)**
PLC_S1	49.9:50.1	80.2:19.8
PLC_S2	50.0:50.0	73.7:26.3
PLC_S3	50.0:50.0	62.8:37.2
PLC_S4	50.0:50.0	57.8:42.2
PLC_S5	50.1:49.9	57.8:42.2
PLC_S6	50.0:50.0	51.9:48.1
PLC_S7	50.0:50.0	49.6:50.4
PLC_S8	50.0:50.0	49.1:50.9
PLC_S9	50.0:50.0	49.0:51.0

As the results in Table 3.6, the L-lactide tended to polymerize preferentially in the initial reaction time, due to its much greater reactivity, resulting in PLC

copolymers which differed in composition from the initial comonomer feed. When increasing the reaction time, polymerization of ε-caprolactone increase; as a result, PLC copolymers have the final copolymer composition close to that of the monomer feed ratio. Thus, it can be concluded that PLC copolymer was successfully copolymerized approximately at 48 hours.

3.1.1.3 Molecular Weight Determination by GPC

The molecular weight ($\overline{M}_n$ and $\overline{M}_w$) and polydispersities (PD = $\overline{M}_w$ / $\overline{M}_n$) of the crude and purified copolymers were determined by GPC as shown in Tables 3.7 and GPC curves in Figures 3.6 - 3.7 respectively.

The molecular weight determined by GPC is not absolute values. This was due to the calibration of the GPC by polystyrene standards, which only give a relative value of the polymer molecular weight. The GPC results were therefore used as a qualitative tool to check the peak sharp, molecular weight distribution and the change in molecular weight.

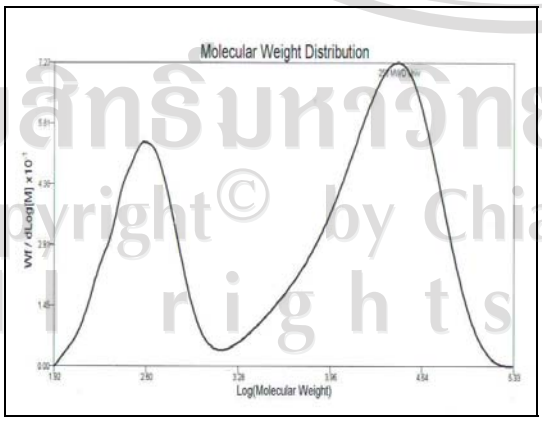

(a)

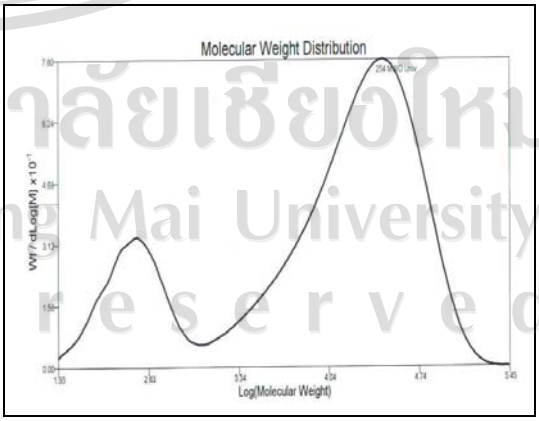

(b)

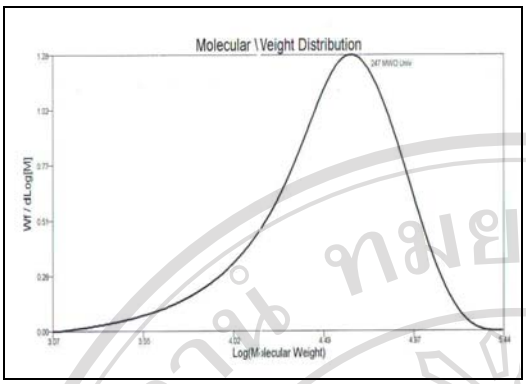

(c)

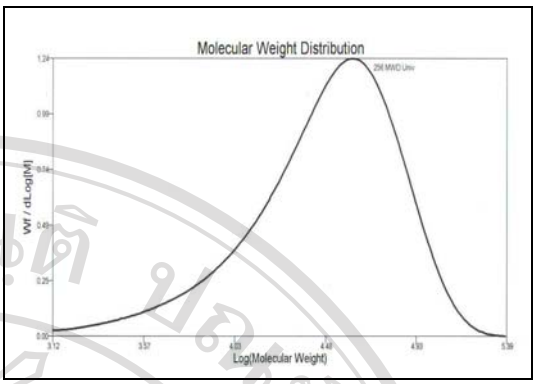

(d)

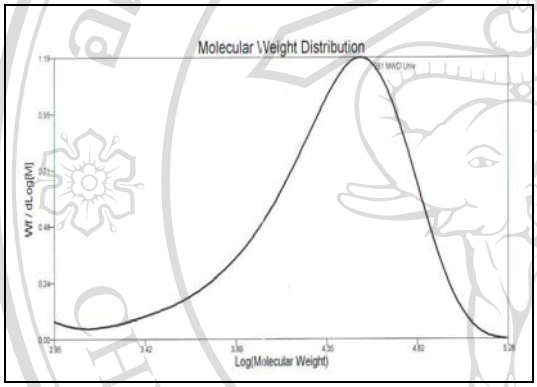

(e)

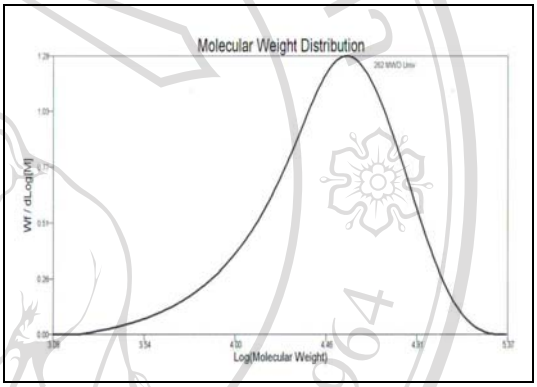

(f)

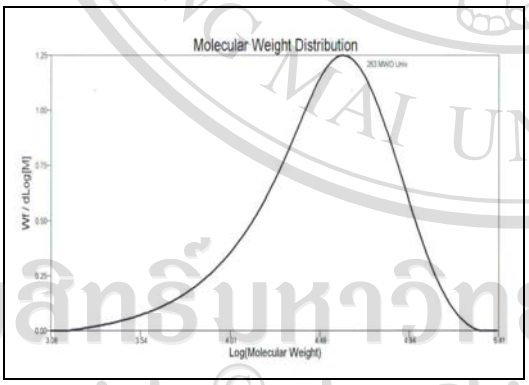

(g)

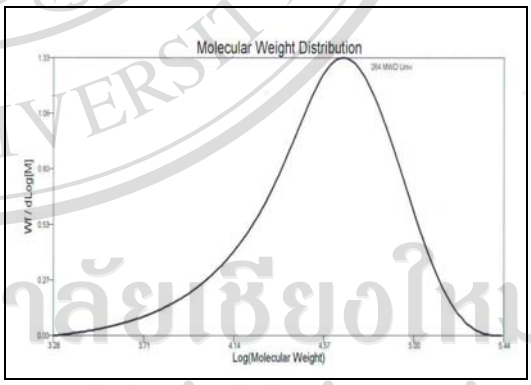

(h)

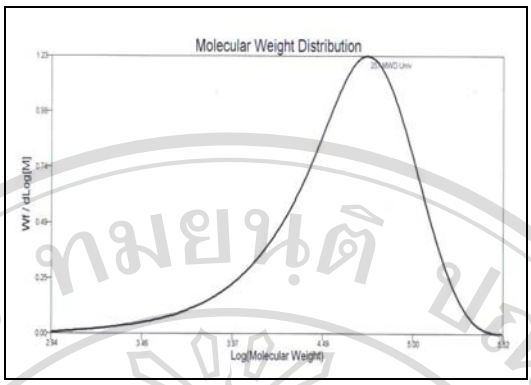

(i)

Figure 3.6 GPC curves of crude PLC copolymers (a) PLC_S1 (b) PLC_S2 (c) PLC_S3 (d) PLC_S4 (e) PLC_S5 (f) PLC_S6 (g) PLC_S7 (h) PLC_S8 and (i) PLC_S9 in small scale (25 g).

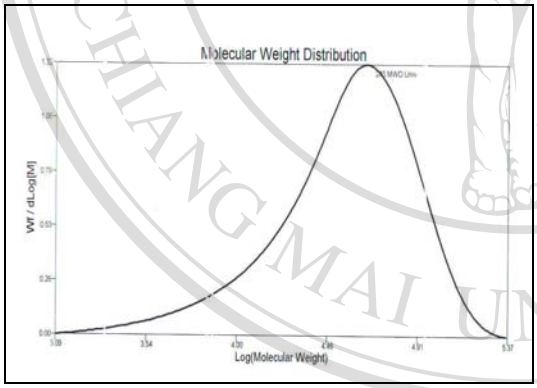

(a)

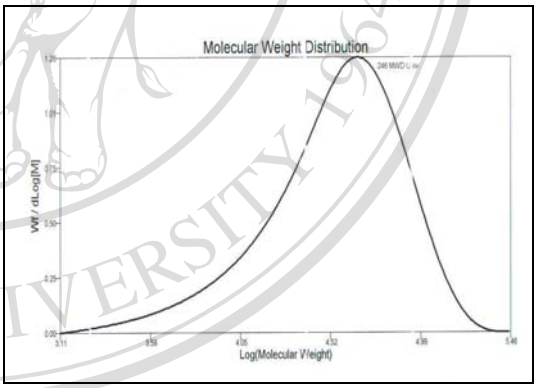

(b)

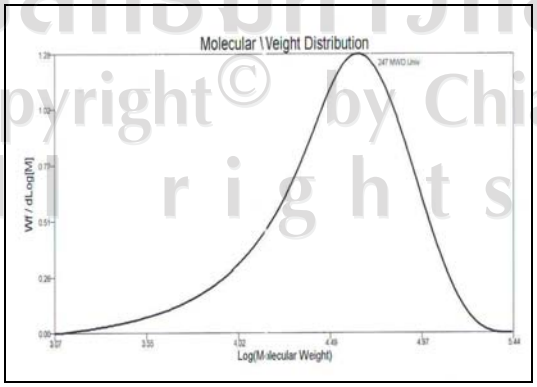

(c)

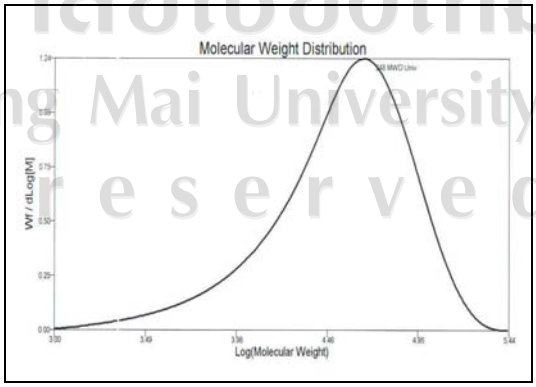

(d)

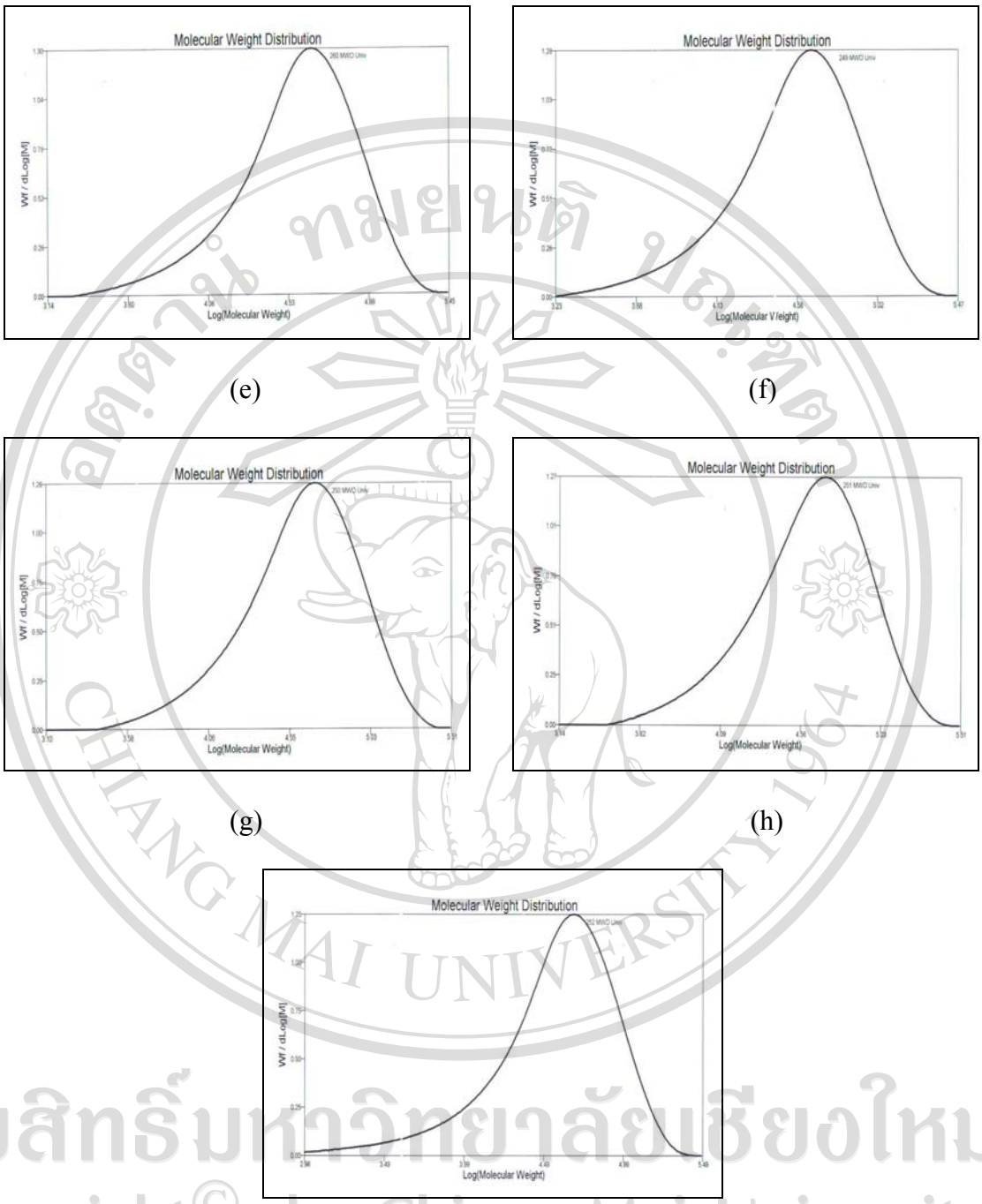

Figure 3.7 GPC curves of purified PLC copolymers (a) PLC_S1 (b) PLC_S2 (c) PLC_S3 (d) PLC_S4 (e) PLC_S5 (f) PLC_S6 (g) PLC_S7 (h) PLC_S8 and (i) PLC_S9 in small scale (25 g).

Table 3.7 GPC molecular weight data of crude and purified PLC copolymers in small scale (25 g).

Copolymer	Crude			Pure		
	$\overline{M}_n$	$\overline{M}_w$	**PD** ($\overline{M}_w / \overline{M}_n$)	$\overline{M}_n$	$\overline{M}_w$	**PD** ($\overline{M}_w / \overline{M}_n$)
PLC_S1	951	19,630	20.64	23,080	45,370	1.97
PLC_S2	1,272	22,990	18.07	21,990	44,730	2.03
PLC_S3	17,300	32,420	1.87	22,310	44,330	1.99
PLC_S4	18,660	39,430	2.11	20,940	45,350	2.17
PLC_S5	13,340	31,560	2.37	26,120	48,340	1.85
PLC_S6	20,770	38,090	1.83	24,710	47,520	1.92
PLC_S7	21,320	40,690	1.91	28,620	52,680	1.84
PLC_S8	26,520	47,780	1.80	28,920	52,480	1.81
PLC_S9	23,470	53,970	2.30	20,850	48,950	2.35

Figure 3.8 shows the effect of the reaction time on the weight-average molecular weight ($\overline{M}_w$) of crude and purified PLC copolymers. For crude PLC copolymers, in the initial reaction time of 2 to 4 hours have low $\overline{M}_w$ and high PD because in the polymerization system has the residue monomers and oligomers. Moreover, in Figures 3.6 (a) and 3.6 (b), exhibit 2 peaks in the GPC curve. This clearly shown that in the polymerization system consist of different molecular weight with the mixture of short and long polymer chains of PLC copolymers. Rise of the reaction time caused higher $\overline{M}_w$ and lower PD.

For the purified PLC copolymers, it has high $\overline{M}_w$ in the initial reaction time (<12 hours) and slightly increase due to residual monomer and oligomers were

eliminated in the purification step *via* re-precipitation in cold methanol. Therefore, residual monomers in the synthesized polymer have profound effect on the average molecular weight by GPC method. Finally, it was found that the PLC_S7 copolymer gives the highest $\overline{M}_w$ (40,000-50,000) with low PD (1.8-2.2) that suitable for either fiber or tube fabrication.

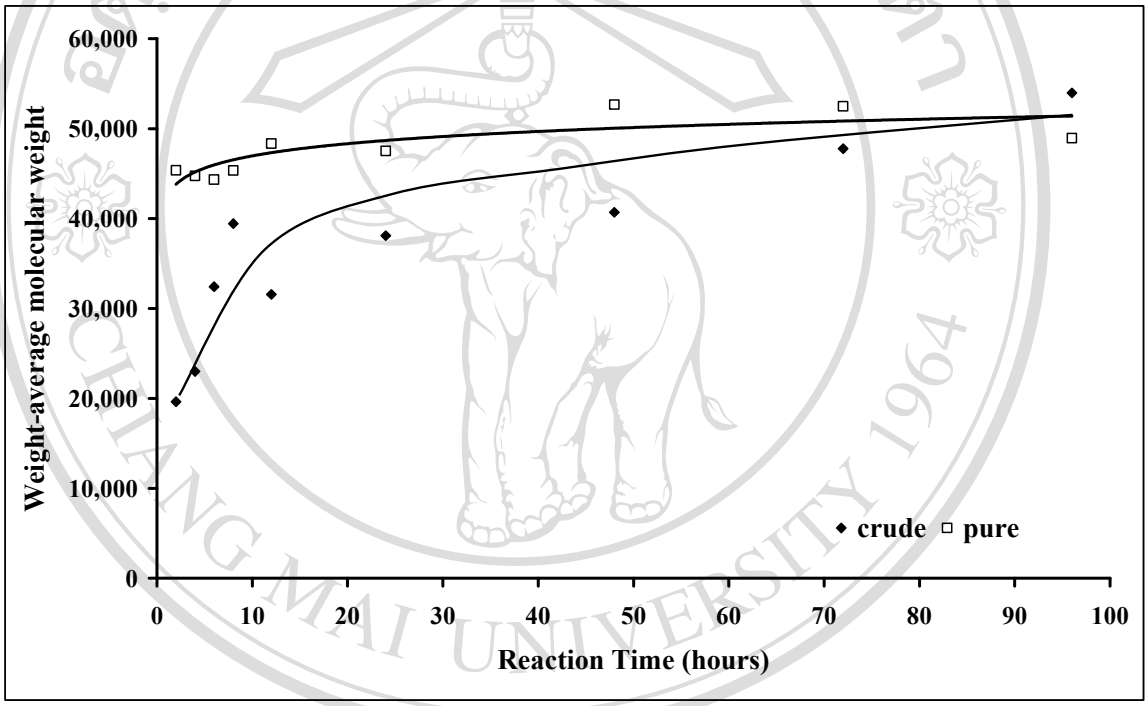

Figure 3.8 Weight-average molecular weight-time profile of crude and purified PLC copolymers in small scale (25 g).

3.1.1.4 Thermal Characterization by DSC Analysis

The DSC thermograms are shown in Figures 3.9 – 3.10 and the results compared in Table 3.8. From the DSC results in Table 3.8, the values of glass transition temperature (T_g), crystalline temperature (T_c) and melting temperature (T_m) of first run and second run tend to follow copolymer composition. For example, the

initial period of polymerization (<48 hours), copolymer showed a T_m because of the higher L-lactide content which has high degree of crystalline, but this subsequently decreased as the *ε*-caprolactone content increased with increasing reaction time. Because of the structure of *ε*-caprolactone consists of five methylene groups which show flexible properties. Furthermore, the values of ΔH_m decrease with increasing structural irregularity. Finally, the final copolymer composition is nearly 50:50 mole%, the absence of T_m peak of PLC copolymer was obtained. The morphology of PLC copolymers was amorphous at 48 hours.

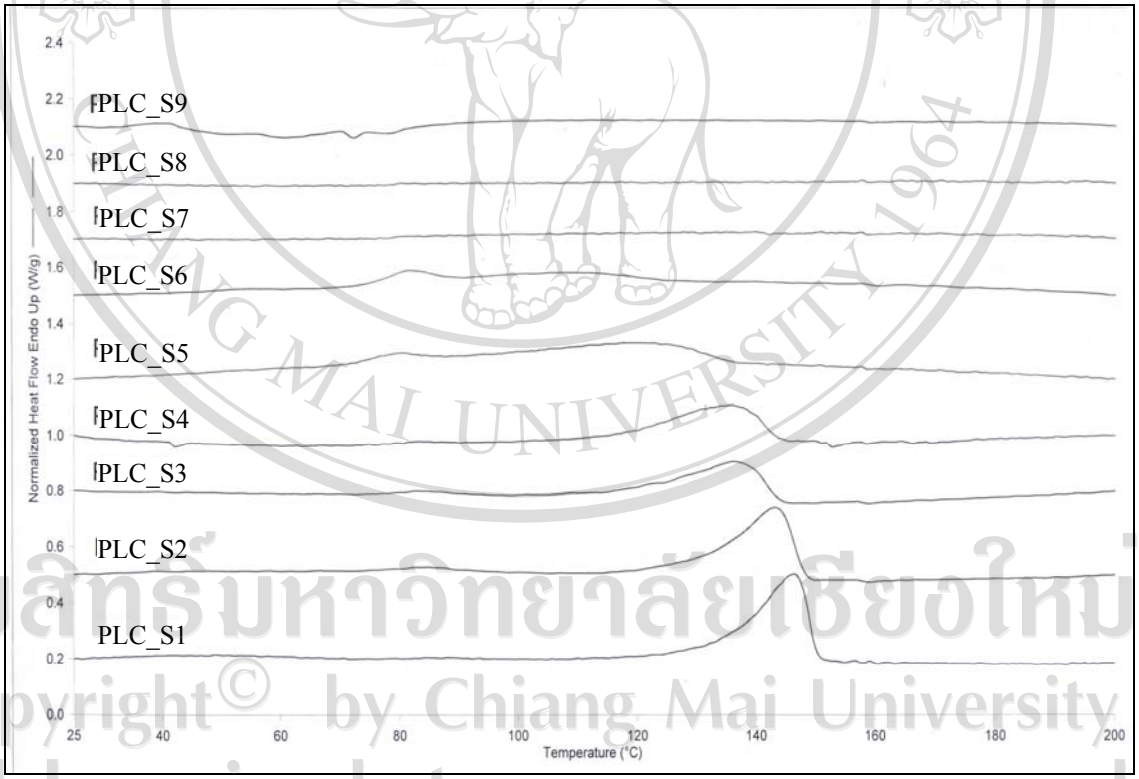

Figure 3.9 Comparison of the DSC thermograms first run of PLC copolymers in small scale (25 g).

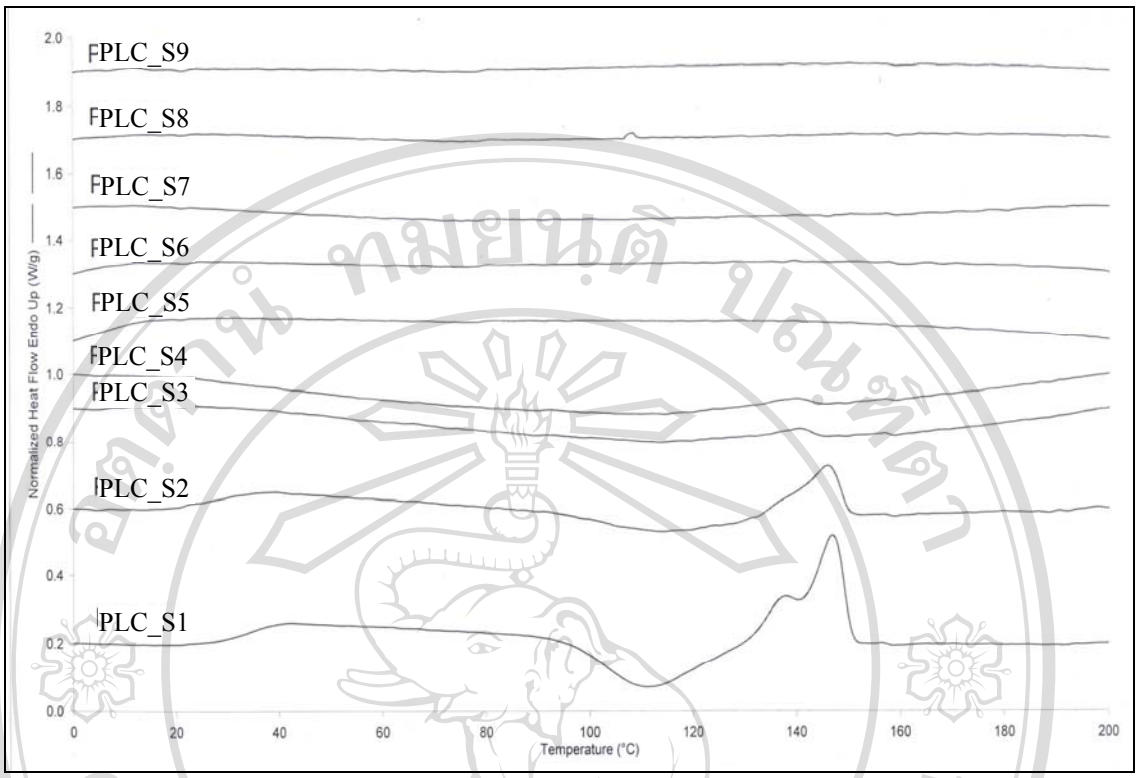

Figure 3.10 Comparison of the DSC thermograms second run of PLC copolymers in small scale (25 g).

Table 3.8 DSC results of the PLC copolymers in small scale (25 g).

Copolymer	DSC 1st run				DSC 2nd run				
	T_g[a] (°C)	T_c[b] (°C)	T_m[c] (°C)	ΔH_m (J/g)	T_g[a] (°C)	T_c[b] (°C)	ΔH_c (J/g)	T_m[c] (°C)	ΔH_m (J/g)
PLC_S1	26.9	nd	146.0	22.4	32.8	111.2	17.8	147.0	17.6
PLC_S2	20.8	nd	143.0	19.8	25.2	113.7	7.9	145.8	7.5
PLC_S3	9.9	nd	136.2	14.7	10.0	113.7	1.5	140.3	0.9
PLC_S4	nd	nd	135.7	12.7	nd	114.2	2.8	139.7	0.8
PLC_S5	nd	nd	117.8	15.4	nd	nd	nd	nd	nd
PLC_S6	nd	nd	81.5	9.4	nd	nd	nd	nd	nd
PLC_S7	nd	nd	nd	nd	nd	nd	nd	nd	nd
PLC_S8	nd	nd	nd	nd	nd	nd	nd	nd	nd
PLC_S9	nd	nd	nd	nd	nd	nd	nd	nd	nd

[a]T_g taken as the mid-point of the glass transition

[b]T_c taken as the peak temperature of the crystalline range

[c]T_m taken as the peak temperature of the melting range

nd = not detected or difficult to estimate

Interestingly, these experimental glass transition temperatures, T_g, for the PLC random copolymers can be reasonably well described by the Fox Equation:

$$\frac{W_{LL}}{T_{g_{LL}}} + \frac{W_{CL}}{T_{g_{CL}}} = \frac{1}{T_{g_{PLC}}} \qquad \text{.....(1)}$$

where W_{LL} and W_{CL} are the respective weight fraction of the L-lactide and ε-caprolactone monomer units in the copolymer, as calculated from the corresponding mole fractions m_{LL} and m_{CL} obtained from the ^{1}H-NMR spectra, as determined in section 3.1.1.2.

Similarly, $T_{g_{LL}}$ and $T_{g_{CL}}$ are the respective T_g (K) values of the PLL (65°C = 338 K) and PCL (-60°C = 213 K) homopolymers respectively. The predicted T_g values from Fox Equation for PLC copolymers are shown in Table 3.9. Agreement between the observed and calculated values is seen to be reasonably good considering that the Fox Equation only takes account of composition, not the chain microstructure.

Table 3.9 The calculated values of T_g from Fox Equation for the PLC copolymers in small scale (25 g).

Copolymer	Final copolymer compositions LL:CL (mole%)	Calculated values of T_g (°C)
PLC_S1	80.2:19.8	35.4
PLC_S2	73.7:26.3	26.3
PLC_S3	62.8:37.2	11.7
PLC_S4	57.8:42.2	5.2
PLC_S5	57.8:42.2	5.2
PLC_S6	51.9:48.1	-2.3
PLC_S7	49.6:50.4	-5.1
PLC_S8	49.1:50.9	-5.7
PLC_S9	49.0:51.0	-5.8

3.1.1.5 Mechanical Properties Determination by Tensile Testing

In this study, mechanical properties such as tensile strength (stress at break), %elongation (strain) at break and Young's modulus were determined with the Lloyds LPX+ Universal Mechanical Testing Machine. The PLC_S7 can be prepared by solvent casting method. The mechanical test results in the form of stress-strain curves are shown in Figure 3.11. Error analysis in testing usually is conducted by repetition of the measurement for at least 5 identical samples in order to the standard deviation in the measurement. The stress-strain curves for a given sample were reasonably consistent within an acceptable range of variation.

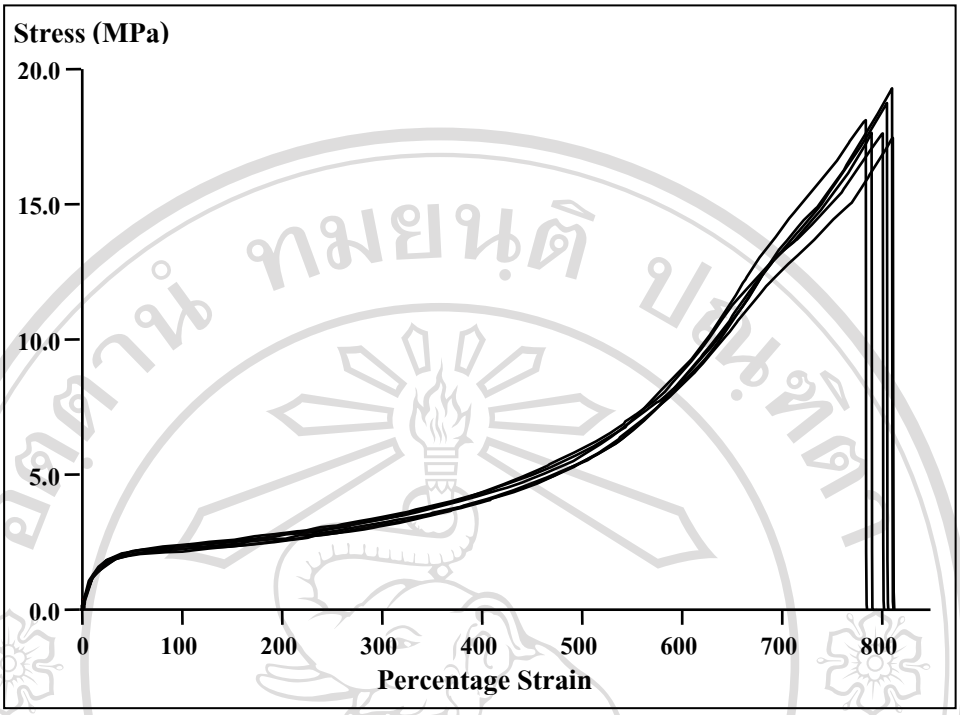

Figure 3.11 The stress-strain curve of PLC_S7 copolymers in small scale (25 g).

From the stress-strain curve, it was found that PLC_S7 copolymer had a tensile strength of 15.9±2.5 MPa, a strain at break of 810±54.7% and Young's modulus of 14.4±1.9 MPa. The PLC_S7 copolymer films showed low stress and high strain because the morphology of PLC_S7 copolymer was amorphous. These results meant PLC_S7 copolymer was soft and tough.

3.1.2 Effect of the Reaction Temperature on the Polymer Properties

To study the effect of the reaction temperature on the PLC 50:50 copolymer properties, polymerizations were carried out with the reaction temperature varying between 110 and 140°C at constant the monomer to initiator molar ratio ([M]:[I] = 100:0.01 mole%) and 0.1 mole% $SnOct_2$ catalyst. The ROP was carried out in bulk

for 48 hours. The influence of the reaction temperatures on the %yield, physical appearance, final copolymer composition and weight-average molecular weights of PLC copolymers are shown in Tables 3.10-3.11 and Figure 3.12.

Table 3.10 The effect of the reaction temperature on the %yield and physical appearance of PLC copolymers in small scale (25 g) using [M]:[I] molar ratio 100:0.01 mole%, 0.1 mole% $SnOct_2$ as a catalyst for 48 hours.

Copolymer	Reaction temperature (°C)	%yield	Physical Appearance
PLC_T1	110	87.39	translucent brittle solid
PLC_T2	120	90.11	transparent rubbery-like solid
PLC_T3	130	89.84	transparent yellow rubbery-like solid
PLC_T4	140	89.10	transparent brown rubbery-like solid

Table 3.11 The effect of reaction temperature on the final copolymer composition and weight-average molecular weights of PLC copolymers in small scale (25 g).

Copolymer	Reaction temperature (°C)	Final copolymer compositions LL:CL (mole%)	Weight-average molecular weight ($\overline{M}_w$)
PLC_T1	110	50.8 : 49.2	98120
PLC_T2	120	50.0 : 50.0	97440
PLC_T3	130	49.1 : 50.9	61040
PLC_T4	140	49.8 : 50.2	36500

From the results obtained, under examined conditions the optimum reaction temperature is 120°C. Below this temperature the reaction yield of PLC copolymers is relatively low (%yield < 87%). This probably due to the 110°C in bulk polymerization the viscosity of the polymerization system increased which reduced the rate of polymerization. On the other hand, a further increasing the reaction temperature (> 120°C) resulted in a decrease both %yield and molecular weight. Due to the transesterification reactions occurred above the optimum reaction temperature, the physical appearance of PLC copolymers was observed. The yellowish or dark brown colors occur from degradation products which are produced during the transesterification reactions. The transesterification reactions were studied by means of ^{13}C-NMR technique. The ^{1}H-NMR results, all of PLC copolymers have a final copolymer compositions close to that of the monomer feed ratio. Furthermore, from DSC results, the morphology of all PLC copolymers was amorphous.

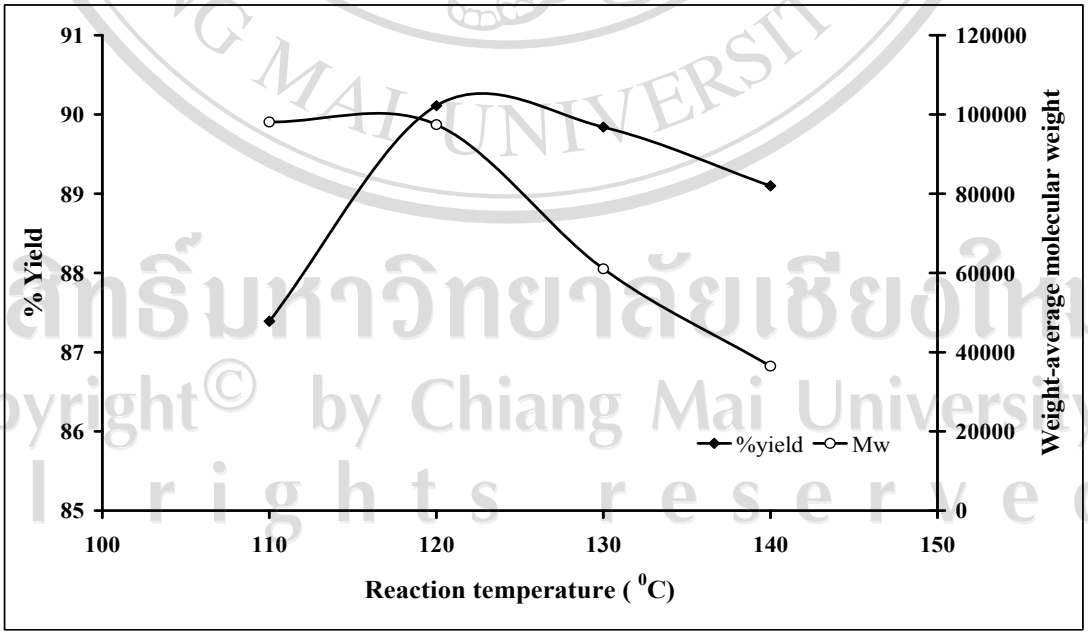

Figure 3.12 %Yield and weight-average molecular weight -temperature profile of PLC copolymers in small scale (25 g).

3.1.2.1 Carbon-13 Nuclear Magnetic Resonance Spectrometry (^{13}C-NMR)

3.1.2.1.1 ^{13}C-NMR Spectra and their Interpretations

The main propose of this ^{13}C-NMR study is to obtain microstructural information particularly on monomer sequence distribution of copolymers while ^{1}H-NMR unable to support. This is the fact that, in ^{13}C-NMR, the chemical shifts are spread over a wide range of over 200 ppm, as compared with the relatively narrow 10 ppm range in ^{1}H-NMR. Therefore, much smaller differences in chemical environment can be distinguished in ^{13}C-NMR making it a much more powerful technique than ^{1}H-NMR for studying copolymer microstructure, in particular monomer sequencing. However, it is not until the carbonyl carbon (C=O) region (165-175 ppm) of the spectrum is expanded, as described in the following section 3.1.2.1.2, that the differences in chain microstructure can be observed.

In this research project, 100 MHz ^{13}C-NMR spectra of the PLC copolymers were obtained using a Bruker Avace 100 MHz NMR spectrometer. Samples were prepared as deuterated chloroform ($CDCl_3$) solutions at room temperature, giving the spectra as shown in Figure 3.13.

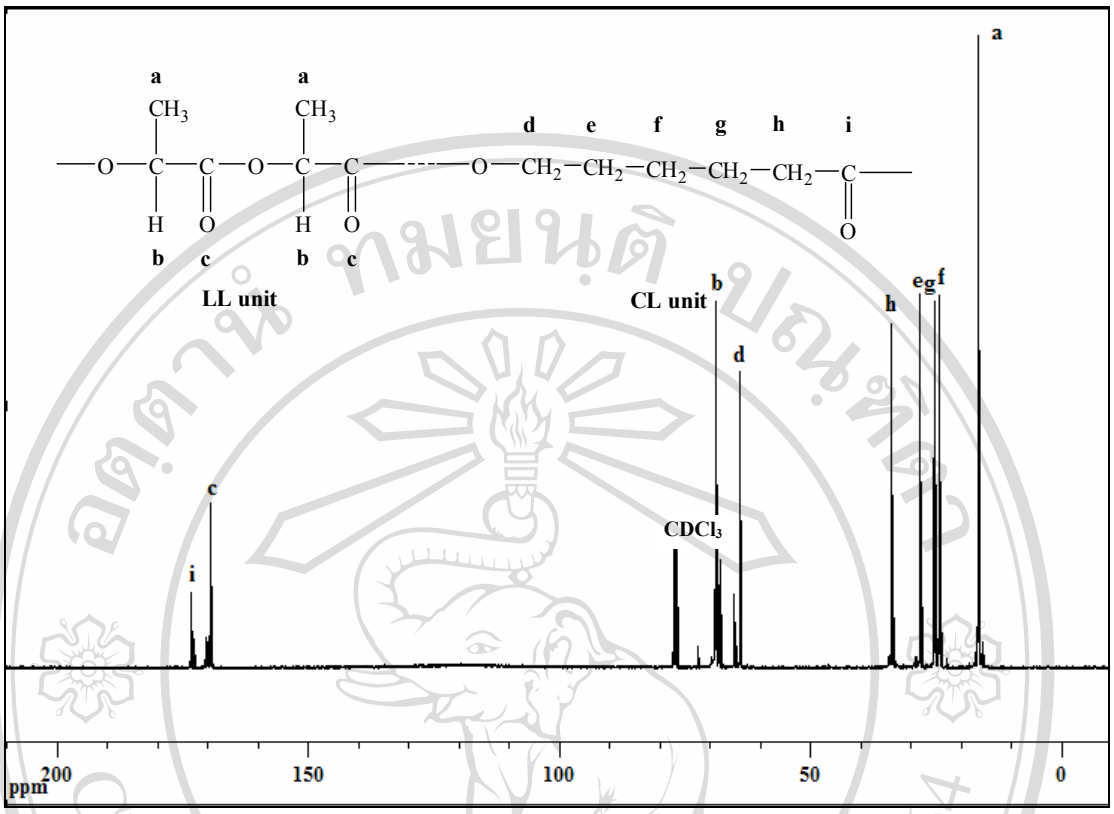

Figure 3.13 100 MHz ^{13}C-NMR spectrum of PLC copolymers in $CDCl_3$ as solvent in small scale (25 g).

3.1.2.1.2 Copolymers Chain Microstructure (Monomer Sequencing)

In ^{13}C-NMR copolyester spectra, the carbonyl C=O carbons signal have been shown to be especially sensitive to sequencing variations, much more so than the C-H carbons (methyl, methylene and methine). Therefore, it is the carbonyl region of the spectrum from δ = 165 – 175 ppm which provides the most information about the copolymer chain microstructures. When this carbonyl region is expanded, as shown in Figures 3.15-3.22, separate peaks due to the various triad sequences, such as *CCC*, *LCC*, *CCL*, *LCL*, *CLC*, *CLL*, *LLC* and *LLL* (where *L* = L-lactate unit (half of L-lactide) and *C* = ε-caprolactone unit), can be identified with reference to previous

work. [71-76] Examples of the triad structures to which these sequence designations correspond are given in Figure 3.14. Each peak comes from the C=O carbon of the middle unit and is influenced by the neighboring units on either side. By conventional, each unit is written with the main chain oxygen atom, -O-, on the left and the carbonyl group, -C(=O)-, on the right. Also, as mentioned previously in the case of diester monomers such as L-lactide, only the ***half-unit*** is taken for *L* in order to take into account the effect of transesterification. Thus, the peak from the triad sequence *CLC* (below), which can only arise via transesterification, becomes a useful indicator that transesterification has occurred.

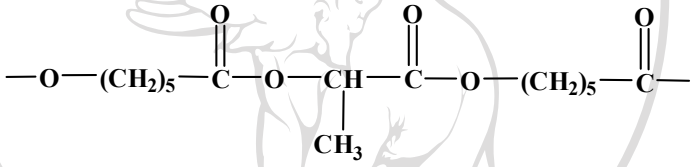

C **L** **C**

However, it must also be said that the actual extent to which transesterification has occurred is impossible to quantify since there are many other triads that are identical both before and after transesterification. The only conclusion that can be draw with any certainly is that transesterification does occur, at least to some extent, and that its effect is to increase the degree of randomness of the monomer sequencing.

Triad Sequences	Corresponding Structures
CCC	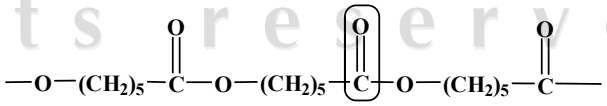
LCC	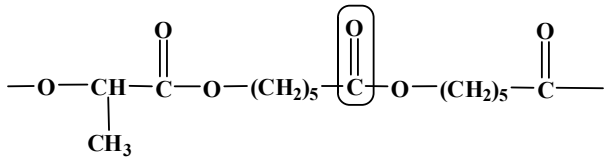

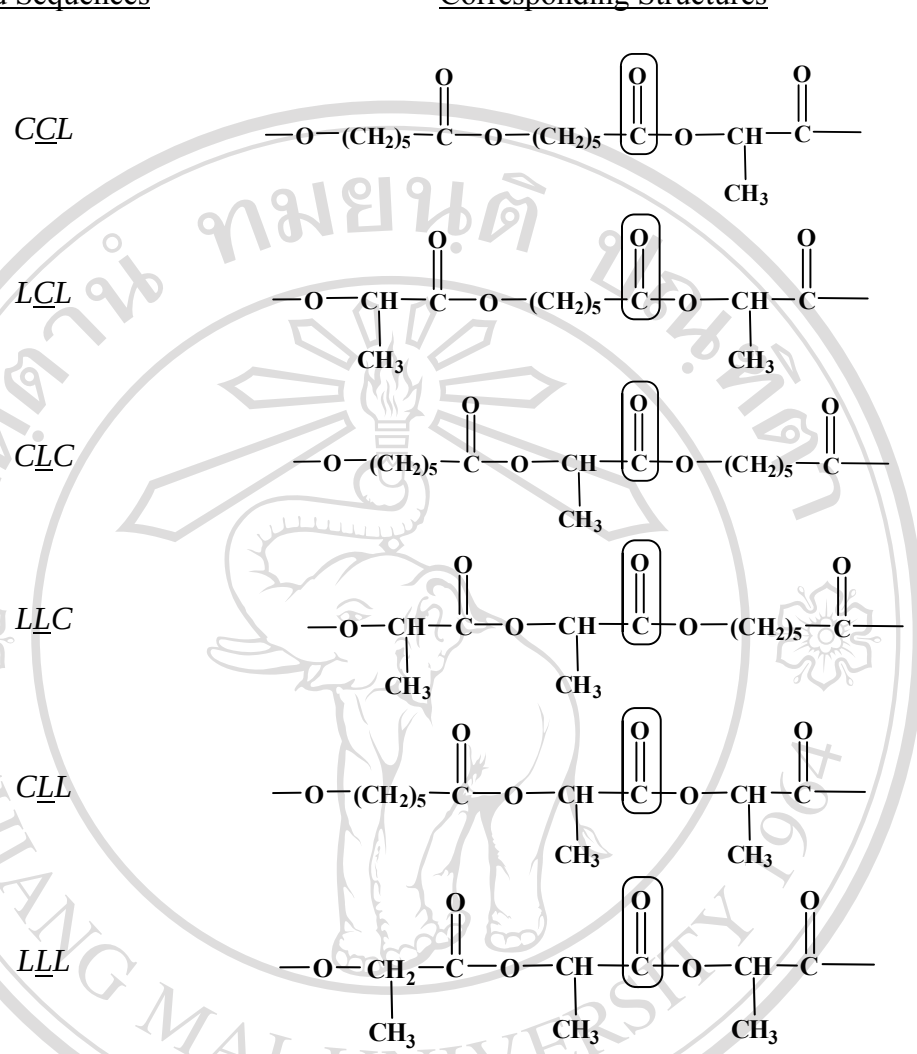

Figure 3.14 Triad sequences and corresponding structures showing the carbonyl groups responsible for the respective chemical shift assignments.

The number-average lengths of the *C* and *LL* sequences were determined on the basis of the attribution of the peaks in the ^{13}C-NMR spectrum, as previously described by Kricheldorf *et al.* [77] and Kasperczyk *et al.* [78]. In addition, two types of transesterification reaction were recognized, referred to as the first and second modes [79], in which a lactidyl unit (*LL*) undergoes bond cleavage leading to the

formation of anomalous sequences of -*CLC*- and -*CLLLC*-, both with an odd number of half-lactidyl (*L*) units. Thus, transesterification plays an important role in the redistribution of monomer sequences, thereby influencing the microstructure. These odd-number *L* sequences cannot be formed by the opening of LA rings alone during the growth reaction of the copolymer chains. Figure 3.15 shows examples of the ^{13}C-NMR carbonyl carbon region between 175.0-168.0 ppm, includes peak assignments as reported by Kasperczyk *et al.*[79]. This second mode transesterification coefficient is defined as follow:

$$T_{II} = [CLC]/[CLC]_R \quad (2)$$

where [*CLC*] is the experimentally determined concentration of the *CLC* sequences from the ^{13}C-NMR spectrum and $[CLC]_R$ is the theoretical concentration for completely random chains as calculated via Bernoulli statistics:

$$[CLC]_R = k^2/(k+1)^3 \quad (3)$$

where $k = [C]/[L]$. The experimental number-average lengths of the lactidyl (l^e_{LL}) and caproyl (l^e_C) sequences are calculated from the following equations:

$$l^e_{LL} = \frac{1}{2}\left[\frac{I_{LLL}+(I_{LLC}+I_{CLL})/2}{(I_{LLC}+I_{CLL})/2+I_{CLC}}+1\right] \quad (4)$$

$$l^e_C = \left[\frac{I_{CCC}+I_{LCC}}{I_{CCL}+I_{LCL}}+1\right] \quad (5)$$

In comparison, the number-average lengths of the lactidyl and caproyl sequences for chains with a random distribution of units, as would be obtained by complete transesterification via the first and second modes, may also be calculated from the following equations:

$$l_{LL}^{R} = (k+1)/2k \quad (6)$$

$$l_{C}^{R} = k+1 \quad (7)$$

Consequently, the degree of randomness (R) of the copolymer chains is given by:

$$R = l_{LL}^{R}/l_{LL}^{e} = l_{C}^{R}/l_{C}^{e} \quad (8)$$

The value of the randomness coefficient R ranges from 0 to 1 for diblock and completely random copolymers respectively. Anomalous values above 1 indicate an increase in the concentration of alternating, i.e. *CLC*, sequences.

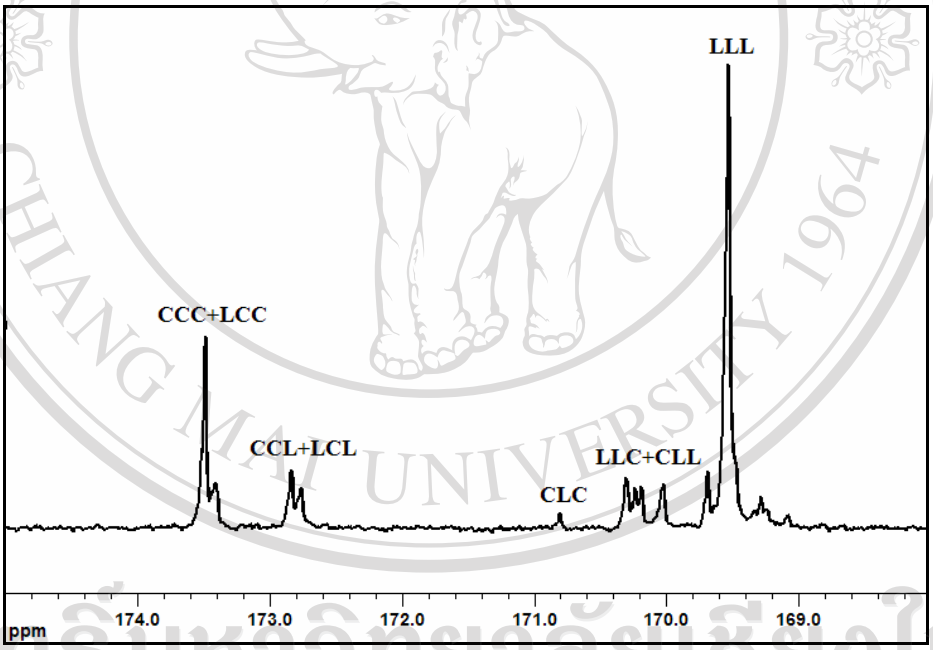

Figure 3.15 Expanded carbonyl region of the 100 MHz ^{13}C-NMR spectrum of crude PLC_T1 in small scale (25 g).

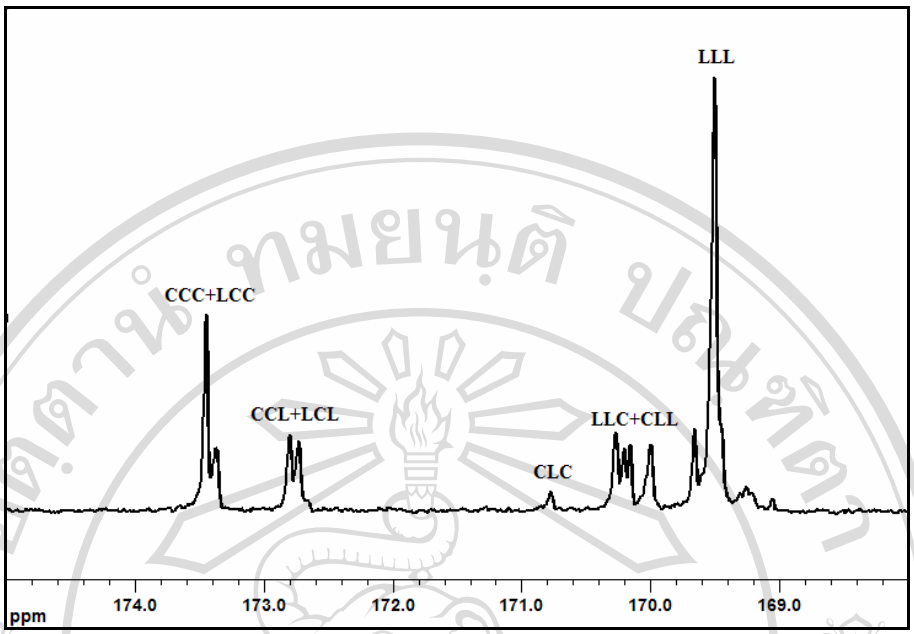

Figure 3.16 Expanded carbonyl region of the 100 MHz ^{13}C-NMR spectrum of crude PLC_T2 in small scale (25 g).

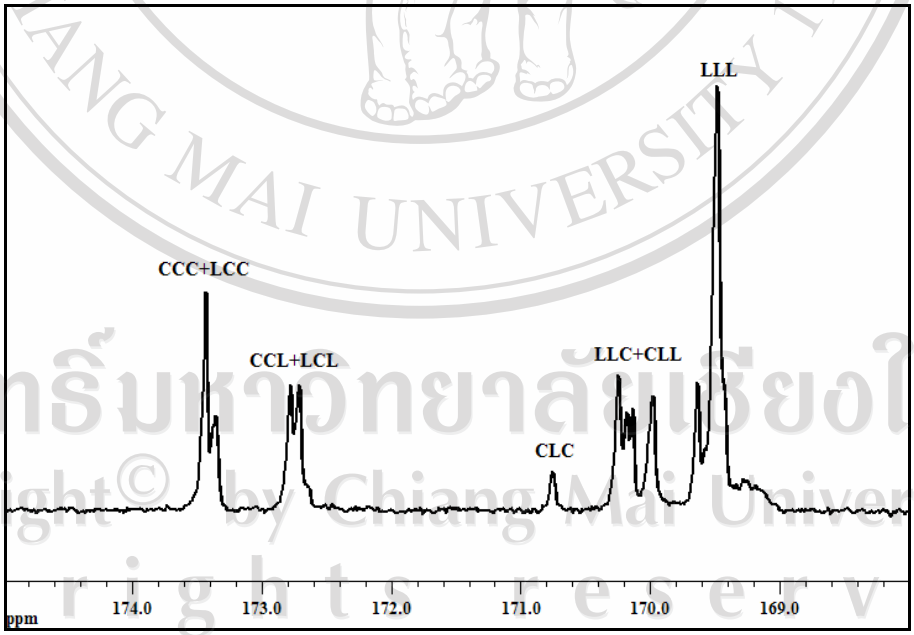

Figure 3.17 Expanded carbonyl region of the 100 MHz ^{13}C-NMR spectrum of crude PLC_T3 in small scale (25 g).

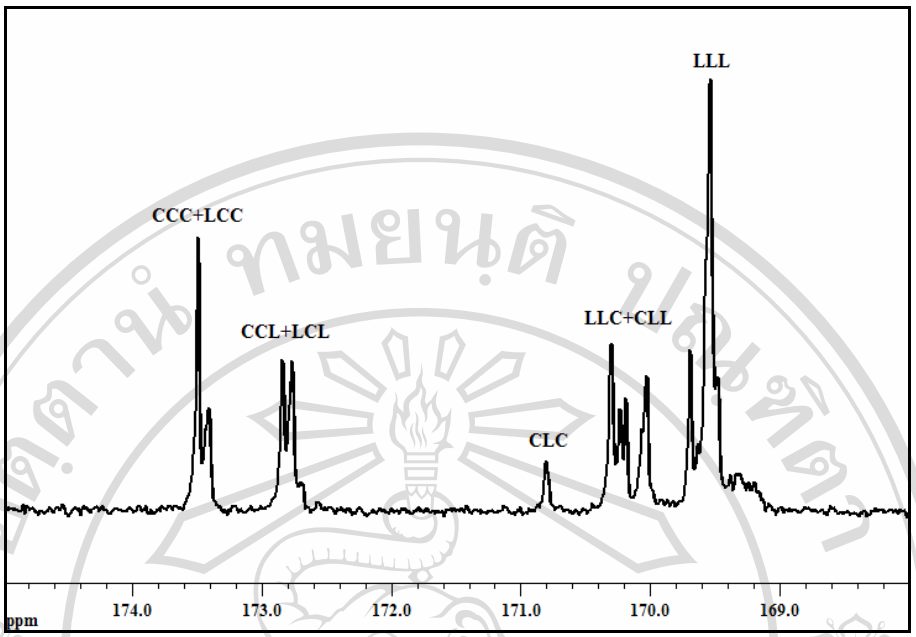

Figure 3.18 Expanded carbonyl region of the 100 MHz ^{13}C-NMR spectrum of crude PLC_T4 in small scale (25 g).

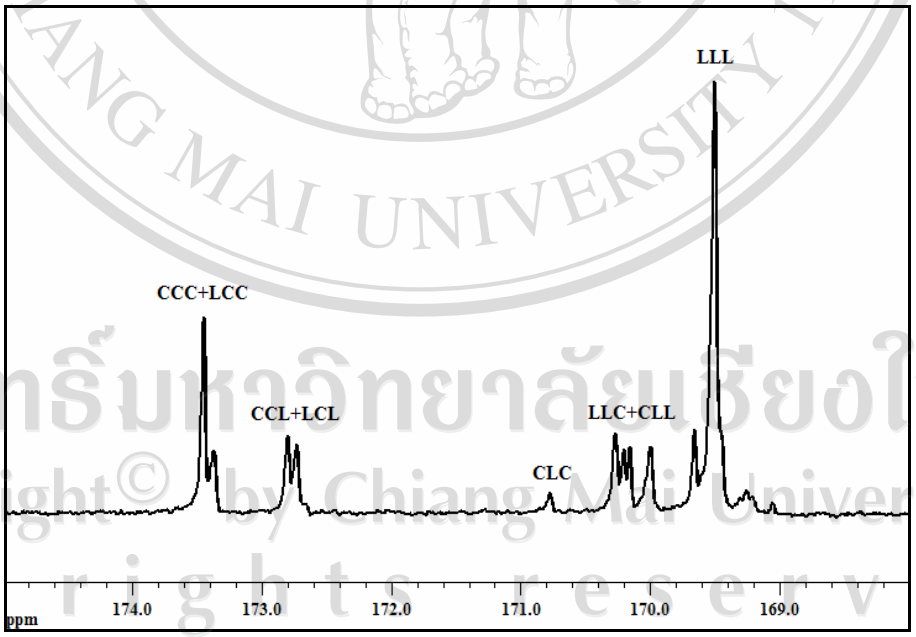

Figure 3.19 Expanded carbonyl region of the 100 MHz ^{13}C-NMR spectrum of pure PLC_T1 in small scale (25 g).

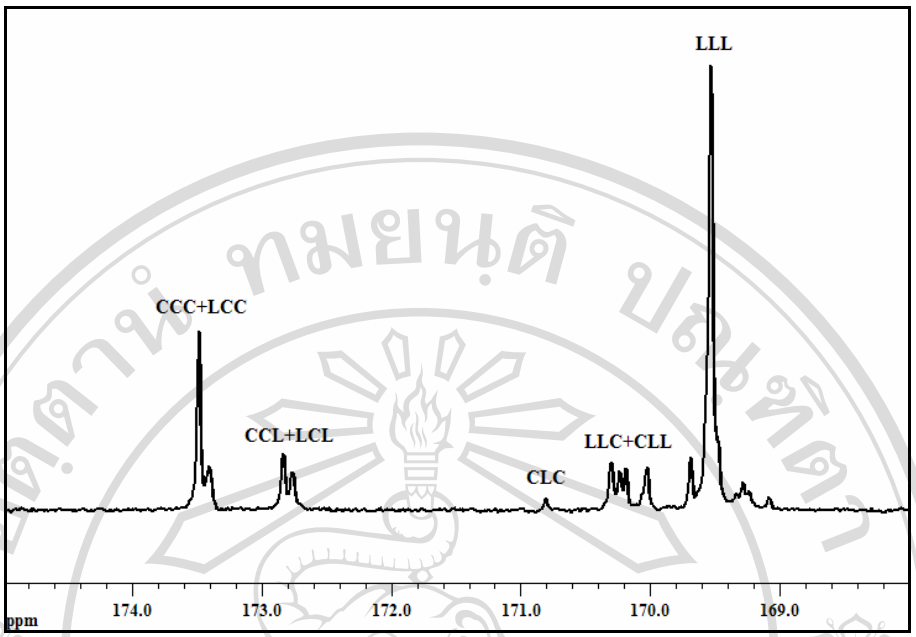

Figure 3.20 Expanded carbonyl region of the 100 MHz ^{13}C-NMR spectrum of pure PLC_T2 in small scale (25 g).

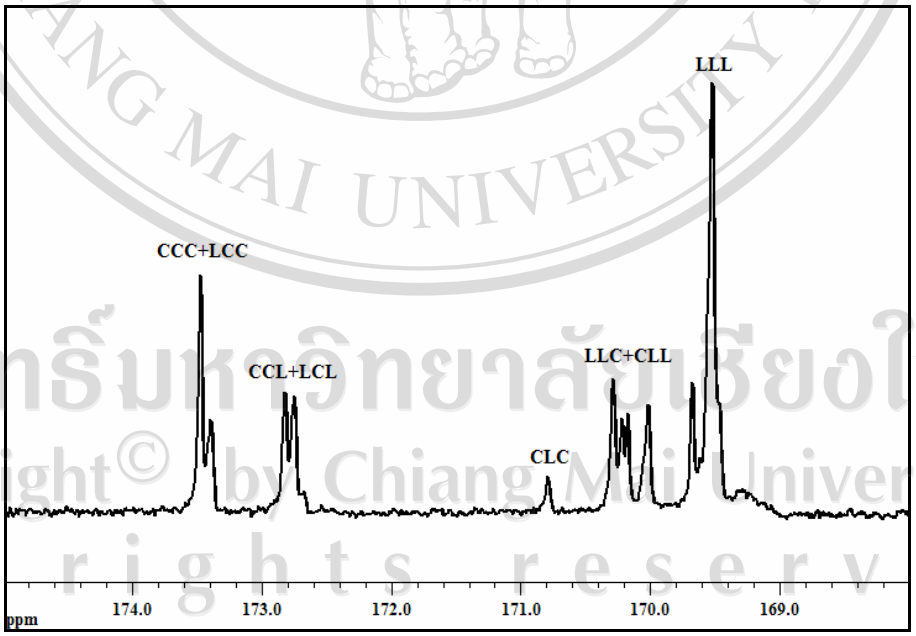

Figure 3.21 Expanded carbonyl region of the 100 MHz ^{13}C-NMR spectrum of pure PLC_T3 in small scale (25 g).

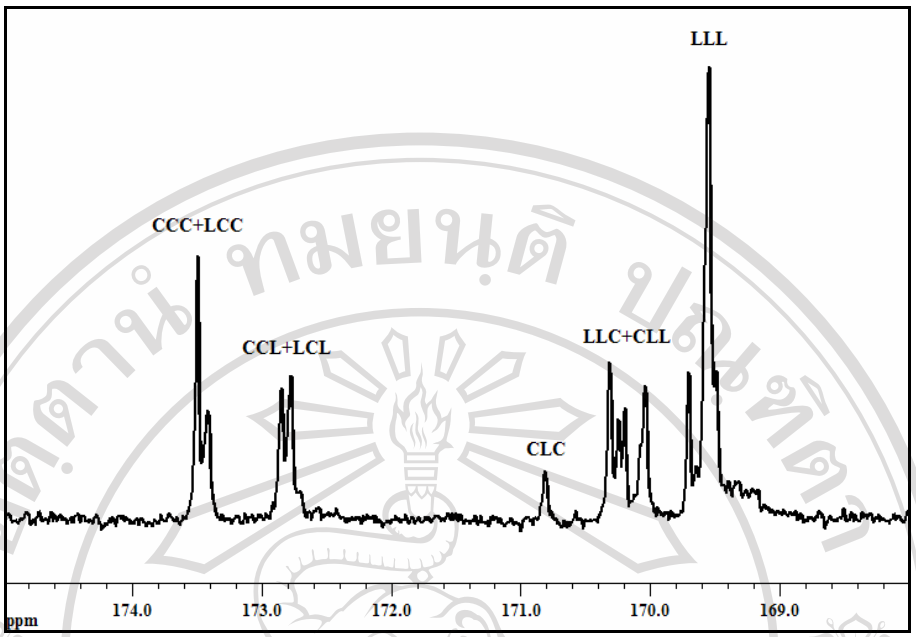

Figure 3.22 Expanded carbonyl region of the 100 MHz ^{13}C-NMR spectrum of pure PLC_T4 in small scale (25 g).

Table 3.12 Intensities of the various triad peaks of PLC copolymers in small scale(25g).

Copolymer	$I_{CCC+LCC}$	$I_{CCL+LCL}$	I_{CLC}	$I_{LLC+CLL}$	I_{LLL}
PLC_T1 crude	1.00	0.51	0.05	0.81	3.21
PLC_T2 crude	1.00	0.57	0.06	1.05	3.30
PLC_T3 crude	1.00	0.92	0.14	1.48	2.90
PLC_T4 crude	1.00	0.98	0.17	1.57	2.97
PLC_T1 purified	1.00	0.55	0.02	1.04	2.98
PLC_T2 purified	1.00	0.50	0.05	0.79	3.14
PLC_T3 purified	1.00	0.84	0.11	1.38	2.78
PLC_T4 purified	1.00	0.95	0.12	1.51	2.98

Table 3.13 Characterization results from ^{13}C-NMR of PLC copolymers in small scale (25 g).

Copolymer	F_{LL} [a]	l_{LL}^{e} [b]	l_{C}^{e} [c]	l_{LL}^{R} [d]	l_{C}^{R} [e]	R [f]	T_{II} [g]
PLC_T1 crude	50.8	4.4725	2.9608	1.4375	1.4843	0.3214	0.697
PLC_T2 crude	50.0	3.7692	2.7544	1.5000	1.5000	0.3980	0.810
PLC_T3 crude	49.1	2.5682	2.0870	1.5740	1.5183	0.6129	1.824
PLC_T4 crude	49.8	2.4660	2.0204	1.5161	1.5040	0.6148	2.277
PLC_T1 purified	49.5	3.7407	2.8180	1.5406	1.5101	0.4118	0.265
PLC_T2 purified	49.1	4.4719	3.0000	1.5740	1.5183	0.3520	0.651
PLC_T3 purified	48.3	2.6688	2.1905	1.6433	1.5352	0.6157	1.389
PLC_T4 purified	48.4	2.6343	2.0526	1.6344	1.5331	0.6204	1.522

[a] F_{LL} L-lactide mole fraction in copolymer from ^{1}H-NMR.

[b] l_{LL}^{e} experimental average length of lactidyl blocks.

[c] l_{C}^{e} experimental average length of caproyl blocks.

[d] l_{LL}^{R} calculated average length of lactidyl blocks.

[e] l_{C}^{R} calculated average length of carproyl blocks.

[f] R degree of randomness.

[g] T_{II} transesterification coefficient.

As mentioned previously, the ^{13}C-NMR, carbonyl carbon region between 168-175 ppm provides valuable information about the sequence distribution of the caproyl (*C*) and lactidyl (*L*) units in the copolymer chains. Since the spectra of the PLA copolymers in this work as shown in Figures 3.15-3.22 show not only peaks due to

the *LLL* and *CCC* sequences but also intermediate peaks due to *CCL, LCL, CLL, LLC* and *CLC* sequences, it confirms that copolymerization has indeed occurred. It is interesting to note in Table 3.13 that l_{LL}^{e} was slightly higher than l_{C}^{e} in the PLC copolymers. This observation is consistent with the findings of previous workers who attributed it to the higher monomer reactivity of L-lactide (LL) compared to *ε*-caprolactone (CL) over a range of temperature. [80]

Comparisons between the experimental and calculated number-average sequence lengths based on Bernoullian statistics and assuming a completely random distribution show significant differences. The experimental l_{LL}^{e} and l_{C}^{e} values are significantly higher than the calculated l_{LL}^{R} and l_{C}^{R} values for every copolymer composition, again possibly due to the higher reactivity of LL compare with CL, as previously described by Kricheldorf *et al.* [31]. In this context, it is relevant to note that all of the synthesized copolymers here are random, as evidenced by their ^{13}C-NMR spectra and interpreted by Kaspercyzk *et al.* [78], but with some blocky character as reflected in their low degrees of randomness (*R*) and transesterification coefficients ($T_{(II)}$) in Table 3.13. Hence, the PLC copolymers were taper microstructure.

When considering the effect of reaction temperature on the degree of randomness, it was found that the increase in the reaction temperature leads to reduced block lengths, enhanced randomization and to the appearance of the transesterification reaction. Moreover, the formation of *CLC* sequences, which give rise to the corresponding signals observed in the ^{13}C-NMR spectra of the PLC copolymers with increasing the reaction temperature. The increase in

transesterification reaction accounts for the enhanced randomization of the copolymer chain.

When comparing the degrees of randomness (R) and the transesterification coefficients ($T_{(II)}$) values of the crude PLC copolymers and purified PLC copolymers, it can be seen that purified PLC copolymers has lower R and $T_{(II)}$ values than crude PLC copolymers. This is possibly due to oligomers which occur during the transesterification reactions were eliminated by re-precipitation in cold methanol.

3.1.3 Effect of the Monomer to Initiator Molar Ratio on the Polymer Properties

To study the effect of the monomer to 1-hexanol initiator molar ratio on the PLC 50:50 copolymer properties, polymerizations were carried out with the monomer to initiator molar ratio ([M]:[I]) varying between 100:0.002 and 100:0.200 at 0.1 mole% $SnOct_2$ catalyst. The ROP was carried out in bulk at 120°C for 48 hours as described in section 2.3.2.

Table 3.14 The effect of the monomer to 1-hexanol initiator molar ratio on the %yield and physical appearance of PLC copolymers in small scale (25 g) using 0.1 mole% $SnOct_2$ as a catalyst at 120°C for 48 hours.

Copolymer	[M]:[I] (mole ratio)	%yield	Physical Appearance
PLC_I1	500 (100 : 0.200)	65.90	transparent pale yellow solid flexible
PLC_I2	1000 (100 : 0.100)	88.70	transparent solid flexible
PLC_I3	10000 (100 : 0.010)	90.00	transparent solid flexible
PLC_I4	20000 (100 : 0.005)	91.80	translucent solid brittle
PLC_I5	50000 (100 : 0.002)	90.60	translucent solid brittle

Table 3.15 The effect of monomer to 1-hexanol initiator molar ratio on the final copolymer composition and weight-average molecular weights of PLC copolymers in small scale (25 g).

Copolymer	[M]:[I] (mole ratio)	Final copolymer compositions LL:CL (mole%)	Weight-average molecular weight ($\overline{M}_w$)
PLC_I1	500 (100 : 0.200)	49.0 : 51.0	45300
PLC_I2	1000 (100 : 0.100)	49.0 : 51.0	55590
PLC_I3	10000 (100 : 0.010)	49.3 : 50.7	83480
PLC_I4	20000 (100 : 0.005)	49.6 : 50.4	82980
PLC_I5	50000 (100 : 0.002)	49.6 : 50.4	67580

The effects of [M]:[I] molar ratio on the copolymerization reaction of PLC were examined as shown in Tables 3.14- 3.15 and Figure 3.23. The increasing [M]:[I] molar ratio, both the %yield and molecular weight of PLC copolymers increase. When the [M]:[I] molar ratio reaches 10000, the molecular weight of PLC copolymers begin to decrease as a result of transesterification reaction which leading to lower molecular weight PLC copolymers. Thus, the polymer molecular weights were controlled by varying the molar ratio of monomer and initiator, consistent with reports from Tangvenichcharoensuk [13], Dong *et al.* [81] and Zhao *et al.* [82]. The $SnOct_2$ acted only as a catalyst, increasing the polymerization rate but having no affect on the molecular weight. [81, 83-84]

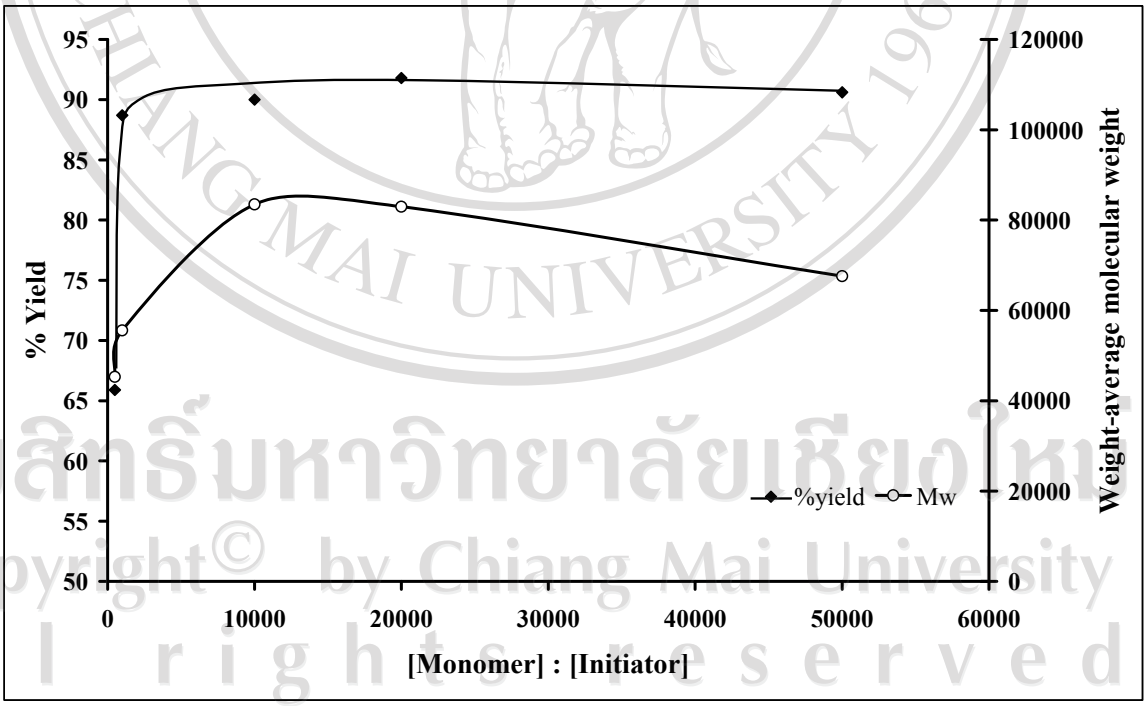

Figure 3.23 %Yield and weight-average molecular weight-[M]:[I] molar ratio profile of purified PLC copolymers in small scale (25 g).

The result indicated that hydroxyl-containing compounds are real initiator, which can stoichiometrically control the molecular weight of the polymer. However, controlled polymerization has been achieved in using very dry systems with a controlled amount of a hydroxyl-containing compound. Transesterification occurred during the ROP results in a broadening of the molecular weight distribution.

These results are in line with both of the mechanistic pathways proposed by Kricheldorf *et al.* and Penczek *et al.* [31, 32]. The polymerization reaction has been interpreted as a 'coordination-insertion' type mechanism. ROP reaction with $SnOct_2$ is carried out in the presence of active hydrogen compounds. If no active hydrogen compound is added, the actual initiating species may be a hydroxyl-containing impurity (*e.g.*, water and/or hydroxyl acid). In this study, it was believed that the monomer is coordinated with the $SnOct_2$ catalyst and is activated. The ROP then proceeds *via* a nucleophilic attack of alcohol leading to the insertion of monomer into metal-oxygen bond by rearrangement of the electrons. [32] The alcohol functionality and the monomer are both coordinated to the $SnOct_2$ complex during propagation. The reaction is terminated by hydrolysis forming a hydroxyl end group.

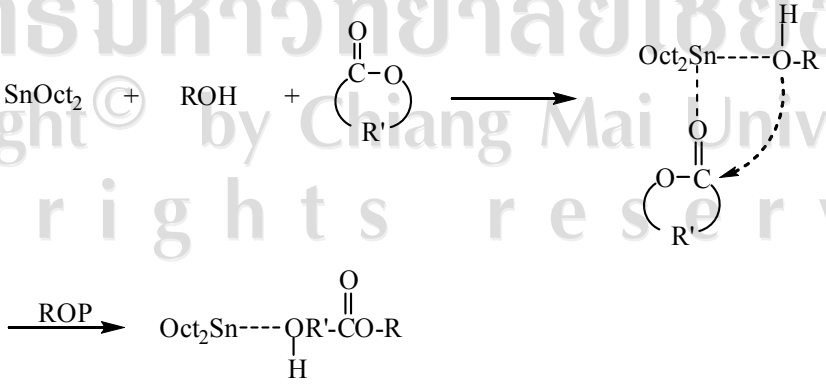

Scheme 3.1 The main ROP mechanism proposed by Kricheldorf *et al.*[1995].

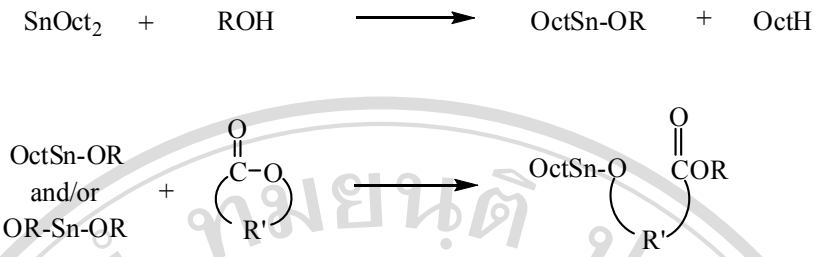

Scheme 3.2 The main ROP mechanism proposed by Penczek *et al.*[1998].

The excess alcohol may act as a chain transfer *via* alcoholysis of the ester bond along the chain, as shown in Scheme 3.3. This would be served to decrease the average molecular weight.

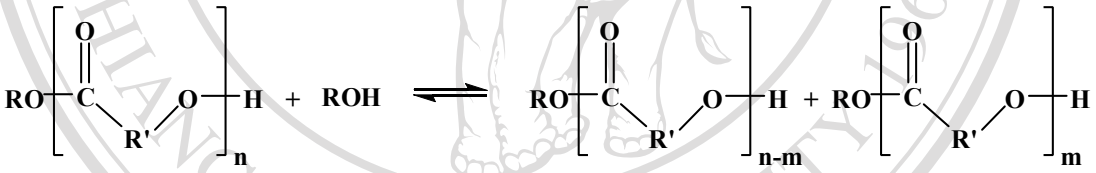

Scheme 3.3 Chain alcoholysis by hydroxyl end group.

Additional, most hydroxyl groups in alcohol were converted into polymer chain segment. The quantitative initiation from an increasing number of sites attached to low molecular weight molecules was increased. This would be also served to decrease the average molecular weight. It can be concluded that alcohol can effect the polymerization through the reaction of initiator formation and transesterification.

The most suitable initiator concentration that gave a high %yield of 90% and high molecular weight approximately 80,000 was 0.01 mole%. The ^{1}H-NMR results,

all of PLC copolymers have a final copolymer compositions close to that of the monomer feed ratio. Moreover, from DSC results, the morphology of all PLC copolymers was amorphous.

3.2 Synthesis of Poly(L-lactide-*co*-ε-caprolactone), PLC 50:50 mole% Copolymers: Medium Scale (250 g)

3.2.1 Effect of the Reaction Time on the Polymer Properties

To study the effect of the reaction time on the PLC 50:50 copolymer properties, polymerizations were carried out with the reaction time varying between 2 and 121 hours at constant the monomer to initiator molar ratio ([M]:[I] = 100:0.01 mole%) and 0.1 mole% $SnOct_2$ catalyst. The ROP was carried out in bulk at 120°C. The conditions used for synthesis and properties of PLC copolymers are shown in Table 3.16.

In the initial period of reaction time (< 24 hours), the physical appearance of PLC copolymers was transparent brittle solid look like poly(L-lactide). From ^{1}H-NMR, the L-lactide tended to polymerize preferentially resulting in PLC copolymers had the final copolymer compositions different from the initial comonomer feed because the reactivity of L-lactide is higher than that of ε-caprolactone as a mentioned in section 3.1.1. When increasing the reaction time (> 24 hours), polymerization of ε-caprolactone increase; as a result, PLC copolymers have the final copolymer composition close to that of the monomer feed ratio and the physical appearance of PLC copolymers became transparent rubbery-like solid. Figure 3.26 shows the effect of the reaction time on the %yield and weight-average molecular weight ($\overline{M}_w$) of

purified PLC copolymers in the medium scale synthesis (250 g), it was found that both %yield and $\overline{M}_w$ of purified PLC copolymers increase with increasing the reaction time.

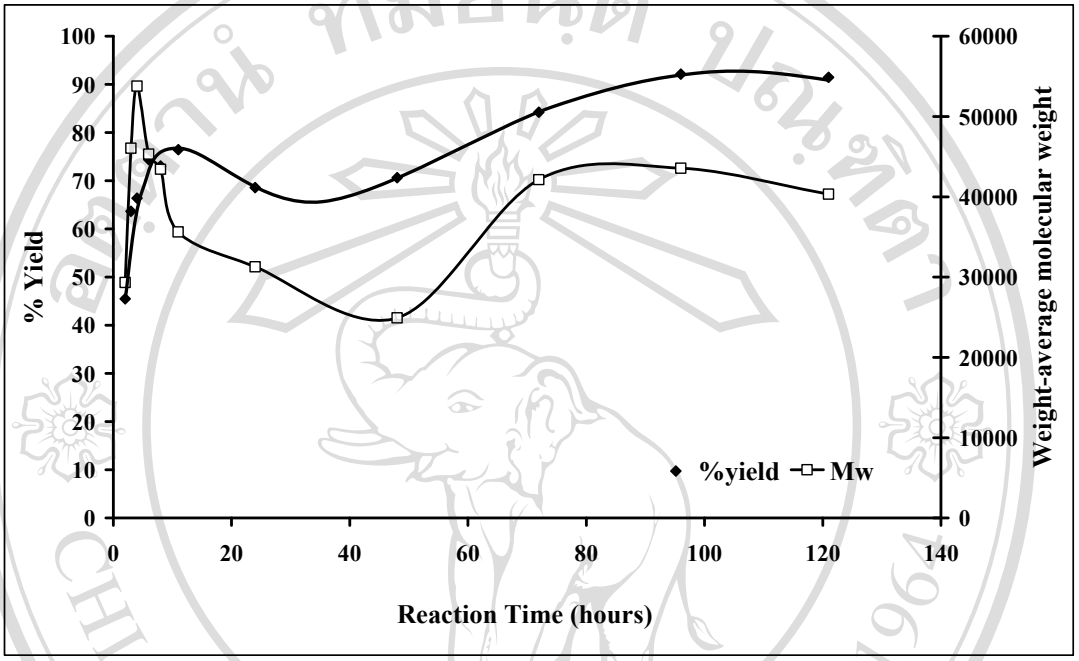

Figure 3.24 %Yield and weight-average molecular weight-reaction time profile of purified PLC copolymers in medium scale (250 g).

When compare the polymerization results of PLC copolymers in the small scale (25 g) with medium scale (250 g) under the same conditions, it was found that both %yield and $\overline{M}_w$ of PLC copolymers in the medium scale obtained is lower than that of the PLC copolymers in the small scale synthesis. It is possible that the problems associated with heat transfer as the mass-to-volume ratio increases resulting in increased temperature variations and transesterification reaction. In the medium scale synthesis, PLC copolymer was successfully copolymerized at 96 hours. It can be concluded that the longer reaction time are required for the larger scale synthesis.

Table 3.16 The PLC polymerization results in medium scale (250 g) using [M]:[I] molar ratio 100:0.01 mole%, 0.1 mole% $SnOct_2$ as a catalyst with different the reaction time at 120°C.

Copolymer	Reaction time (hours)	%yield	Physical Appearance	Final copolymer compositions LL:CL (mole%)	Weight-average molecular weight ($\overline{M}_w$)
PLC_M1	2	45.51	translucent brittle solid	86.5 : 13.5	29320
PLC_M2	3	63.67	translucent brittle solid	75.8 : 24.2	46040
PLC_M3	4	66.36	translucent brittle solid	72.4 : 27.6	53790
PLC_M4	6	74.40	translucent brittle solid	63.4 : 36.6	45310
PLC_M5	8	73.09	translucent brittle solid	63.2 : 36.8	43420
PLC_M6	11	76.45	translucent brittle solid	60.4 : 39.6	35620
PLC_M7	24	68.58	translucent brittle solid	55.0 : 45.0	31270
PLC_M8	48	70.64	translucent brittle solid	51.3 : 48.7	24920
PLC_M9	72	84.23	transparent rubbery-like solid	49.4 : 50.6	42140
PLC_M10	96	92.11	transparent rubbery-like solid	49.3 : 50.7	43570
PLC_M11	121	91.48	transparent pale yellow rubbery-like solid	48.6 : 51.4	40320

3.2.1.1 Thermal Characterization by DSC Analysis

The differential scanning calorimetry (DSC) thermograms are shown in Figures 3.25 – 3.26 and the results compared in Table 3.17. From the DSC results in Table 3.17, the values of T_g, T_c and T_m of first run and second run tend to follow copolymer composition. For example, at the initial period of polymerization (< 72 hours) copolymer showed a T_m because of the higher L-lactide content which has high degree of crystalline, but this subsequently decreased as the ε-caprolactone content increased with increasing reaction time. Moreover, the values of ΔH_m decrease with increasing structural irregularity. Finally, the final copolymer composition was nearly 50:50 mole%, the absence of T_m peak of PLC copolymer was obtained. The morphology of PLC copolymers was amorphous at 72 hours. The predicted T_g values from Fox Equation, as previously described in section 3.1.1.4, for PLC copolymers in medium scale synthesis are shown in Table 3.18.

From the results of the effect of the reaction time on the PLC copolymer properties, it can be concluded that the most suitable reaction time that gave a high % yield (92.11%), high molecular weight ($\overline{M}_w$ = 43570) and copolymer composition (LL:CL = 49.3:50.7 mole%) close to that of the comonomer feed ratio was 96 hours.

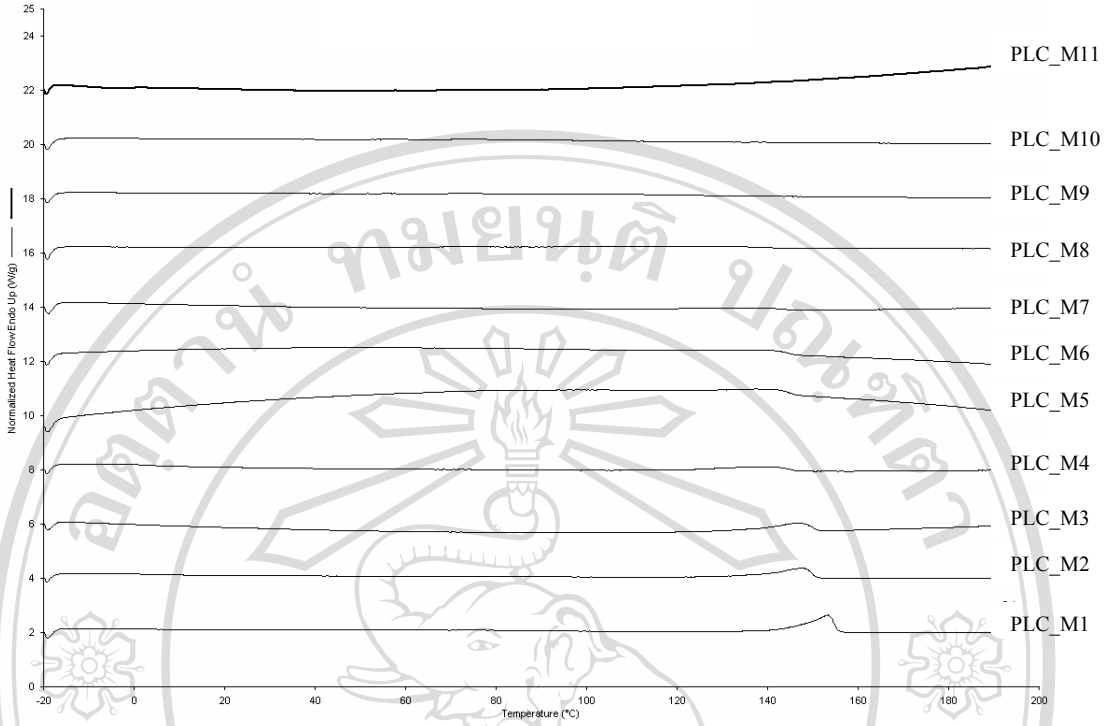

Figure 3.25 Comparison of the DSC themograms first run of PLC copolymers in mediun scale (250 g).

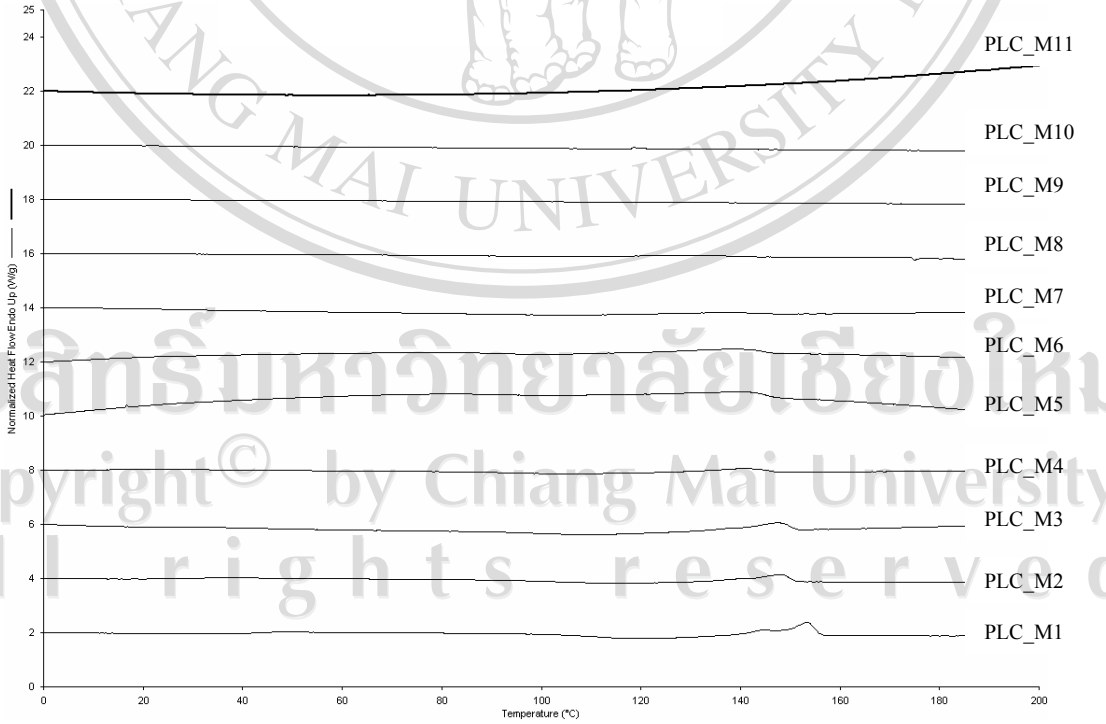

Figure 3.26 Comparison of the DSC themograms second run of PLC copolymers in mediun scale (250 g).

Table 3.17 DSC results of the PLC copolymers in medium scale (250 g)

Copolymer	DSC 1st run				DSC 2nd run				
	T_g (°C)	T_c (°C)	T_m (°C)	ΔH_m (J/g)	T_g (°C)	T_c (°C)	ΔH_c (J/g)	T_m (°C)	ΔH_m (J/g)
PLC_M1	nd	nd	153.2	29.5	nd	119.3	20.9	153.3	21.3
PLC_M2	nd	nd	147.7	22.6	nd	115.0	11.9	148.0	13.2
PLC_M3	nd	nd	146.3	19.1	nd	108.5	17.0	147.5	15.2
PLC_M4	nd	nd	139.2	15.8	nd	105.5	12.9	141.8	7.9
PLC_M5	nd	nd	141.3	11.1	nd	101.5	6.2	140.8	15.9
PLC_M6	nd	nd	139.0	14.3	nd	98.7	6.4	139.0	15.5
PLC_M7	nd	nd	137.2	9.9	nd	101.3	6.1	136.8	5.0
PLC_M8	nd	nd	127.8	9.4	nd	100.0	1.5	133.0	4.1
PLC_M9	nd	nd	nd	nd	nd	nd	nd	nd	nd
PLC_M10	nd	nd	nd	nd	nd	nd	nd	nd	nd
PLC_M11	nd	nd	nd	nd	nd	nd	nd	nd	nd

[a]T_g taken as the mid-point of the glass transition

[b]T_c taken as the peak temperature of the crystalline range

[c]T_m taken as the peak temperature of the melting range

nd = not detected or difficult to estimate

Table 3.18 The calculated values of T_g from Fox Equation for the PLC copolymers in medium scale (250 g).

Copolymer	Final copolymer compositions LL:CL (mole%)	Calculated values of T_g (°C)
PLC_M1	86.5 : 13.5	44.5
PLC_M2	75.8 : 24.2	29.2
PLC_M3	72.4 : 27.6	24.5
PLC_M4	63.4 : 36.6	12.5
PLC_M5	63.2 : 36.8	12.2
PLC_M6	60.4 : 39.6	8.5
PLC_M7	55.0 : 45.0	1.6
PLC_M8	51.3 : 48.7	-3.0
PLC_M9	49.4 : 50.6	-5.4
PLC_M10	49.3 : 50.7	-5.5
PLC_M11	48.6 : 51.4	-6.3

3.2.2 Synthesis of Poly(L-lactide-*co*-*ε*-caprolactone), PLC 50:50 mole% Copolymers

PLC 50:50 mole% copolymer was synthesized by ROP in bulk at 120°C for 96 hours using 0.1 mole% $SnOct_2$ as a catalyst and 0.01 mole% 1-hexanol as initiator for use as absorbable nerve guide. The structure and properties of PLC copolymer were characterized using ^{1}H-NMR, ^{13}C-NMR, GPC, DSC, TGA, DMA as shown in Table 3.19. The physical appearance of crude PLC copolymer was transparent rubbery-like solid and became white solids after precipitation dropwise into cold methanol. The yield of purified PLC copolymer was 97.3%.

Table 3.19 Results of the polymerization of PLC copolymer using 0.1 mole% $SnOct_2$ as a catalyst and 0.01 mole% 1-hexanol as initiator at 120°C for 96 hours in medium scale (250 g).

Polymer properties	**PLC copolymer**	
Physical appearance	transparent rubbery-like solid	
%yield	97.3	
Initial monomer ratio LL:CL (mole %)	50.1 : 49.9	
Final copolymer compositions (^{1}H-NMR) LL:CL (mole %)	crude	pure
	50.7 : 49.3	50.6 : 49.4
Average molecular weight (GPC)	crude	pure
$\overline{M}_n$	93935	89743
$\overline{M}_w$	182907	173876
Polydispersity (PD = $\overline{M}_w$ / $\overline{M}_n$)	1.9	1.9
Thermal properties		
T_g (°C) (DMA)	-6.3	
T_g (°C) (DSC)	nd	
T_m (°C) (DSC)	nd	
ΔH_f (J/g) (DSC)	nd	

3.2.2.1 Structure and Copolymer Composition Analyses by ^{1}H-NMR Spectroscopy

The ^{1}H-NMR spectra of PLC copolymer in deuterated chloroform solutions were recorded using a Bruker Avace 400 MHz NMR Spectrometer at room temperature and the data obtained from MestRe-C data processing software. The spectra of crude and purified PLC copolymer are shown in Figures 3.27-3.28 respectively. The summarized interpretations from the proton assignments of corresponding chemical shift and peak area integration are given in Tables 3.20.

The evaluation of average copolymer compositions of PLC could be calculated as described previously in section 3.1.1.2 and the results are presented in Table 3.21. As would be expected, the final copolymer compositions was also very similar to the comonomer feed ratio (50.1:49.9) because polymerization reaction was taken to near-quantitative (> 97%) conversion. From these results, it can be concluded that the polymerization conditions for the polymer synthesis employed (temperature, time, catalyst and initiator concentrations) were suitable for the purpose of obtaining near-quantitative conversion for PLC copolymer in medium scale (250 g).

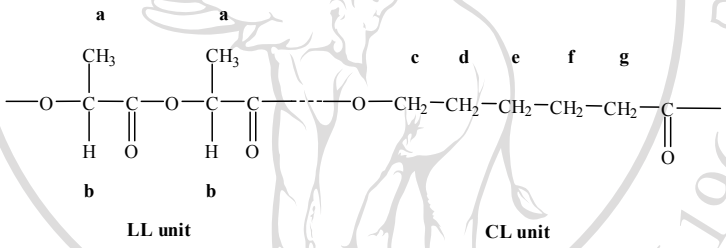

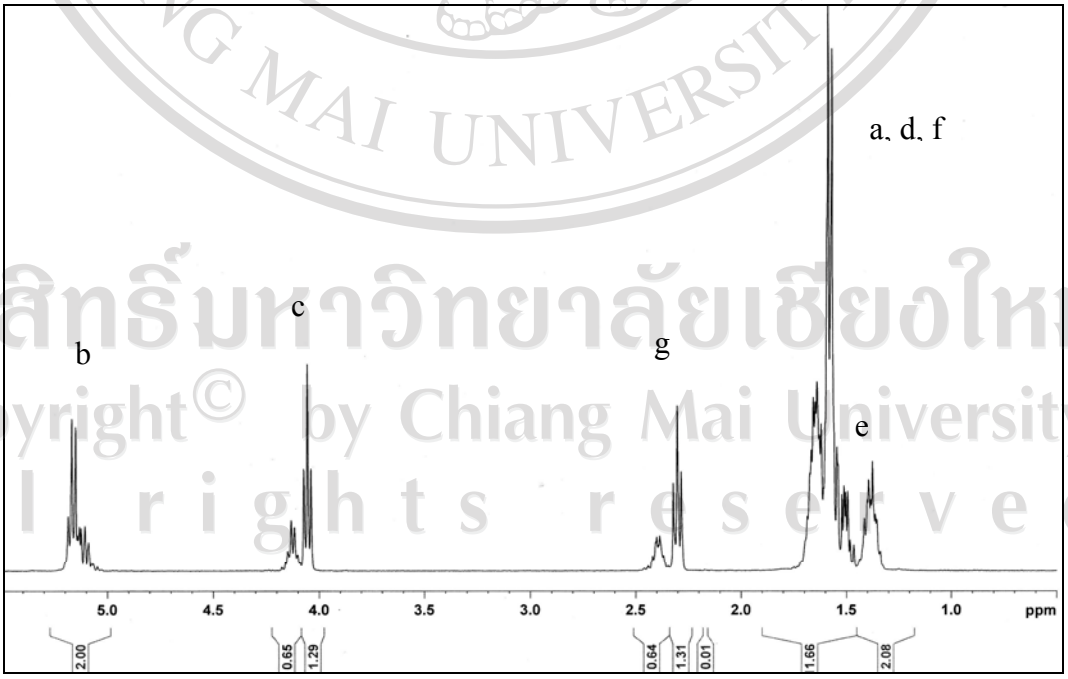

Figure 3.27 ^{1}H-NMR (400 MHz) spectrum of crude PLC in medium scale (250 g).

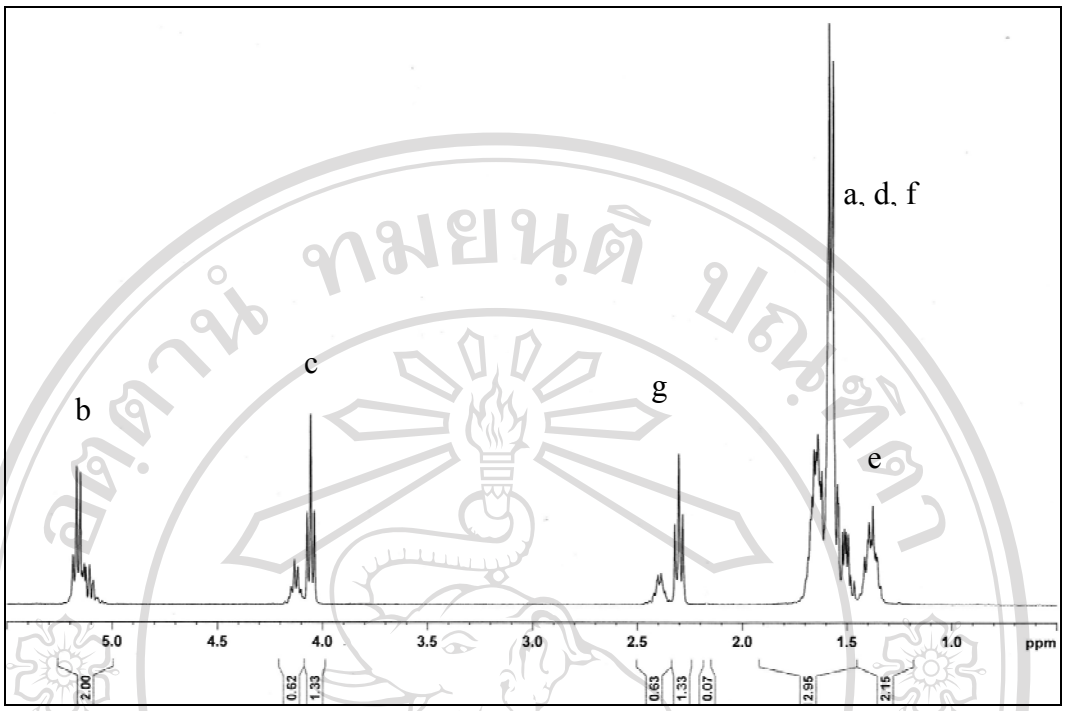

Figure 3.28 ^{1}H-NMR (400 MHz) spectrum of purified PLC in medium scale (250g).

Table 3.20 Proton assignments and corresponding chemical shift ranges and peak area integrations for the various resonance peaks in the ^{1}H-NMR spectra of the crude and purified PLC copolymers in medium scale (250 g).

Proton assignment	Chemical shift range, δ (ppm)		Peak area integration	
	Crude PLC	Purified PLC	Crude PLC	Purified PLC
b	5.0-5.2	5.0-5.2	2.00	2.00
c	4.0-4.2	4.0-4.2	1.94	1.95
g	2.2-2.5	2.2-2.5	1.95	1.96
a, d, f	1.3 - 1.8	1.3 - 1.8	13.74	15.10
e				

Table 3.21 Comparison of the initial comonomer feeds with the final copolymer compositions of the crude and purified PLC copolymer in medium scale (250 g).

Copolymer	Initial comonomer feeds LL:CL (mole%)	Final copolymer compositions LL:CL (mole%)
Crude PLC	50.1 : 49.9	50.7 : 49.3
Purified PLC	50.1 : 49.9	50.6 : 49.4

3.2.2.2 Copolymers Chain Microstructure (Monomer Sequencing) by ^{13}C-NMR Spectrometry.

Copolymer chain microstructure, particularly the monomer sequencing of the L-lactide (L) and ε-caprolactone (C) can be determined by a Bruker Avace 100 MHz ^{13}C-NMR spectrometer. The ^{13}C-NMR spectra of PLC copolymer are shown in Figures 3.29-3.30 and the chemical shifts that corresponding to peak assignments was tabulated in Table 3.22. The spectra all conform to the copolymer chemical structures.

As mentioned in section 3.1.2.1, the carbonyl (C=O) carbon atoms have been shown to be the most sensitive to the sequencing variations, with the results that triad splitting of the carbonyl carbon region (165-175 ppm) can be observed. The carbonyl carbon regions of the spectra are expanded in Figures 3.31-3.32, that the differences in chain microstructure can be observed.

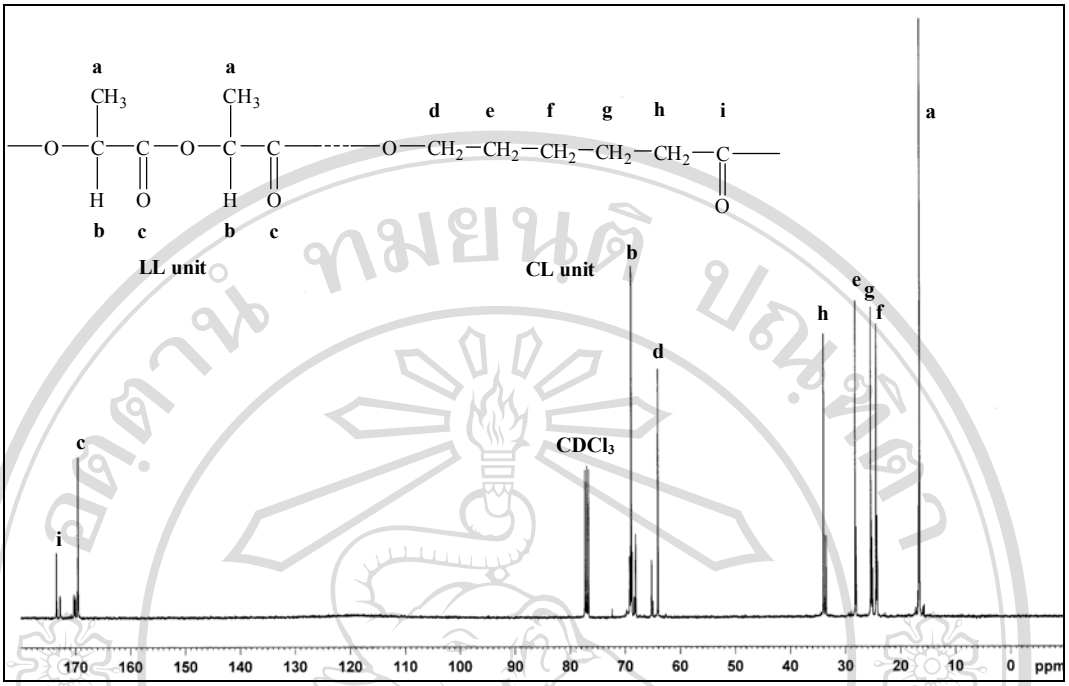

Figure 3.29 100 MHz ^{13}C-NMR spectrum of crude PLC copolymers in $CDCl_3$ as solvent in medium scale (250 g).

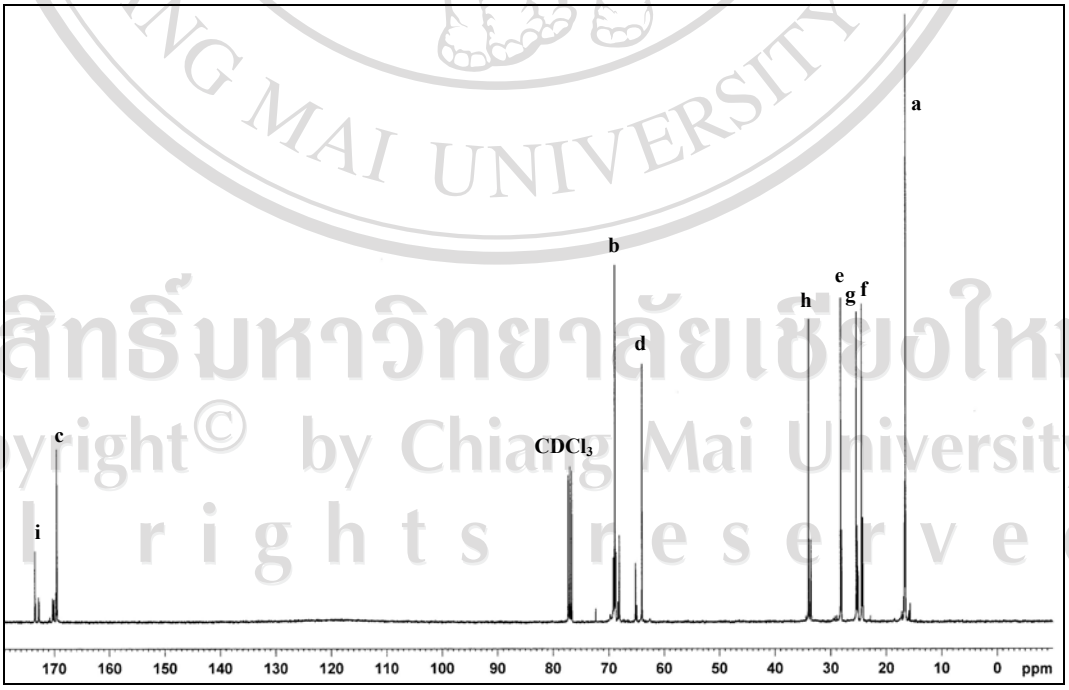

Figure 3.30 100 MHz ^{13}C-NMR spectrum of purified PLC copolymers in $CDCl_3$ as solvent in medium scale (250 g).

Table 3.22 Carbon-13 assignments and corresponding chemical shifts for the various resonance peaks in the ^{13}C-NMR spectra of crude and purified PLC copolymer in medium scale (250 g).

Proton assignment	Chemical shift range, δ(ppm)	
	Crude PLC	Purified PLC
i	173.5	173.5
c	169.5	169.5
b	68.8	68.8
d	64.1	64.1
h	34.0	34.0
e	28.2	28.2
g	25.4	25.4
f	24.5	24.5
a	16.8	16.8
$CDCl_3$	77.3-76.7	77.3-76.7

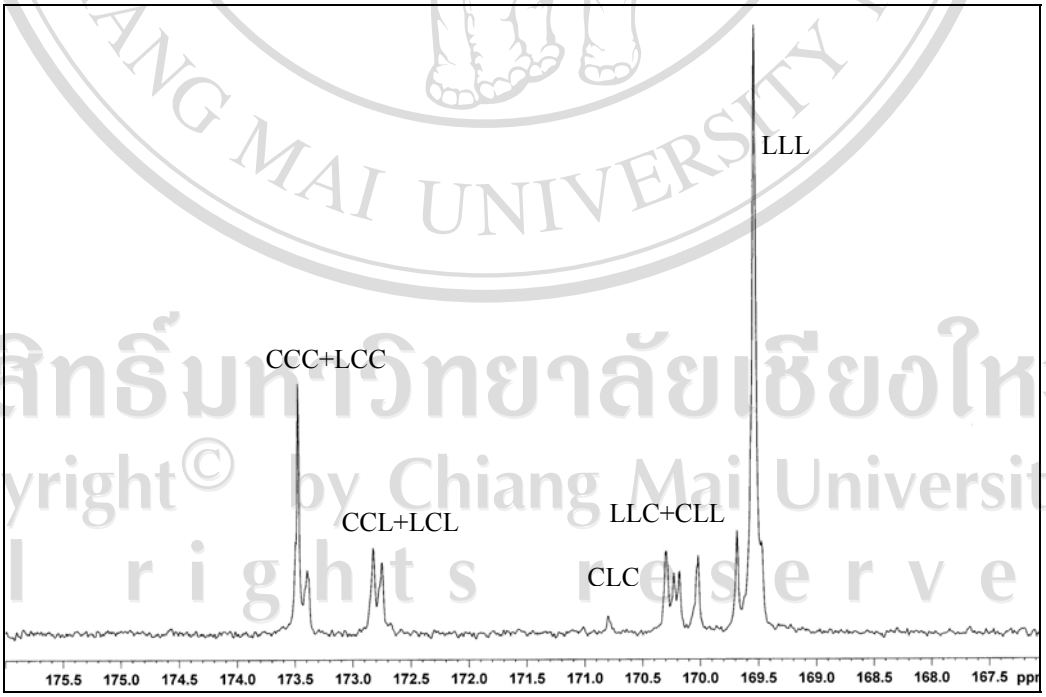

Figure 3.31 Expanded carbonyl region of the 100 MHz ^{13}C-NMR spectrum of crude PLC copolymer in medium scale (250 g).

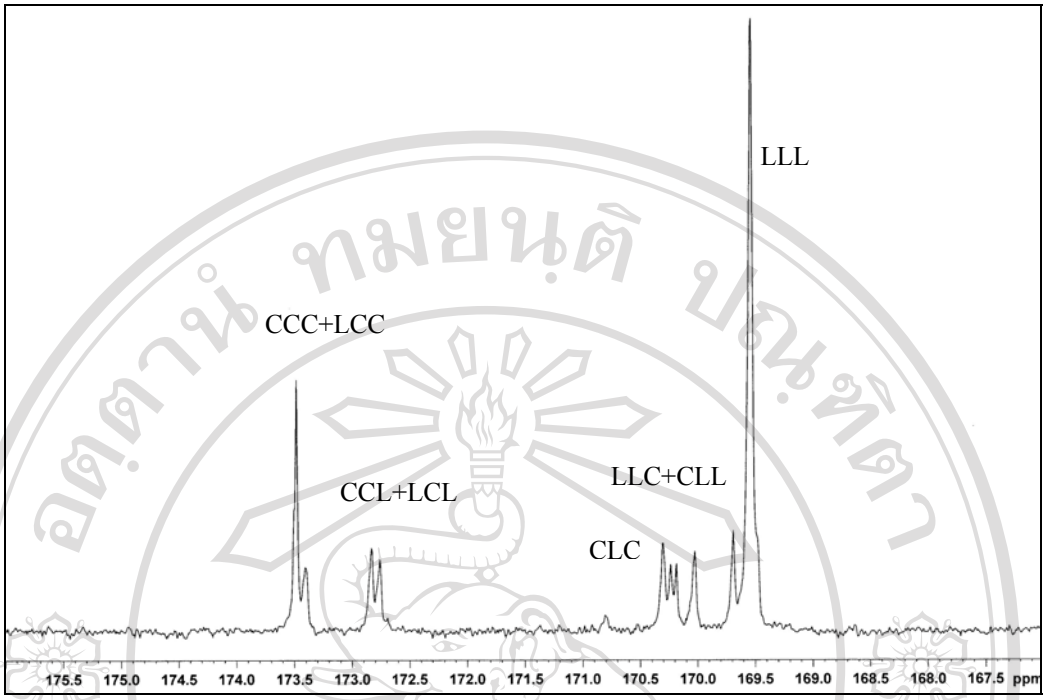

Figure 3.32 Expanded carbonyl region of the 100 MHz ^{13}C-NMR spectrum of purified PLC copolymer in medium scale (250 g).

Table 3.23 Monomer sequence assignments and intensities for the various carbonyl carbon peaks in the expanded ^{13}C-NMR spectra of crude and purified PLC copolymer in medium scale (250 g).

Monomer sequence (triad)	**C=O carbon chemical shift (ppm)**	
	Crude PLC	**Purified PLC**
CCC + LCC	173.6 -173.3	173.6 -173.3
CCL + LCL	172.9 - 172.6	172.9 - 172.6
CLC	170.9	170.9
LLC + CLL	170.4 - 169.9	170.4 - 169.9
LLL	169.5	169.5

Table 3.24 The results of calculated average monomer sequence lengths and degree of randomness of PLC copolymer in medium scale (250 g).

Copolymer	F_{LL} [a]	l_{LL}^{e} [b]	l_{C}^{e} [c]	l_{LL}^{R} [d]	l_{C}^{R} [e]	R [f]	T_{II} [g]
Crude PLC	50.7	3.5470	2.5604	1.4452	1.4862	0.4074	0.855
Purified PLC	50.6	3.2401	2.6002	1.4529	1.4881	0.4484	1.214

[a] F_{LL} L-lactide mole fraction in copolymer from ^{1}H-NMR.

[b] l_{LL}^{e} experimental average length of lactidyl blocks.

[c] l_{C}^{e} experimental average length of caproyl blocks.

[d] l_{LL}^{R} calculated average length of lactidyl blocks.

[e] l_{C}^{R} calculated average length of carproyl blocks.

[f] R degree of randomness.

[g] T_{II} transesterification coefficient.

From the expanded carbonyl regions of crude and purified PLC copolymer spectra in Figures 3.31-3.32 respectively and the results are summarized in Table 3.23. The evidence for PLC 50:50 that apart from the expected preponderance of *LLL* sequence, the other component, *C*, are indeed distributed at various points along the copolymer chain. The appearance of the additional C=O peaks (*LCC*, *CCL*, *LCL*, *LLC*, *CLL*) indicated that various mixed triad sequences are also presented, as would be expected in tapered microstructure. Investigation of transesterification in the polymerization reaction can be observed by ^{13}C-NMR. The phenomenon of transesterification is presented by *CLC* (δ = 170.9 ppm) sequence because this sequence cannot be formed by opening the lactide ring during the growth reaction of

the copolymer chain. The triad sequence *CLC* could formed in this study, become a useful indicator that transesterification has occurred.

The number-average lengths of the C and LL sequences were determined on the basis of the attribution of the peaks in the ^{13}C-NMR spectrum, as previously described in section 3.1.2.1.2. Table 3.24 show the calculated average monomer sequence lengths (l^e_{LL}, l^e_C) and degree of randomness (*R*) for the crude and purified PLC copolymer. It was found that PLC copolymer was tapered microstructure due to the effect of the monomer reactivity ratio that the reactivity of L-lactide is higher than that of ε-caprolactone.

3.2.2.3 Molecular Weight Determination by GPC

The molecular weight ($\overline{M}_n$ and $\overline{M}_w$) and polydispersities ($\overline{M}_w / \overline{M}_n$) of the crude and purified PLC copolymer were determined by gel permeation chromatography (GPC) as shown in Table 3.25 and GPC curves in Figures 3.33 - 3.34 respectively. From GPC results, the PLC copolymer has high number-average molecular weight and low polydispersity that suitable for fabrication.

Table 3.25 GPC molecular weight data of crude and purified PLC copolymer in medium scale (250 g).

Copolymer	Molecular weight		
	$\overline{M}_n$	$\overline{M}_w$	$\overline{M}_w / \overline{M}_n$
Crude PLC	93,935	182,907	1.9
Purified PLC	89,743	173,876	1.9

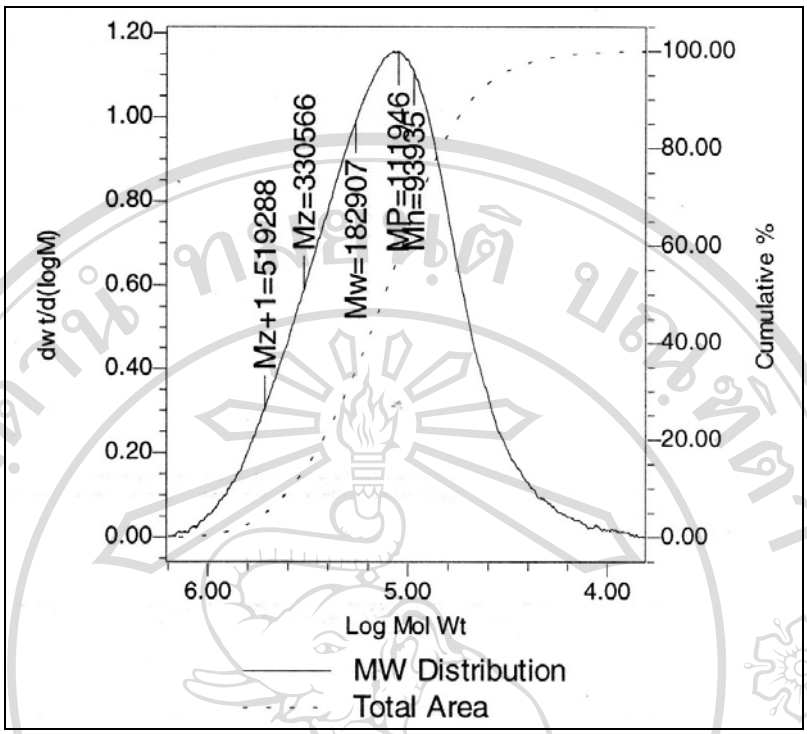

Figure 3.33 GPC curve of crude PLC copolymer in medium scale (250 g).

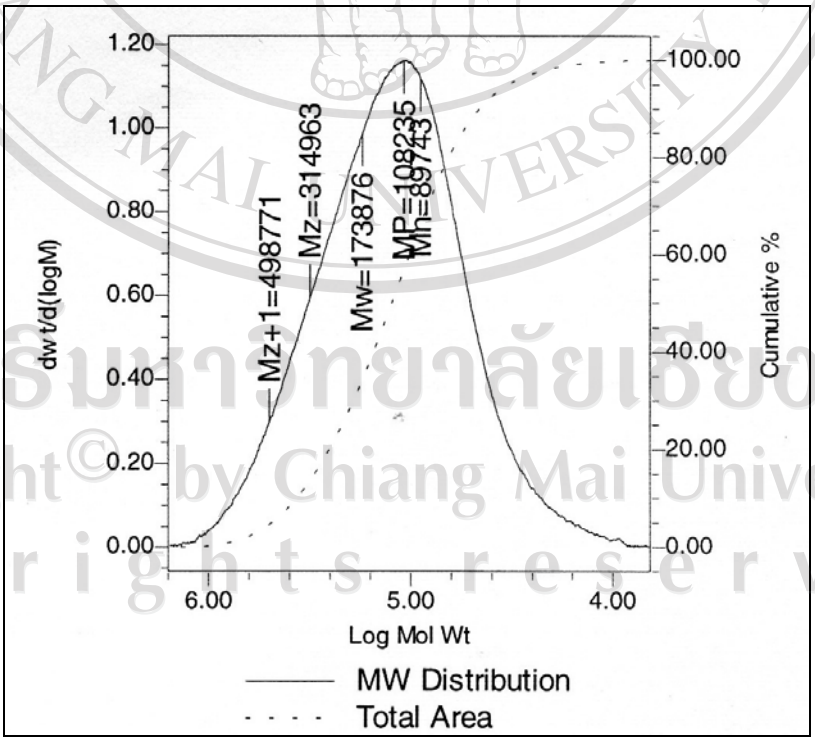

Figure 3.34 GPC curve of purified PLC copolymer in medium scale (250 g).

3.2.2.4 Intrinsic Viscosity Determination by Dilute-Solution Viscometry

Viscosity of the synthesized PLC copolymer was measured at 25.0°C in chloroform ($CHCl_3$) solution. Under a series of PLC concentrations, reduced viscosities (η_{red}) and inherent viscosities (η_{inh}) were measured and evaluated. Furthermore, intrinsic viscosity [η] was estimated via the extrapolation of the η_{red} and η_{inh} versus polymer concentration plot and the result was shown in Figure 3.35. It was found that the intrinsic viscosity of PLC copolymer was 1.19 dl/g.

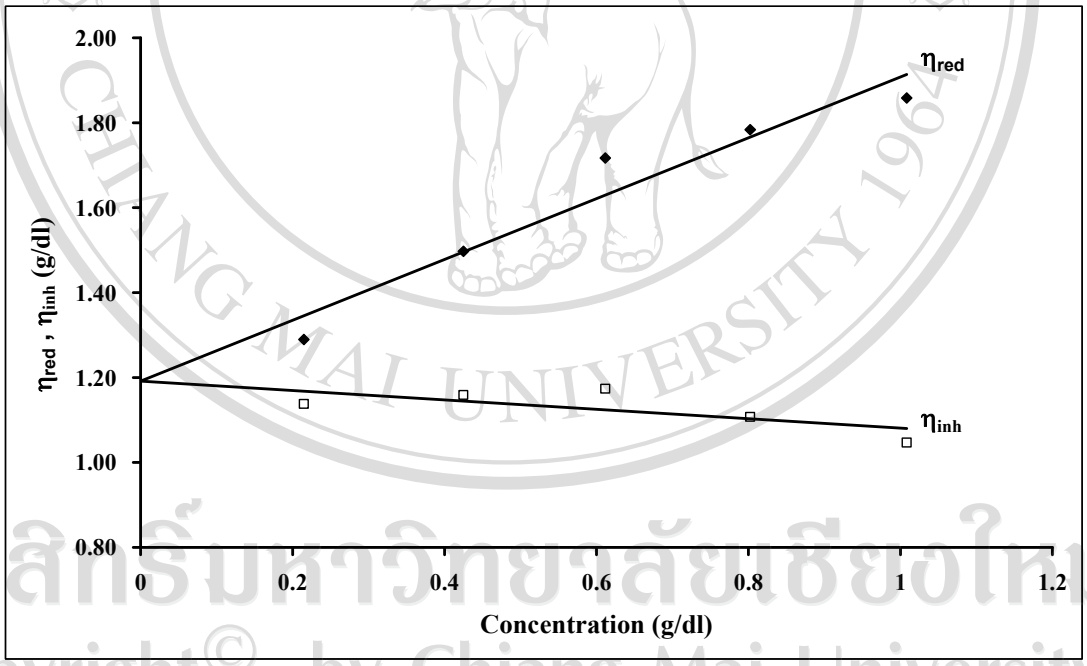

Figure 3.35 Double extrapolation plots of the reduced, η_{red}, and inherent, η_{inh}, viscosities against concentration for PLC copolymer in medium scale (250 g).

3.2.2.5 Thermal Characterization by DSC Analysis

DSC analyses of the PLC copolymer samples were conducted at the heating rate 10°C/min under dry nitrogen atmosphere. From the DSC results, the absence of T_g, T_c and T_m of first run and second run of crude and purified PLC copolymer was obtained. It can be concluded that both crude and purified PLC copolymer was amorphous. The predicted T_g values from Fox Equation for crude and purified PLC copolymer are -3.74°C and -3.87°C respectively.

3.2.2.6 Thermal Characterization by TGA Analysis

The thermogravimetric analysis measurement of the PLC copolymer was obtained at a heating rate of 20°C/min under dry nitrogen atmosphere and is shown in Figure 3.36. Samples were in the 5-10 mg range and of as small a particle size as possible in order to minimize diffusion-controlled weight loss processes.

From the TG thermogram in Figure 3.36, the weight loss profile is seen to be single-step. TG is not a particularly informative technique as far as the microstructure characterization of the copolymer is concerned. Its usefulness and main purpose in this study was to define the upper temperature limit for polymer processing below which the copolymer could be safety melt without accompanying degradation. The weight loss proceeded to completion (100% weight loss) with no involatile residual remaining. The thermal degradation of PLC copolymer was in the temperature range of 215 - 520°C. This temperature as estimated from the initial and final weight loss temperature. In aliphatic polyesters such as PLC copolymer, the main mechanisms of thermal degradation are either intra- or intermolecular transesterification reactions.

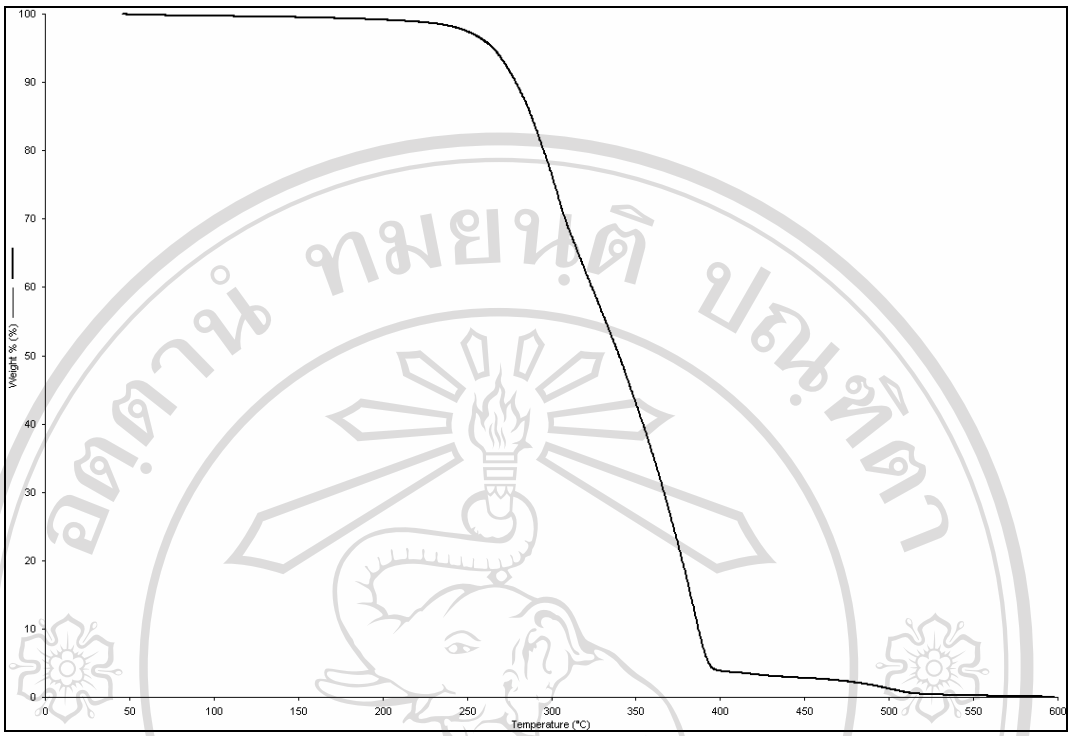

Figure 3.36 TG thermogram of PLC copolymer in medium scale (250 g).

3.2.3.7 Mechanical Properties Determination by Tensile Testing

The mechanical properties of polymer are of fundamental interest as mentioned earlier because they must fall within a specified range for a given application. In this study, mechanical properties such as tensile strength (stress at break), %elongation (strain) at break and Young's modulus were determined with Lloyds LRX+ Universal Mechanical Testing Machine. Error analysis in testing usually is conducted by repetition of the measurement for at least 5 identical samples in order to the standard deviation in the measurement. The mechanical test results in the form of stress-strain curve are shown in Figure 3.37.

From the stress-strain curve, it was found that PLC copolymer had a stress at break of 16.3±2.3 MPa, a strain at break of 807±18.5% and Young's modulus of

11.6±2.2 MPa. As expected, PLC copolymer giving soft and flexible properties that suitable to modulate the mechanical properties for nerve guides application.

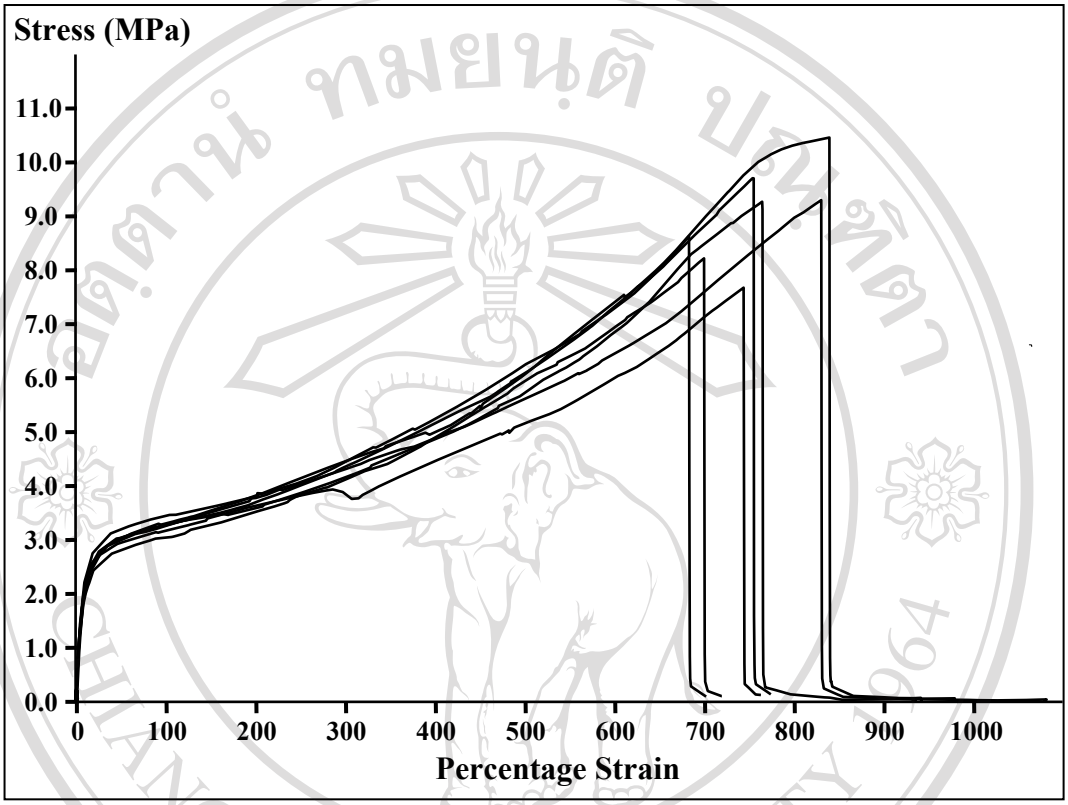

Figure 3.37 Stress-strain curve of PLC copolymer in medium scale (250 g).

3.2.3.8 Dynamic Mechanical Analysis (DMA)

Dynamic mechanical properties of polymers were investigated in the solid state below the respective melt temperatures using a Dynamic Mechanical Analyzer (Mettler Toledo DMA/SDTA 861^e) with the films in shear mode. The film obtained finally with a thickness of about 0.65 mm (5.37mm×4.85 mm) was used for the DMA measurements. Values of the storage modulus (E′), the loss modulus (E″) and the damping (tan δ) were calculated over the temperature range -100 to 150°C, the rate of heating was with 4°C/min and applied at a frequency of 1 Hz, Maximum force 3 N

and Maximum displacement amplitude 20 μm as previously described in section 2.4.8.

The dynamic moduli (E′ and E″) and tan δ of PLC copolymer, with the typical observations in glass (brittle) and rubbery (tough and leathery) starts are plotted as a function of temperature shown in Figure 3.38.

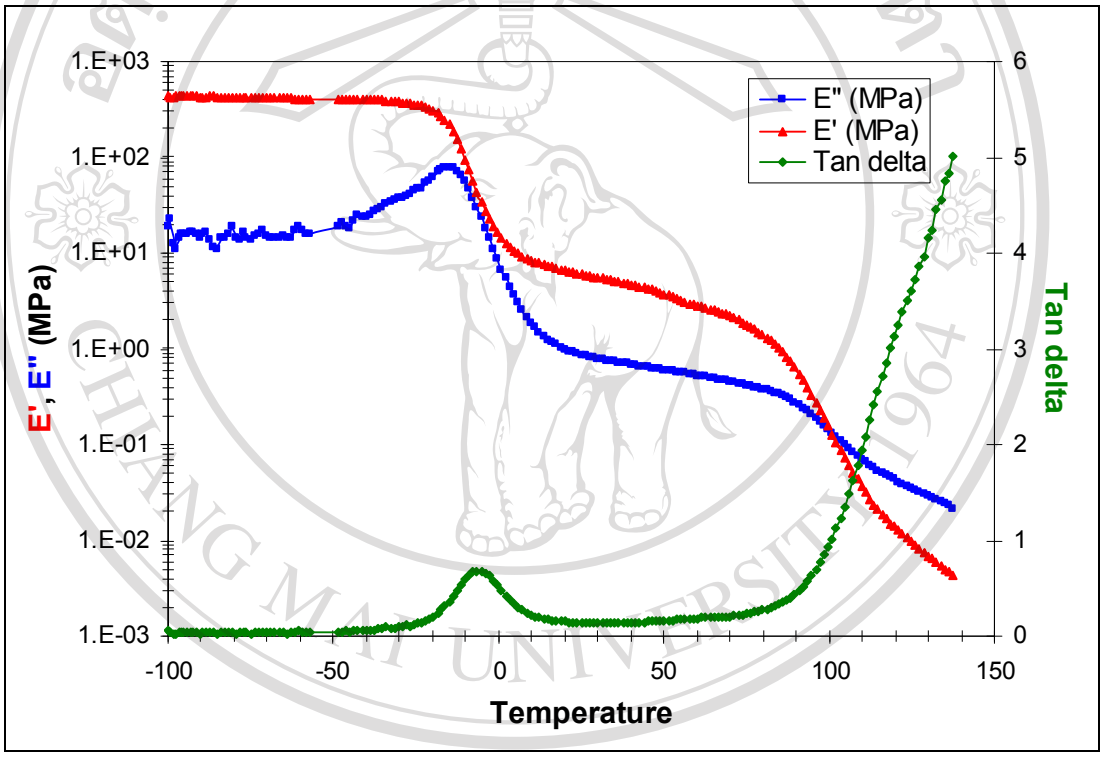

Figure 3.38 The E′, E″ and tan δ curves as a function of temperature for PLC copolymer film.

The storage modulus E′ value of rigid PLC copolymer sample is roughly 10^3 MPa and the E′ decreases very slowly as the temperature increases in the glassy state over the range -100°C to -20°C. In the neighborhood of the glass transition temperature (T_g), E′ decreases over a short temperature interval due to the

transformation from the glassy to the rubbery state. In this region PLC is semi-rigid and has a leathery feel. At temperature above the transition region, PLC is in a rubbery state with an E′ value of about 1 MPa. The E′ drops further at higher temperature (100°C) due to the increasing role of viscous flow. The upper temperature region cannot be seen the crystalline melting temperature (T_m). Thus, it was concluded that PLC copolymer was amorphous.

The changes in the loss modulus (E″) and the damping (tan δ) of the PLC copolymer over the same temperature range are shown in Figure 3.38. The E″ value increase at lower glass transition temperature (T_g) and drops further at higher T_g. A damping peak can be seen around -6.3°C (α-transition). This is corresponding to E′ changing from approximately 10^3 MPa in the glassy state to about 1 MPa in the soft rubbery state. In the transition region, tan δ is high in intensity because some chain segments are free to move while others are not. The α-transition peak (-6.3°C) is assigned to the glass transition temperature (T_g). Hence, PLC copolymer was soft and elastic at room temperature that suitable for fabrication of nerve guide tubes.

As we already known that the relative sensitivity of DMA to DSC vary, it appears that DMA is 10 to 100 times more sensitive to the changes occurring at the T_g. These transition was normally too weak or too broad for determination by DSC method.

3.2.3.9 Rheological Properties by Melt Rheology

One of the best methods to characterize the mechanical properties of polymer melts with respect to structure is melt rheology. From melt rheology the complex

shear modulus (G^*) can be obtained as a function of frequency and temperature. G^* is composed of shear storage modulus (G') and shear loss modulus (G'') component parts, being representative of the 'elastic' and 'viscous' behavior of the polymer, respectively. The rheological properties of the PLC were determined using a Bohlin Gemini HR^{nano} Rotational Rheometer. PLC copolymer is a hygroscopic material, in order to remove any absorbed moisture and avoid hydrolytic degradation, the copolymer chips were dried under vacuum at 100°C for 24 hours before measurements.

Dynamic measurements of the PLC copolymer under strain-controlled conditions were performed on a parallel plate Bohlin Gemini HR^{nano} rotational rheometer. The diameter of the plates was 25 mm and the gap between the plates was set to 0.5 mm. The copolymer was placed between the plates and heated to the test temperature (150°C) in order to eliminate previous deformation and thermal history. After adjusting the gap to 0.5 mm, the molten copolymer was trimmed off to give smooth-edged surfaces and the appropriate cylindrical sample form.

Table 3.26 The shift factor values for used construct a master curve at reference temperature.

Temperature (°C)	**Shift factor ($\log(a_T)$) at reference temperature**		
	130°C	**140°C**	**150°C**
30	9.39	9.88	9.84
40	7.45	7.94	7.90
50	6.15	6.64	6.60
60	4.89	5.38	5.34
70	4.11	4.60	4.56

Table 3.26 continued

Temperature (°C)	Shift factor ($\log(a_T)$) at reference temperature		
	130°C	**140°C**	**150°C**
80	2.95	3.44	3.40
90	2.17	2.66	2.62
100	1.50	1.99	1.95
110	0.933	1.42	1.38
120	0.304	0.796	0.754
130	0	0.492	0.450
140	-0.486	0	-0.035
150	-0.450	0.042	0

The frequency dependences of G′ and G″ measured within the frequency range of 0.628 to 628 rad/s with a 5% strain at various temperatures (30 to 170°C) were used to construct a master curve representing a broad-range frequency dependence of these quantities. Table 3.26 shown the shift factor values (log (a_T)) were calculated for used to construct a master curve at the reference temperature (130, 140 and 150°C) from the William Landel and Ferry (WLF) equation. [68-69]

$$\log(a_T) = -\frac{C_1(T-T_0)}{C_2+(T-T_0)}$$

where a_T is the shift factor, T is the temperature, T_0 is the reference temperature and C_1 and C_2 are material constants which depend on the reference temperature and polymer system. The C_1 and C_2 values from WLF equation for used construct a master curve at reference temperature as shown in Table 3.27.

Table 3.27 The C_1 and C_2 values from WLF equation for used construct a master curve at reference temperature.

Reference temperature (°C)	C_1	C_2
130	7.64	180.55
140	7.92	197.92
150	5.34	183.02

The master curve showing the frequency dependence of G′ and G″ for PLC at a reference temperature (T_0) of 150°C is shown in Figure 3.39. G′ and G″ are frequency dependent and, by increasing the frequency, both moduli increase. At low frequency, the PLC shows predominantly viscous properties (G″ > G′). By increasing the frequency, G′ increases faster than G″ so that the G′ curve crosses the G″ curve at a frequency called the "crossover frequency" (ω_c). At frequencies higher than ω_c, the G′ prevails over G″ and the sample is predominantly elastic. The polymer melt displays a high degree of elasticity with G′ only weakly dependent on frequency and greater than G″ over the rubbery plateau region. The curve for G′ indicates that the copolymer melt has a high rigidity and elasticity at high frequency. If the width of the rubbery plateau region increases, so does the elasticity of the copolymer. In the terminal region where flow is dominant, G′ drops rather rapidly and G′ and G″ are proportional to ω^2 and ω respectively.

Due to the amorphous nature of the PLC 50:50 copolymer, it is difficult to determine the melt flow temperature for use in melt extrusion. A frequency sweep was therefore performed to determine the temperature at which the PLC melted and flowed homogeneously.

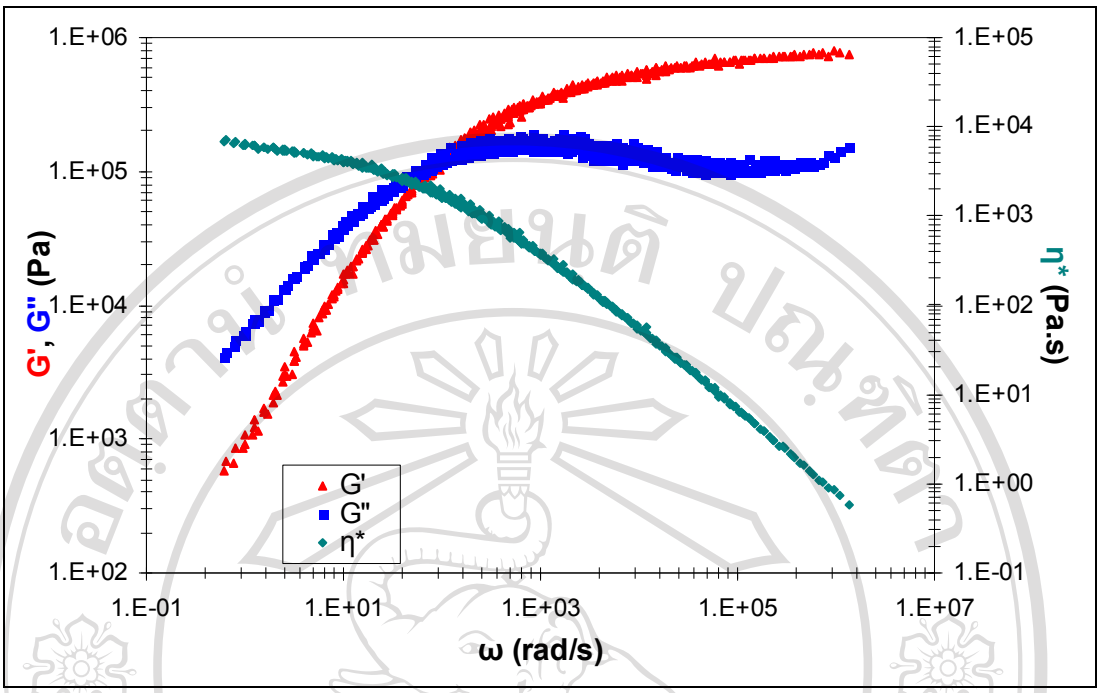

Figure 3.39 Master curve showing G′, G″ and η^* of PLC at a reference temperature of 150°C.

A comparison of the master curves at reference temperatures of 130°C and 140°C is shown in Figure 3.40. Both G′ and G″ at these reference temperatures in the rubbery plateau region are quite similar as the moduli in this region are not a function of temperature but depended on molecular weight and polymer chain length. In the terminal region, the effect of temperature on the moduli increases. The moduli at T_0 = 130°C are higher than at T_0 = 140°C. At reference temperatures of 140°C and 150°C, as shown in Figure 3.41, the curves of G′ and G″ are quite similar, especially in the terminal zone. PLC melts and flows approximately homogeneously in the temperature range of 140-150°C. This data is applied to determine the most appropriate temperature for preparing a polymer rod in order to avoid air bubbles and void formation during melt extrusion.

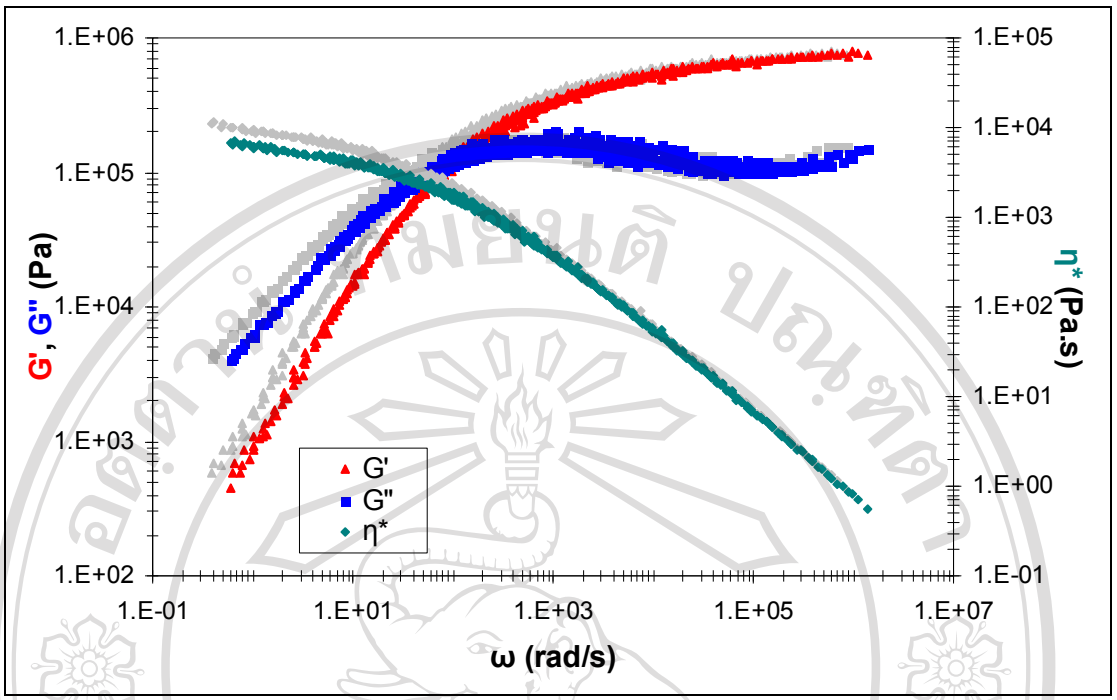

Figure 3.40 Comparison of the master curve at reference temperatures of 130°C (gray curves) and 140°C.

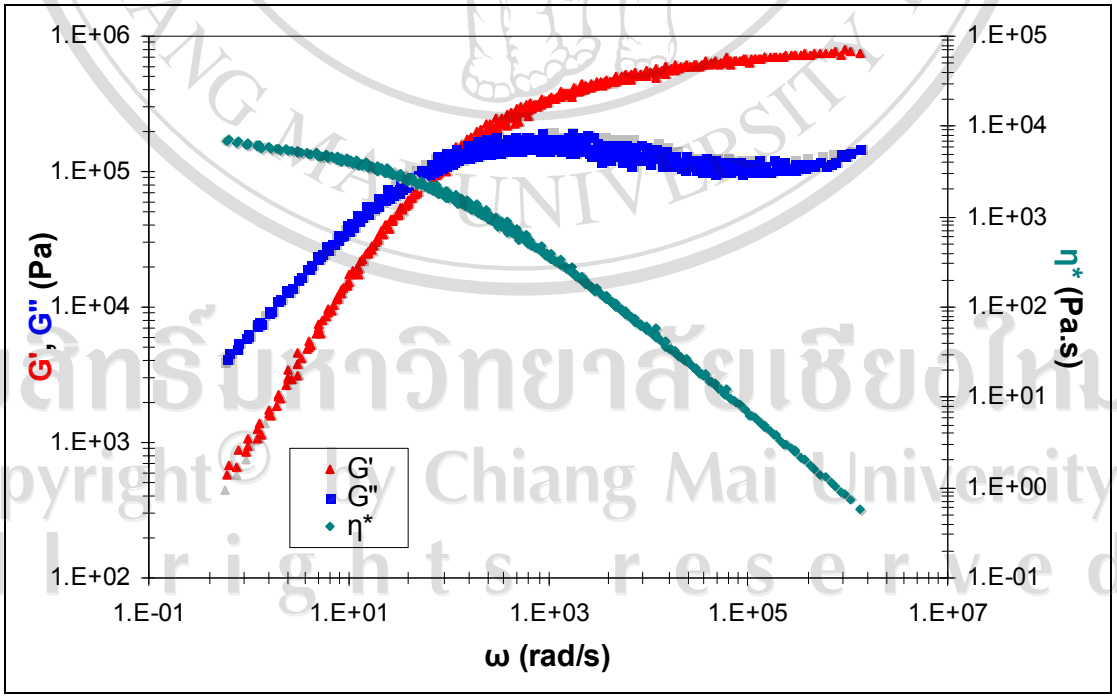

Figure 3.41 Comparison of the master curve at reference temperatures of 140°C (curves in gray color) and 150°C.

To observe the rheological changes in the PLC copolymer during a temperature ramp of 10°C/min, a strain of 5% at a frequency of 1 Hz were used.

The temperature dependences of G′, G″, loss factor (tan δ) and complex viscosity (η*) are shown in Figure 3.42. The PLC melt exhibited a transition from a solid-like to a liquid-like state at the crossover of G′ and G″ at 83°C. At the temperatures below 83°C, the value of G′ is greater than G″ so that PLC behaves like a solid. In contrast, when G″ is higher than G′ and G′ drops dramatically, the PLC exhibits liquid-like properties at higher temperature above 83°C. In the terminal region, G′ and G″ generally decrease linearly (G′ α ω^2 and G″ α ω). However, in this work, at temperature above 160°C, the variation in both moduli deviated from linearity due to thermal degradation. Thus, the experimental data was applied over the range of extrusion temperature of 83-150°C.

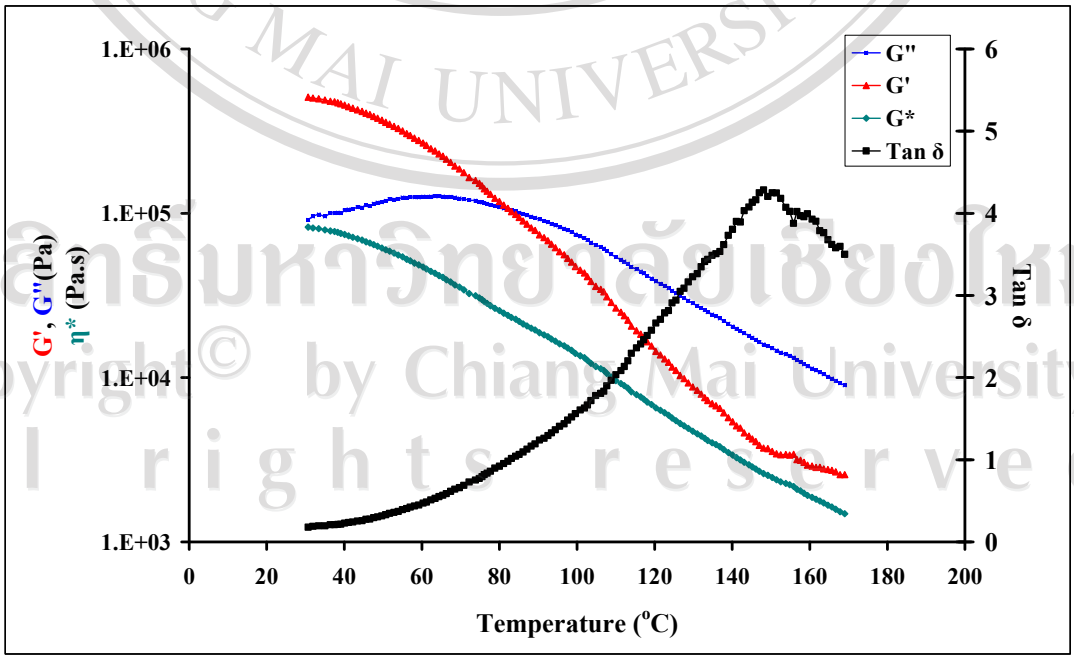

Figure 3.42 Temperature dependence of G′, G″, tan δ and η* of PLC copolymer.

3.2.3 Fabrication of Small Tubes.

3.2.3.1 Fabrication of Small Tubes by Dip-coating.

The PLC copolymer was dissolved in distilled chloroform (15%w/w) and Kirchner (K) wires with diameters of 1.2 mm used as moulds. After drying in air, the tube was stored in desiccators under vacuum for complete drying before being manually removed from the K-wire. A photograph and SEM images of the tube obtained are shown in Figure 3.43 (a-d). Transparent rubber-like tubes with an internal diameter and wall thickness of 1.2 mm and 0.3-0.4 mm respectively have been produced by the dip-coating method which, although rather laborious and time-consuming, yields tubes of uniform and controllable dimensions.

(a) (b)

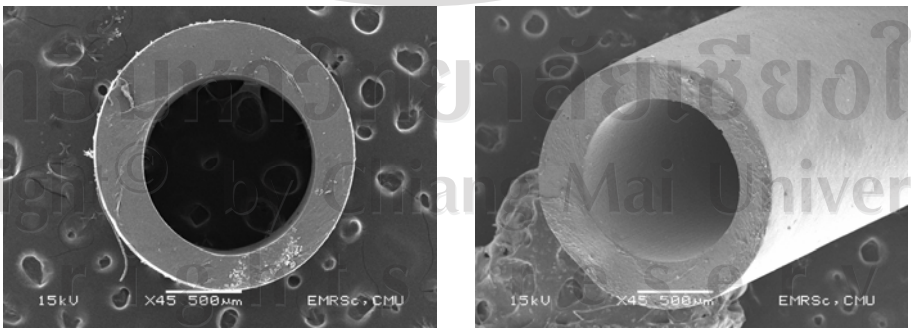

(c) (d)

Figure 3.43 (a) Camera (b) Photograph, (c) and (d) SEM images of the PLC copolymer small tube prepared by dip-coating.

3.2.3.2 Fabrication of Small Tubes by Melt extrusion.

An alternative technique, melt extrusion, was also used to prepare small tubes of similar dimensions. A small-scale melt spinning apparatus was modified by using a tubular-shaped die instead of a spinneret. From rheological property of PLC copolymer as mentioned in section 3.2.5, PLC melts and flows approximately homogeneously in the temperature range of 140°C to 150°C. Thus, a PLC copolymer rod was first made by heating at 140°C under compression with a maximum load of 400 kg. The temperature was then held constant for 15 min before cooling to room temperature and removing from the cylinder. For melt extrusion, the copolymer rod was carefully inserted into the extrusion cylinder, heated up to 135°C and melt extruded as a tube at a ram speed of 2 mm/min through a tubular-shaped die. The tube was drawn down manually to a designated diameter and cooled in the water bath (10-15°C).

(a) (b)

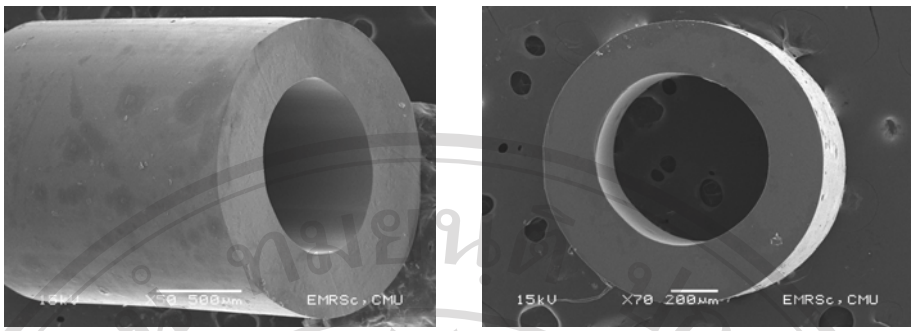

(c) (d)

Figure 3.44 (a) Camera (b) Photograph, (b) and (c) SEM images of the PLC copolymer small tube prepared by melt extrusion.

Melt extrusion can produce longer tubes, is quicker and more convenient than dip-coating, and also avoids the use of an organic solvent. Photographs and SEM images of the tube obtained are shown in Figure 3.44 (a-d). Transparent elastic tubes with an internal diameter and wall thickness of 0.7 mm and 0.2 mm respectively were obtained. However, the tube from melt extrusion was less uniform in its dimensions than that from dip-coating due to the multivariate nature of melt extrusion process and the viscoelastic properties of the polymer melt.

3.3 Large Scale Synthesis (500 g)

The ROP of L-lactide and ε-caprolactone was performed in bulk with a composition ratio of 50:50 mole% respectively and using $SnOct_2$ as the catalyst and 1-hexanol as the initiator. Each batch of preparation was for 500 g of the random copolymer. The polymerizations were carried out in a Parr Reactor Model 4520 as shown in Figure 3.45.

Figure 3.45 Parr Reactor Model 4520.

3.3.1 Parr Reactor Instrument

The Parr Reactor instrument consists of 2 main assemblies such as a 4520 Bench Top Reactors and a 4843 Temperature Controllers as shown in Figure 3.46 (a) and (b) respectively.

(a) (b)

Figure 3.46 (a) 4520 Bench Top Reactors (b) 4843 Temperature Controllers.

The use of 4520 Bench Top Reactors comprised the following steps:

(1) Lower the heater and push it aside before attempting to remove the split ring and head.

(2) To open the vessel, open the gas release valve to discharge any internal pressure. Loosen and remove the split ring. If the vessel is equipped with a drop band first loosen the screw and lower the band. The head with all attached fittings is free to be lifted from the cylinder. Handle the head carefully so as not to damage the stirring shaft and other internals when they are outside of the cylinder.

(3) Before closing the vessel, examine the head seal carefully to be sure that it is in good condition. The seal should not have any nicks or be hardened, discolored or deformed. Examine the mating surfaces on the cylinder and head to be sure they are clean and free from burrs; then raise the cylinder up to the head.

(4) To close the vessel, slide the two split rind halves around the cylinder and head flanges. If equipped with a drop band raise the band to secure them. Position the band so that the cone pointed screw enters the indent in one of the ring halves and tightens the screw lightly to hold the band in place.

(5) Sealing vessels with PTFE gaskets, if your split ring has compression bolts, tighten each of the bolts with the wrench furnished. Apply a firm but hard pull to each bolt. Or, if a torque wrench is available, apply 25 ft-lbs to each bolt. Tightening should proceed in a criss-cross pattern rather than progressively around the circle. Let the vessel stand for about five minutes after the initial tightening; then retighten the bolts again. This will

compensate for any tendency of the PTFE gasket to flow under the loading pressure.

(6) Set the vessel in the heater with the gage facing forward. Swing the drive arm into position and connect the spline coupling onto the drive of the reactor.

A 4843 temperature controller has three illuminated switches on the front panel as shown in Figure 3.48, along with a speed control potentiometer and a high limit indicator light to show the status of the system.

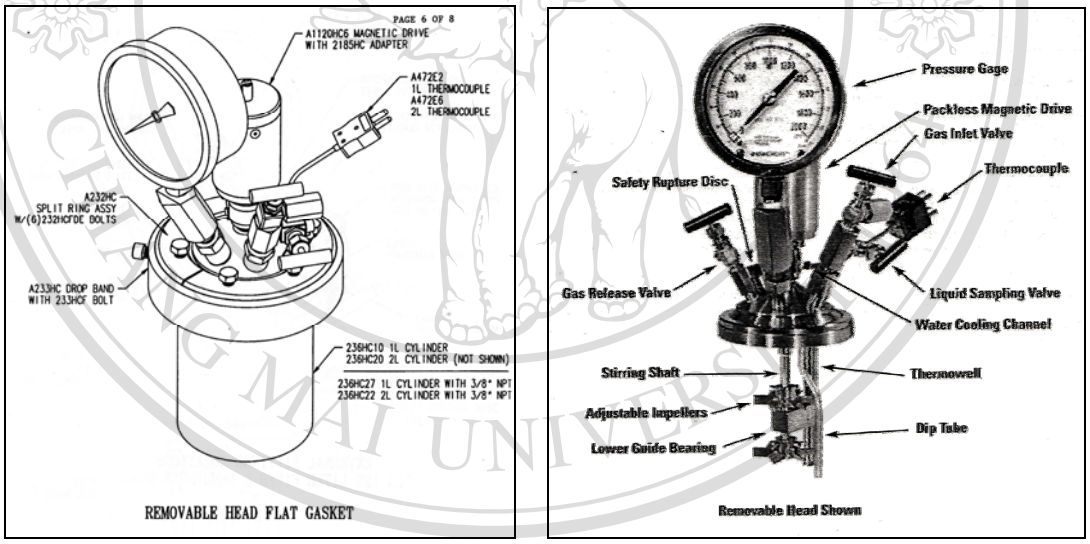

(a) (b)

Figure 3.47 The assembly of removable head vessels (a) external (b) internal.

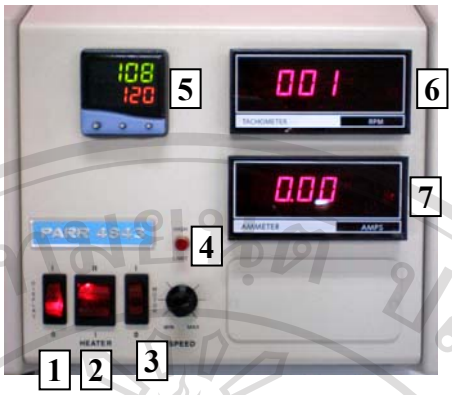

Figure 3.48 The assembly of 4843 temperature controller

(1) the instrument switch (2) the heater switch

(3) the motor controls (4) the high limit indicator light

(5) the temperature module (6) the optical tachometer module

(7) the digital ammeter display module.

The heater switch is a manual, three positions, illuminated switch which controls the amount of power sent to the heater. In the HIGH (II) position, full power is developed by the heater. In the middle (0) position the heater is off. In the LOW (I) position, a diode is switched into the system to allow only one-half of the rated power to be developed by the heater. This low setting will be useful when operating the reactor at temperatures below 175°C. Both the instrument switch and the heater switch must be turned on to activate the heater as power for the heater is supplied through a solid state relay controlled by the temperature control module. The light in the heater switch will glow only when current is flowing to the heater. Turning off the instrument switch will also turn off the heater.

The motor controls consist of an on-off switch and a potentiometer to control the speed of the DC motor furnished on current stirred reactors. The speed control knob should be turned down to a minimum setting before turning on the motor switch to minimize electrical surges within the speed control unit.

The high limit indicator light will glow if the controller receives an indication from any of its sensors that a high temperature or pressure limit has been reached and the lockout relay has opened. When the light comes on, the user must find the source of the problem, correct it, and then manually reset the system using the high limit reset button on the back of the controller.

The temperature module, two lines of information are shown on the display during normal operations. The upper line (green display) shows the actual temperature as read by the control thermocouple. The lower line (orange display) shows the set point. The set point can be raised or lowered by holding down the (*) key and pressing the up or down arrows.

The optical tachometer module showed the digital RPM display module which provides a means for continuously monitoring the stirring speed in a Parr reactor. It consists of a digital readout mounted in the controller cabinet connected to an optical sensor installed in the over arm drive on the reactor. The connecting cable has a microphone plug which fits into a marked socket on the back panel of the controller. The digital display will show the stirring speed over a range from 0 to 1999 rpm with a 1 rpm resolution and ± 10 rpm accuracy.

The digital ammeter display module provides a means for continuously monitoring the current being drawn by the stirrer motor. Since the motor speed control will provide a constant stirring speed at any given setting, changes in the

current drawn by the motor will correspond to changes in the viscosity of the fluids in the vessel. This will be a useful option for users who want to monitor the progress of a polymerization reaction in which there are viscosity changes as the reaction proceeds.

3.3.2 Calibration Thermocouple

Thermocouple in the Parr reactor is a Type J (iron-constantan) thermocouple in a 1/8″ diameter. Stainless steel sheath is furnished with the reactor. Insert this thermocouple into the head thermowell and connect it to the thermocouple socket on the rear panel of the temperature controller using the extension wire furnished with the reactor. The total resistance of the thermocouple and the lead wires should not exceed 20 ohms. If the resistance of the thermocouple circuit is higher, it will reduce the sensitivity of the control system.

In this study, thermocouple was calibrated with the three accurately thermometers. The zero setting in the temperature controller program was set at -10.0, 0.0 and +10.0 and the time-temperature profiles are shown in Figure 3.49 (a) to (c) respectively. It was concluded that the suitable zero setting that gave the accurately temperature of thermocouple was +10.0. Thus, in the large scale synthesis (500 g) used zero setting at +10.0.

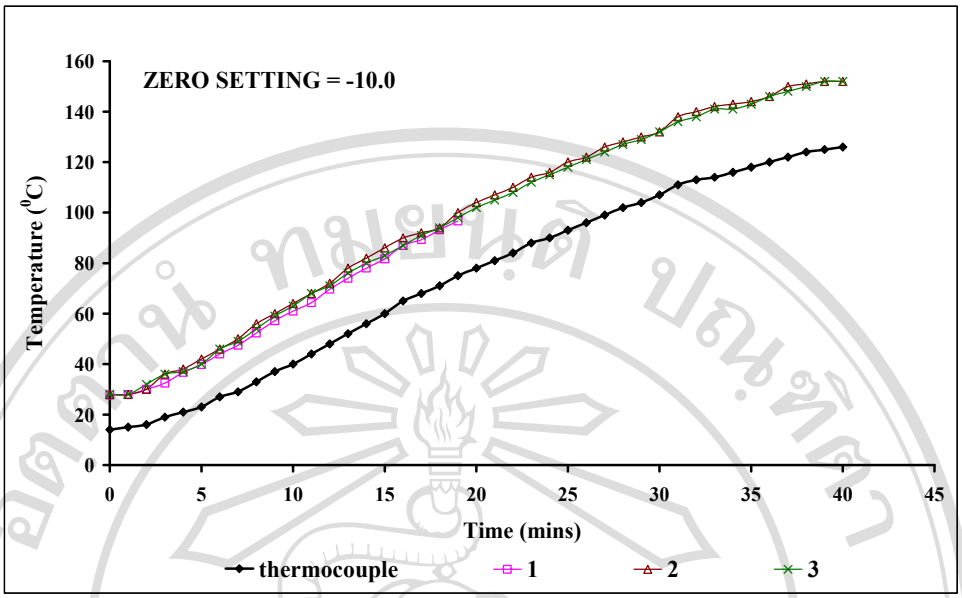

(a)

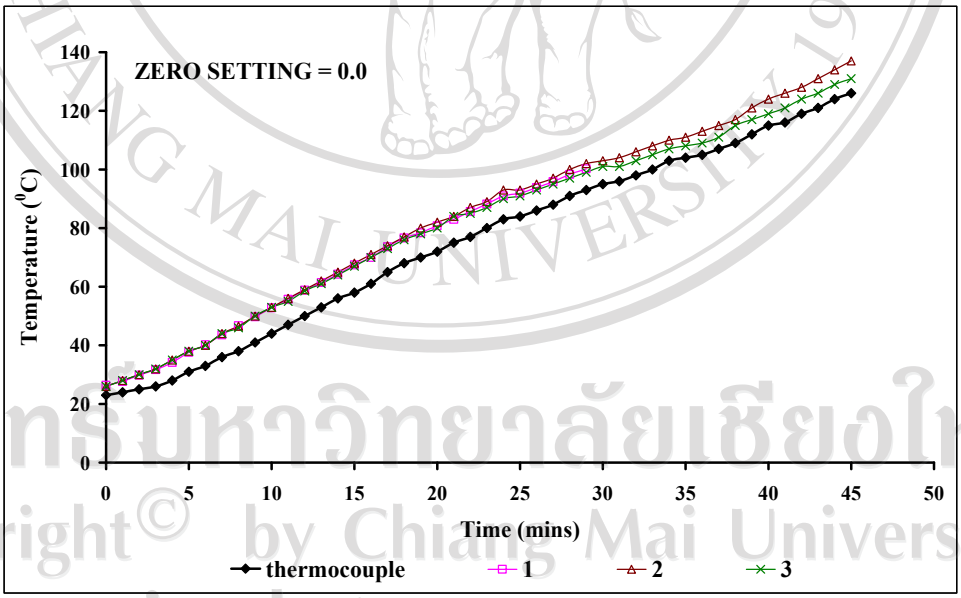

(b)

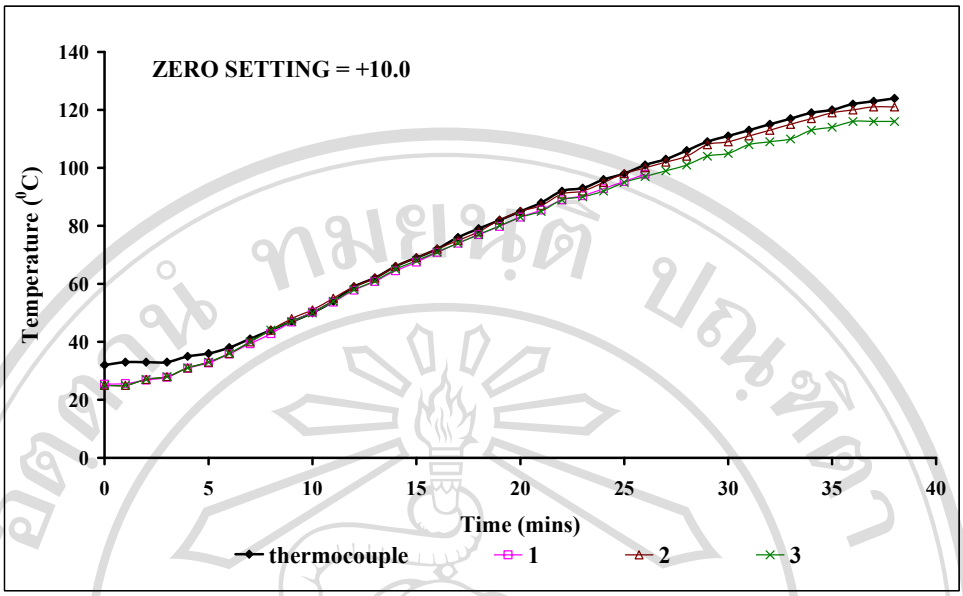

(c)

Figure 3.49 Time-temperature profiles of different zero setting value

(a) -10.0 (b) 0.0 (c) +10.0 in large scale synthesis (500 g).

3.3.3 Test Parr Reactor

An initial operating test should be made, with only water, to check the apparatus before starting the first experimental runs. For this initial test, fill the cylinder not more than half full of water and run the temperature up to 150°C while checking the apparatus for leaks and observing the performance of the temperature controller. Figure 3.50 shows the time and temperature profile of water in this test; it was found that in the initial of time, the temperature increase with the increasing time. When the temperature closely the set point (150°C), the temperature was obtained levels off at a constant value.

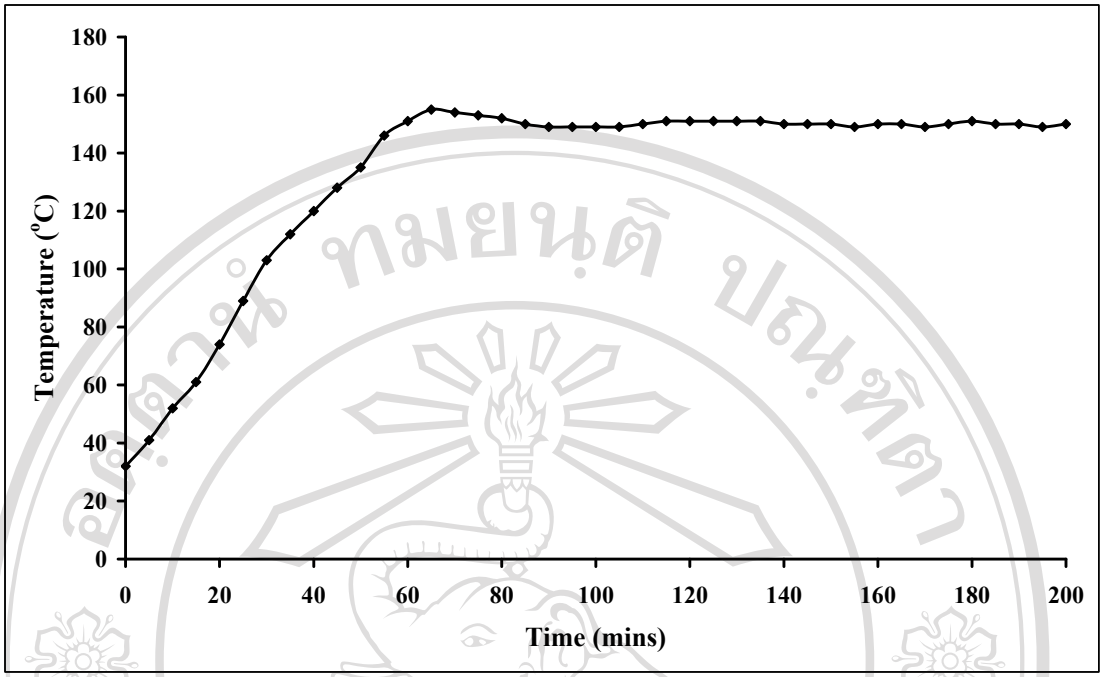

Figure 3.50 Time-temperature profile of water in the initial operating test.

3.3.4 Synthesis of Poly(L-lactide-*co*-*ε*-caprolactone), PLC 50:50 mole% Copolymers : Large Scale (500 g)

To study the effects of the reaction temperature and time on PLC 50:50 copolymer properties, polymerizations were carried out at constant the monomer to initiator molar ratio ([M]:[I] = 100:0.01 mole%) and 0.1 mole% $SnOct_2$ catalyst in large scale synthesis (500 g). The conditions used for synthesis and properties of PLC copolymers are summarized in Table 3.28 and the details as follow.

Batch 1

From the results of PLC copolymerization in the medium scale (250 g), the suitable conditions that gave a high %yield, high molecular weight and final copolymer compositions close to that of the comonomer feed ratio was 96 hours at

120°C. Thus, the first experiment, the PLC copolymer was synthesized by the ROP in bulk using 0.1 mole% $SnOct_2$ as a catalyst and 0.01 mole% 1-hexanol as an initiator at 120°C for 96 hours. The results of PLC copolymer properties were shown in Table 3.28. It was found that the PLC copolymer was dark brown caramel as shown in Figure 3.51, gave low molecular weight ($\overline{M}_w \approx$ 14000) due to the degradation products was produced during the polymerization reaction. The PLC copolymer composition (LL: CL = 55.1: 44.0 mole%) is nearly the monomer feed ratio (LL: CL = 50.0: 50.0 mole%). However, the ε-caprolactone monomer still remained in the polymerization system that was confirmed by ^{1}H-NMR spectrum as shown in Figure 3.52. Randolf *et.al.* [55] and Minglong *et.al.* [56] report that the %yield and molecular weight of polymer began to decrease with longer reaction time due to transesterification reactions leading to low molecular weight oligomers.

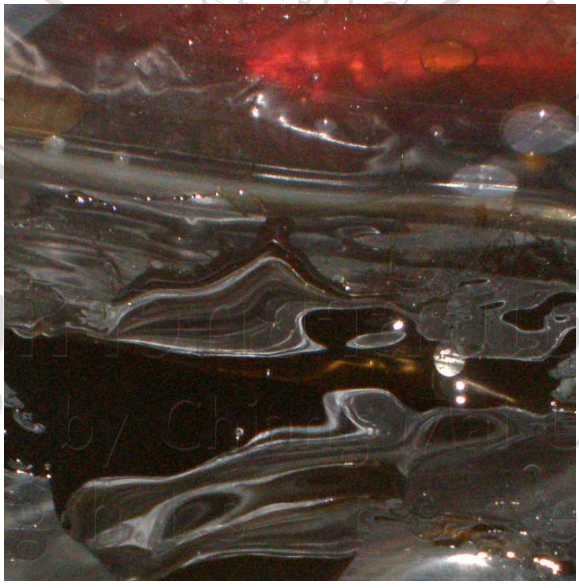

Figure 3.51 The dark brown caramel of crude PLC copolymer (Batch 1 in large scale (500 g)).

Table 3.28 Results of the polymerization of PLC copolymer in large scale (500 g).

Copolymer	**Batch 1**		**Batch 2**		**Batch 3**	**Batch 4**		**Batch 5**		
Reaction Temperature (°C)	120		120		100	120	100	120	120	120
Reaction Time (hours)	96		48		96	6	18	6	9	24
Physical appearance	crude	pure	crude	pure	viscous liquid	opaque hard brittle solid	transparent flexible solid	opaque hard brittle solid	transparent flexible solid	pale yellow transparent solid
	dark brown caramel	dark brown caramel	brown caramel	brown caramel						
% yield (after reprecipitation)	nd		nd		nd	72.21	88.32	74.44	87.77	32.70
Initial monomer ratio LL:CL (mole %)	50.0 : 50.0		49.6 : 50.4		50.1:49.9	50.1 : 49.9		50.1 : 49.9		
Final copolymer compositions (^{1}H-NMR) LL:CL (mole %)	crude	pure	crude	pure	nd	70.1:29.9	51.8:48.2	68.0:32.0	56.3:43.7	50.9:49.1
	55.1:44.9	59.3:40.7	48.7:51.3	48.0:52.0						
Average molecular weight (GPC)	crude	pure	crude	pure						
$\overline{M}_w$	14050	23740	17340	15630	nd	21130	17610	355300	280000	43050
Intrinsic viscosity, [η] (dl/g)	nd	nd	nd	nd	nd	0.16	0.34	0.60	0.99	0.32

nd = not detected or difficult to estimate

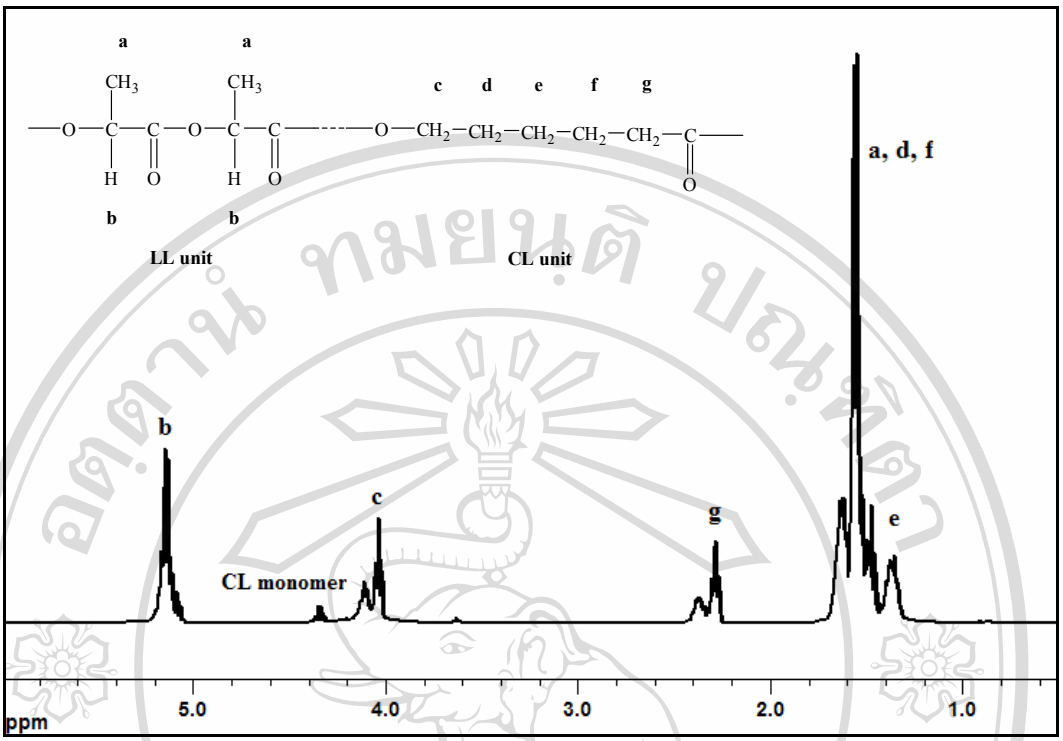

Figure 3.52 ^{1}H-NMR (400 MHz) spectrum of crude PLC copolymer at 120°C for 96 hours (Batch 1 in large scale (500 g)).

Batch 2

In batch 2, the reaction time was decreased from 96 to 48 hours. The final copolymer composition (LL: CL = 48.7: 51.3 mole%) close to that of the monomer feed ratio (LL: CL = 49.6: 50.4 mole%) as determined by ^{1}H-NMR spectrum as shown in Figure 3.53. However, physical appearance of copolymer product was brown caramel. The molecular weight of PLC copolymer increased slightly when compared with Batch 1 as compared in Table 3.28. Figures 3.54 and 3.55 show the temperature variation with the reaction time and the increasing in the current from the ammeter module that correspond to increase in the viscosity of the copolymer product in the vessel respectively. It confirmed that the PLC copolymer product was

decomposed at high temperature. The ^{13}C-NMR shown that transesterification reaction occurred. From the expanded carbonyl regions (165-175 ppm) of crude PLC copolymer spectra in Figures 3.56, the triad sequence *CLC* could formed, become a useful indicator that transesterification has occurred. This is due to the problems associated with heat transfer as the mass-to-volume ratio increases resulting in increased temperature variations during 110°C to 160°C as shown in Figure 3.54. The transesterification reaction occurred at temperature higher than 130°C as previously described in section 3.1.2.

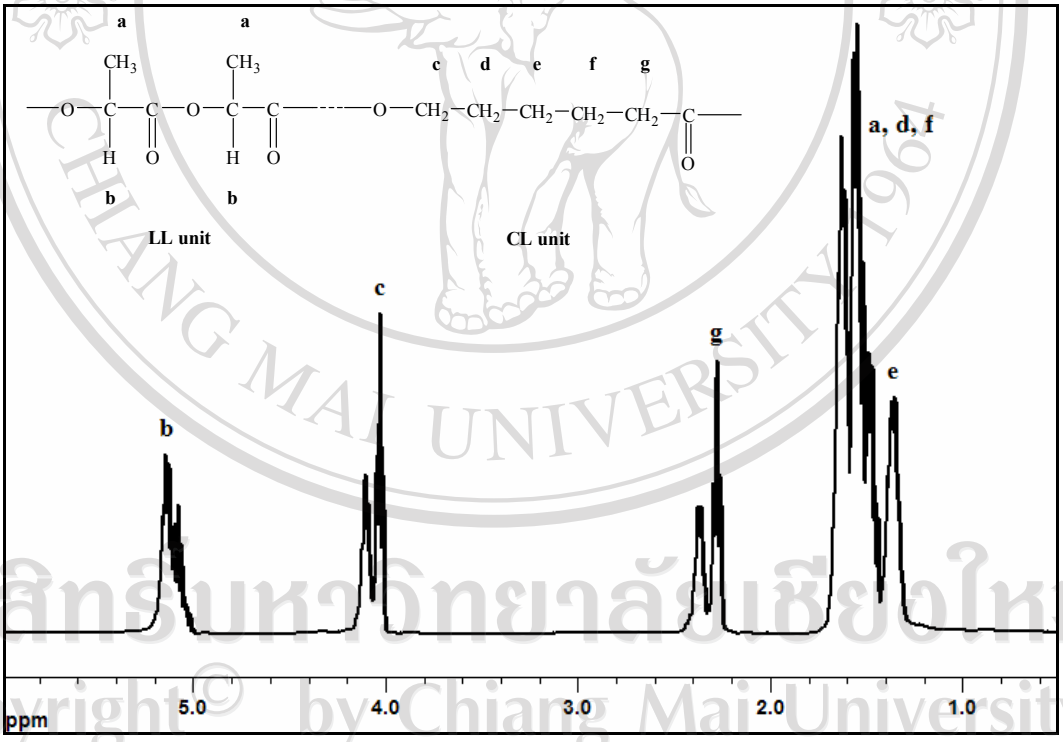

Figure 3.53 ^{1}H-NMR (400 MHz) spectrum of crude PLC copolymer at 120°C for 48 hours (Batch 2 in large scale (500 g)).

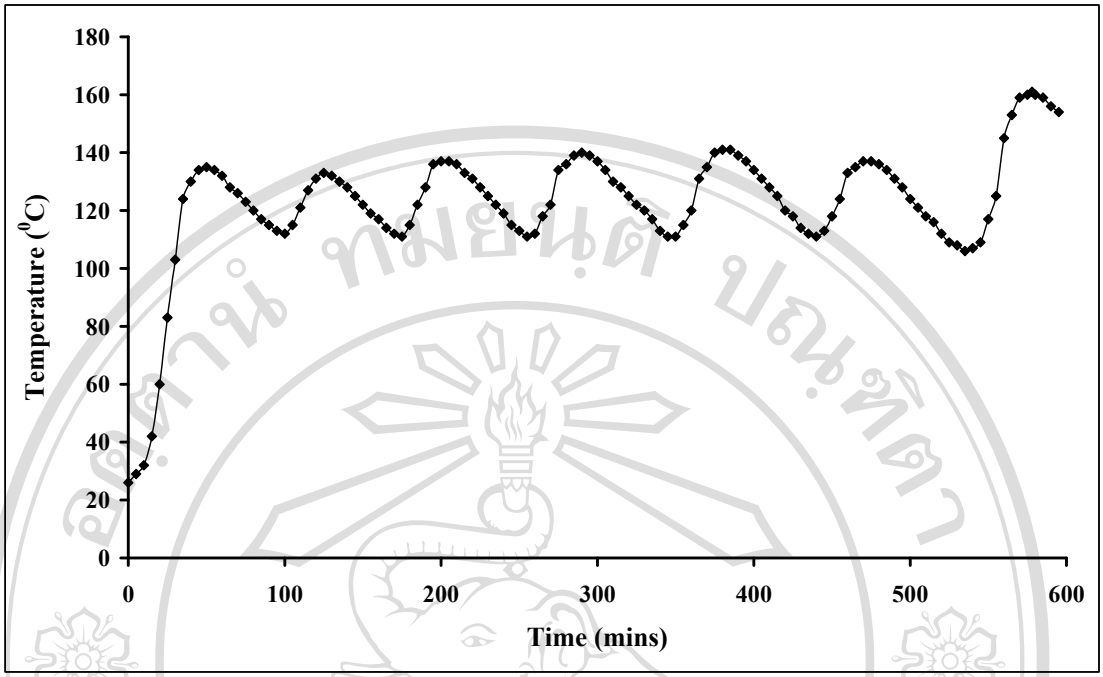

Figure 3.54 Reaction time-temperature profile of PLC copolymer in Batch 2 for large scale (500 g).

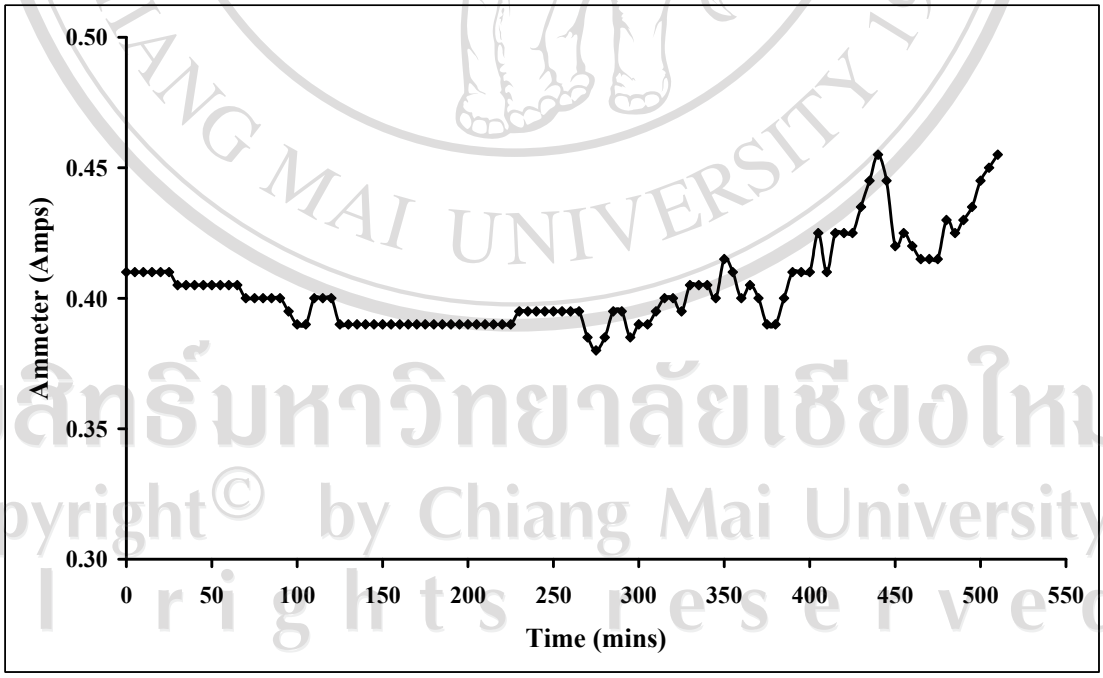

Figure 3.55 Reaction time-ammeter module profile of PLC copolymer in Batch 2 for large scale (500 g).

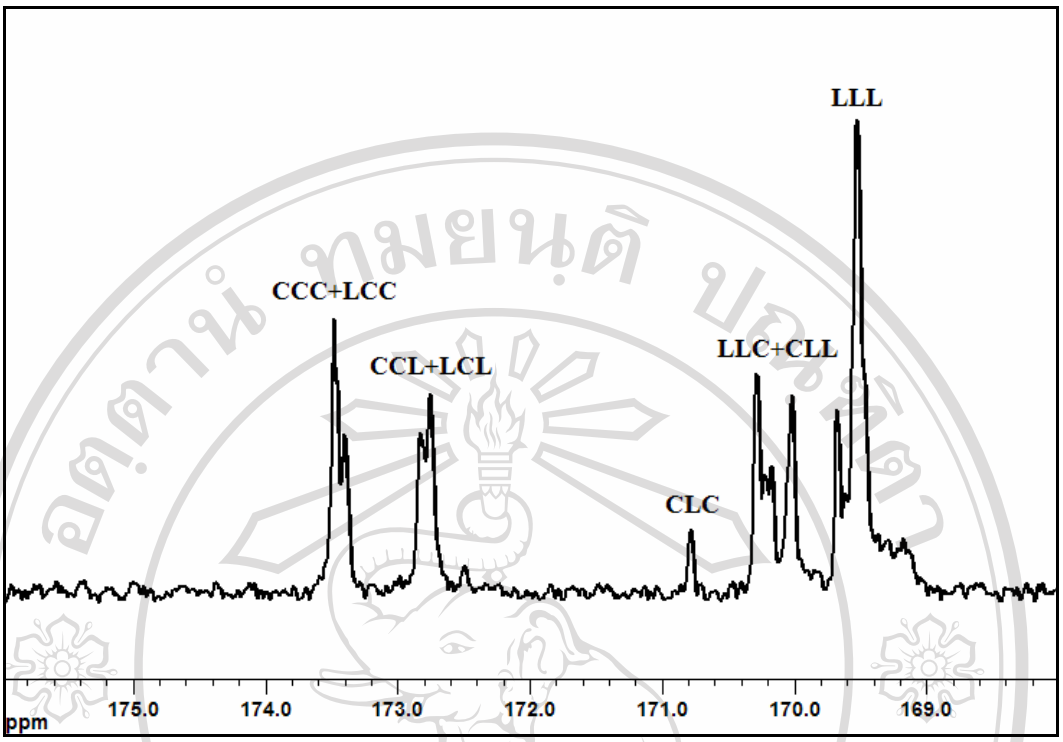

Figure 3.56 Expanded carbonyl region of the 100 MHz ^{13}C-NMR spectrum of crude PLC copolymer at 120°C for 48 hours (Batch 2 in large scale (500 g)).

Batch 3

In batch 3, the PLC copolymer was synthesized at 100°C for 96 hours. It was found that the polymerization reaction could not occur because this temperature is not suitable. Thus, it can be concluded that the suitable initial temperature is 120°C. The main problem associated with the increasing in the reaction time leading to the increasing in the viscosity of the copolymer product and that cause of really poor heat transfer. Hence, the copolymer products in Batch 1 and Batch 2 were easily decomposed by the exceed of temperature.

Batch 4

In batch 4, the PLC copolymer was polymerized in two steps. Firstly, the polymerizations were carried out at 120°C for 6 hours. It was found that the copolymer product was opaque hard brittle solid, low %yield (72%) and low molecular weight ([η] = 0.16 dl/g). From ^{1}H-NMR, it was found that the LL content in the copolymer composition is higher than CL content (LL: CL = 70.1: 29.9 mole%) and CL monomer is still remaining in the reaction as shown in Figure 3.57.

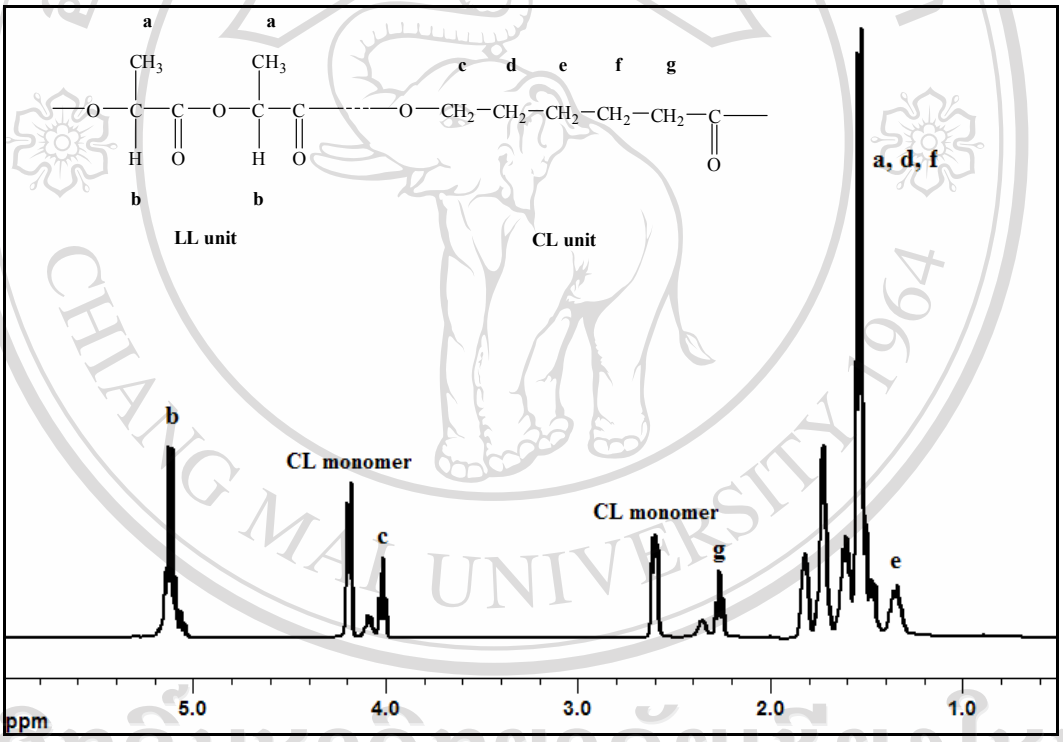

Figure 3.57 ^{1}H-NMR (400 MHz) spectrum of crude PLC copolymer at 120°C for 6 hours (Batch 4 in large scale (500 g)).

Later, the reaction temperature was decreased to 100°C for 18 hours in order to solve the heat transfer problem. It was found that the copolymer product became transparent flexible solid as shown in Figure 3.58 and copolymer composition (LL:

CL = 51.8: 48.2 mole%) close to that of the monomer feed ratio (LL: CL = 50.1: 49.9 mole%) as shown in Figure 3.59.

Figure 3.58 The transparent flexible solid of crude PLC copolymer at 100°C for 18 hours (Batch 4 in large scale (500 g)).

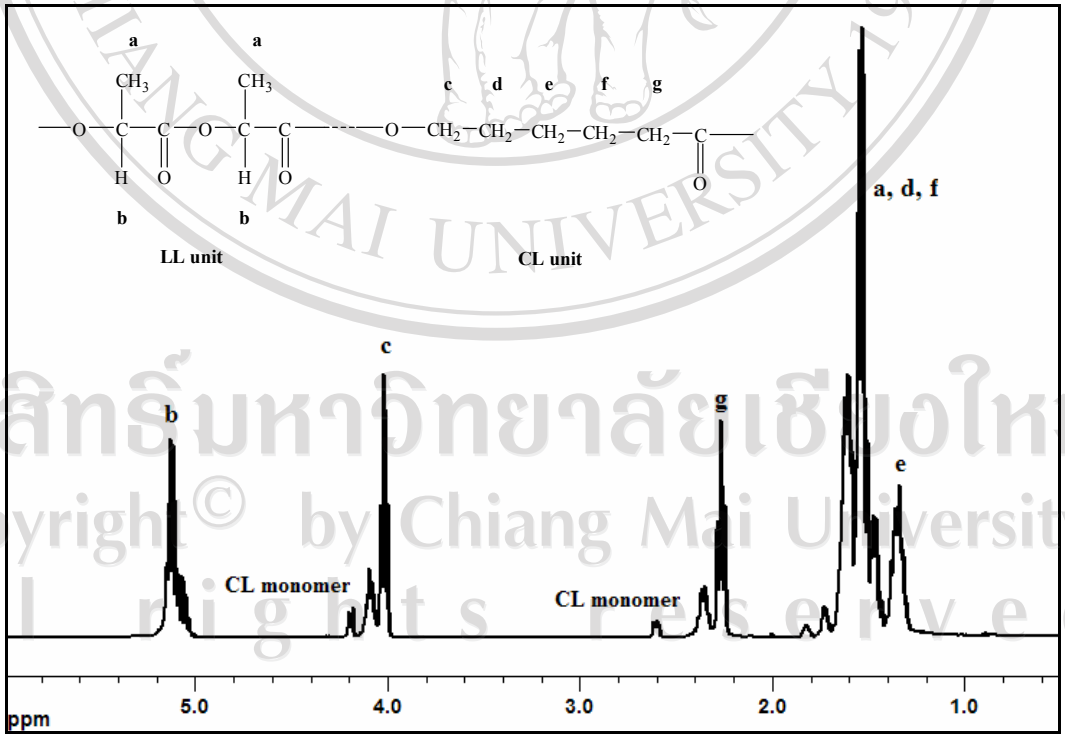

Figure 3.59 ^{1}H-NMR (400 MHz) spectrum of crude PLC copolymer at 100°C for 18 hours (Batch 4 in large scale (500 g)).

When increasing the reaction time from 6 to 18 hours, both of a %yield (88%) and the intrinsic viscosity ([η] = 0.33 dl/g) increased due to the high molecular weight of PLC copolymer was produced.

Batch 5

In batch 5, the PLC copolymer products were synthesized at 120°C for various the reaction times such as 6, 9 and 24 hours. Figures 3.60 – 3.62 showed the ^{1}H-NMR spectra of crude PLC copolymer at 120°C for 6, 9 and 24 hours respectively and Figure 3.63 showed the double extrapolation plots of the reduced, η_{red}, and inherent, η_{inh}, viscosities against concentration for PLC copolymer at 120°C for 9 hours. It was found that increasing the reaction time from 6 to 9 hours, both of a %yield (from 74% to 88%) and the intrinsic viscosity ([η] from 0.61 to 0.99 dl/g), increased and copolymer composition close to that of the monomer feed ratio. However, with longer reaction time, example reaction time reaching 24 hours, both of a %yield (33%) and the intrinsic viscosity ([η] = 0.32 dl/g), decreased and the copolymer product became pale yellow transparent solid due to transesterification reaction occurred. This suggests that the reaction temperature and time are very important for the polymerization reactions.

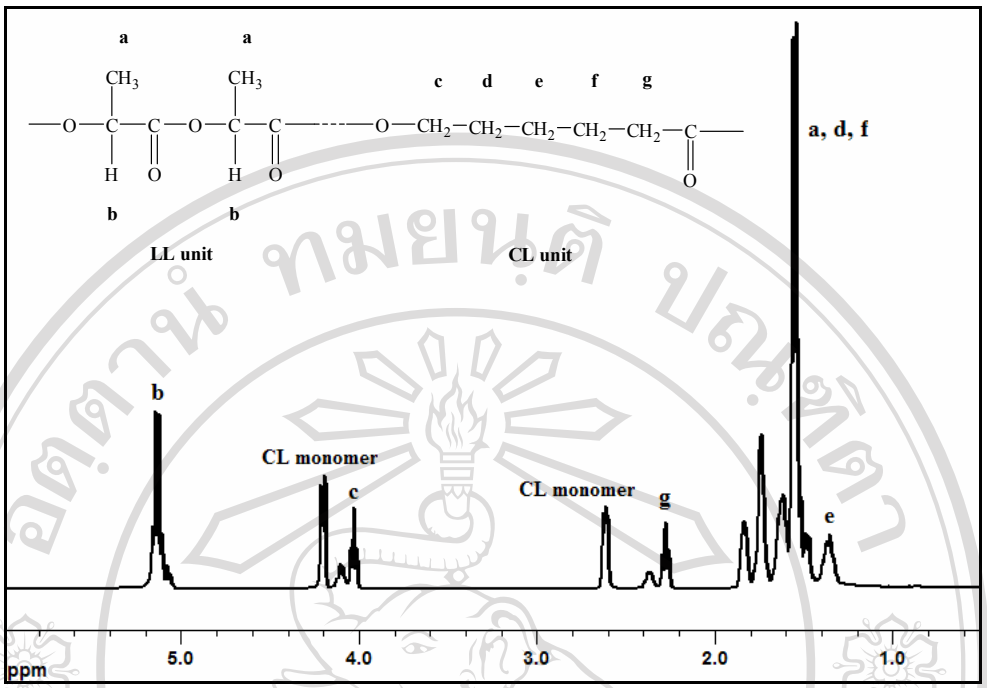

Figure 3.60 ^{1}H-NMR (400 MHz) spectrum of crude PLC copolymer at 120°C for 6 hours (Batch 5 in large scale (500 g)).

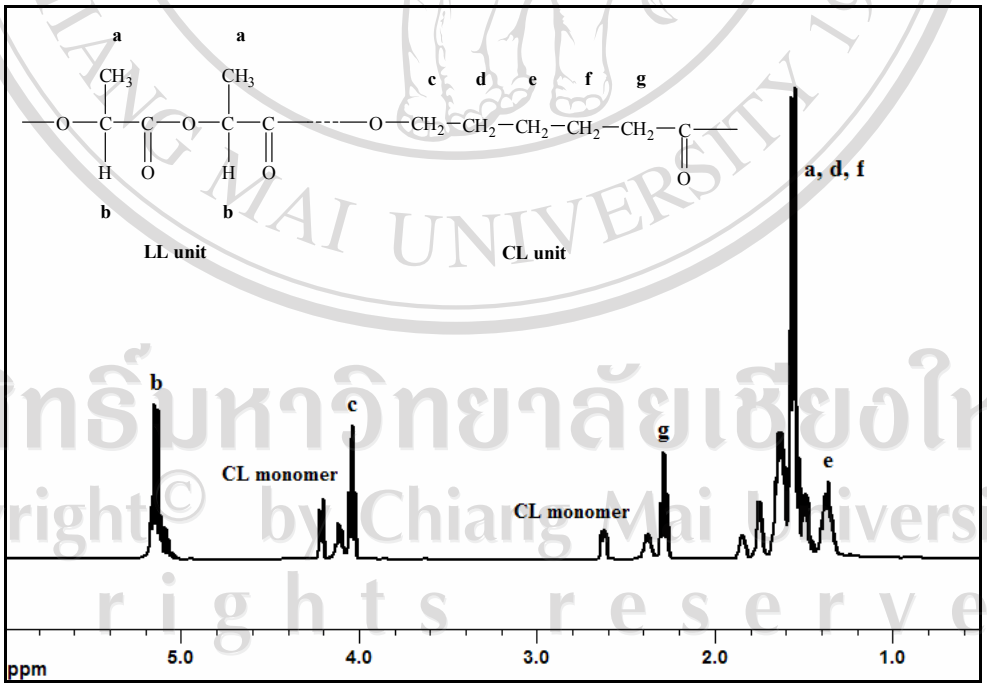

Figure 3.61 ^{1}H-NMR (400 MHz) spectrum of crude PLC copolymer at 120°C for 9 hours (Batch 5 in large scale (500 g)).

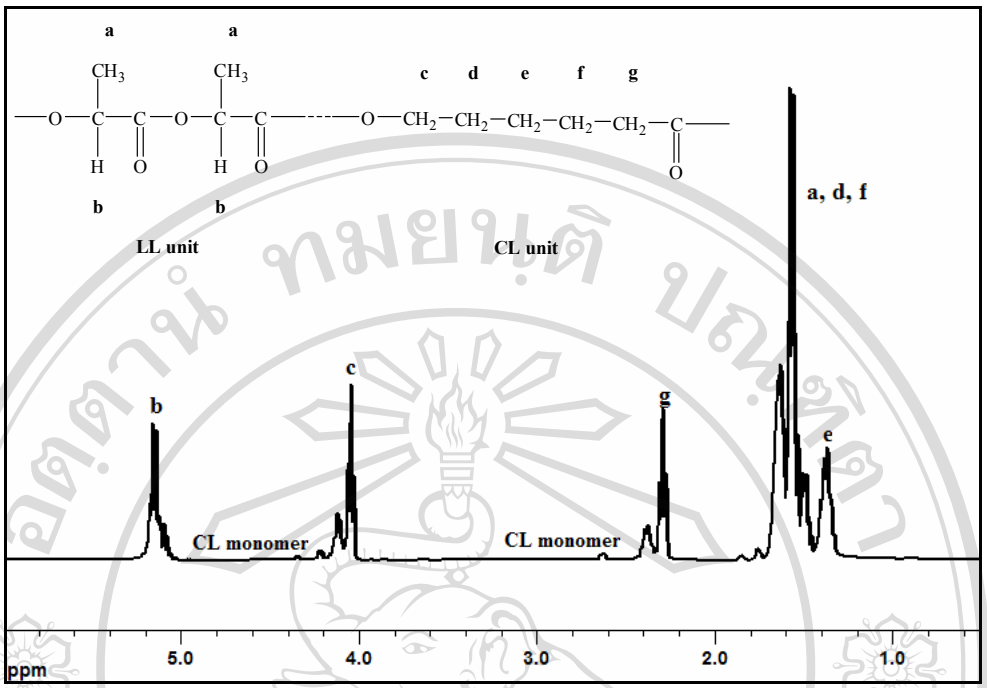

Figure 3.62 ^{1}H-NMR (400 MHz) spectrum of crude PLC copolymer at 120°C for 24 hours (Batch 5 in large scale (500 g)).

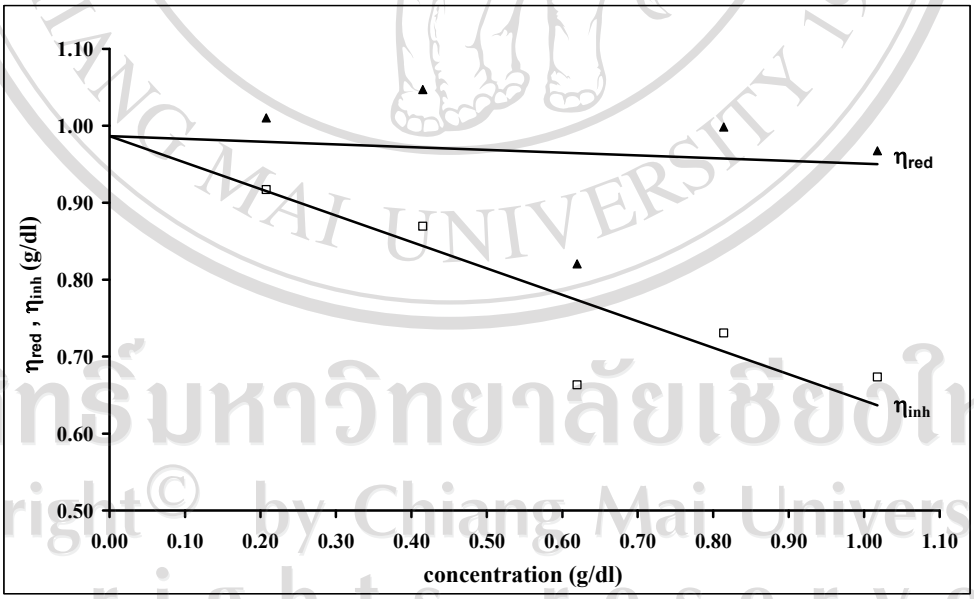

Figure 3.63 Double extrapolation plots of the reduced, η_{red}, and inherent, η_{inh}, viscosities against concentration for PLC copolymer at 120°C for 9 hours (Batch 5 in large scale (500 g)).